Doctoral Dissertation(Shinshu University)

Potential applications of advance functional polymeric nanofibers in biomedical and environmental engineering (優れた機能性を備えた高分子ナノファイバーの医療用・環境工学への応用の可能性に関する研究)

March 2021

HASHMI MOTAHIRA

Contents

List of figure

Abstract

Potential applications of advance functional polymeric nanofibers in biomedical engineering

Hashmi Motahira

Directed by: Professor Ick Soo Kim

Nanomaterials plays the vital role in the main areas of advance research such as electronic, waste water treatment, detection and diagnose of various diseases, drug delivery, tissue engineering and nano medicine. Nanotechnology shows the different picture of materials. This thesis mainly focus on the biomedical applications like mask, wound dressing and antibacterial properties of nanomaterials using Electrospinning. For mask application, Copper oxide was selected as antibacterial agent due to its good antimicrobial properties as well as its production is economical as compared to other metallic nanoparticles which are being used as antibacterial agents i.e. Copper nanoparticles, gold nanoparticles, and silver nanoparticles. Presence of copper oxide nanoparticles exhibited excellent morphological, mechanical, structural, surface, and antimicrobial properties (samples having 1.00% CuO exhibited optimum results). Momordica charantia MC (bitter gourd) is a natural wound dressing for diabetic patients. Keeping in view valuable and fruitful properties of MC, we have loaded bitter gourd extract in combination with polyvinyl alcohol (PVA) on electrospinning and characterized for possible testing. It is expected that prepared composite nanofibers have potential applications as sustainable antibacterial wound dressings for smooth and speedy recovery of open wounds. Antibacterial property is very important for biomedical application. For this purpose silver sulfadiazine (AgSD) was loaded for the first time on electrospinning as well as self-synthesized AgSD on PAN nanofibers by solution immersion method and then compared the results of both. The antibacterial properties of PAN nanofibers impregnated with AgSD were determined with both types of bacteria strains to compare with control one. Excellent antibacterial efficiency was indorsed to samples with AgSD by immersion method.

Cellulose is one of the most hydrophilic polymers with sufficient water holding capacity but it's unstable in aqueous conditions and it swells. Cellulose itself is not suitable for electrospun nanofibers' formation due to high swelling, viscosity, and lower conductivity. Carboxymethyl cellulose (CMC) is also super hydrophilic polymer, however it has same trend for nanofibers formation as that of cellulose. Due to above stated reasons,

applications of CMC are quite limited in nanotechnology. Loading of CMC has been optimized for electrospun tri-component polyvinyl alcohol (PVA), polyvinylpyrrolidone (PVP), and carboxymethyl cellulose (CMC) nanofibers aiming widening its area of applications. It was observed that at weight ratio of PVP 12 and CMC 3 was as highest as possible loading to produce smooth nanofibers.

Chapter 1

Introduction of nanotechnology

1. Introduction

There are various methods of nanofibers production. One of the most flexible and cost-effective is electrospinning, allowing formation under the influence of high electrical voltage of long, continuous fibers with diameter ranging from few nanometers to several micrometers. Electrospun nanofibers are created from electrically charged jets of polymer solution or polymer melt. A typical electrospinning scheme is given in Figure 1. Unusual properties of resulting fibers predispose them for plenty of biomedical applications like tissue engineering, drug delivery, nanomedicine, implantation, antiviral mask, wound dressing and protective clothing.[1–3]

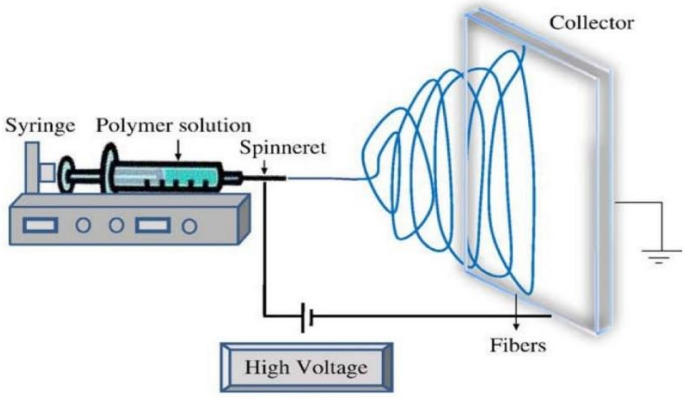

Figure 1.1 Typical Electrospinning scheme

1.1. Nanofibers as wound dressing

Wound dressings are pieces of fabric which are used to cover a cut or a wound. They can be woven, knitted or non-woven fabric. With the increasing demand for effective wound care technology, a number of researchers are carrying out research in the field of wound care systems. Nanofiber mats have been used as wound dressings for a couple of years. It is stated that about 60% of total nanofiber production is used for biomedical purposes only. This can be for wound dressings, self-healing features, drug delivery, or implants.[1,4–8]

1.2. Nanofibers as drug carrier

To achieve a desired therapeutic effect, a drug requires the correct drug-delivery system to assure its specific release profile. The location, timing, and rate of release of a drug need to be adjusted as closely as possible to the therapeutic target of the drug. However, this can be a major challenge in the design of drug-delivery systems. Among the potential drug-delivery systems, nanofibers offer a promising solution. Nanofibers are solid fibers that have a diameter from a few nanometers to 1000 nm, and unique functionality and inherent nanoscale characteristics. Thus, they are among the most universal and promising of drug-delivery systems, and they can be designed for a wide range of drug-release kinetics. They can be used for a number of routes of administration, including oral, topical, transdermal, and trans mucosal. In addition, nanofibers can protect a drug from decomposition in the body prior to arrival at the required target.[9,10]

1.3. Nanofibers in tissue engineering

Tissue engineering is a multidisciplinary field that provides substitute methods for repairing damaged tissues by implanting natural, synthetic, and semisynthetic implants, which mimic fully functional tissues and organs. Today, remunerating nonfunctional tissue into functional forms is the biggest challenges in the field of tissue engineering. Currently, there are three important methods available for fabricating nanofibrous scaffolds, phase separation, electrospinning, and self-assembly. Among these methods, electrospinning is the most widely used technique for tissue engineering applications. The synthesis of nanofibrous scaffolds by the electrospinning process can be achieved using a variety of natural and synthetic biomaterials. The development of 3D biodegradable scaffolds provides excellent support for cell adhesion, proliferation, and differentiation. Therefore, electrospun scaffolds are used for such distinct tissue engineering as epidermal, vascular, neural, musculoskeletal (including bone, cartilage, ligament, and skeletal muscle), and corneal applications.

1.4. Nanofibers as mask filter

A facemask is a loose-fitting, disposable device that creates a physical barrier between the mouth and nose of the wearer and potential contaminants in the immediate environment. They are generally labelled

as surgical, isolation, dental or medical procedure masks. A face masks consists entirely or substantially of filter material or comprises a face piece in which the main filter(s) form an inseparable part of the device. Nanofibers could be the key elements for filter materials in face masks. They have a very high surface area per unit mass that enhances capture efficiency and other surface area-dependent phenomena that may be engineered into the fiber surfaces (such as catalysis or ion exchange). They could enhance filter performance for capture of naturally occurring nanoparticles such as viruses, as well as micron-sized particles such as bacteria or man-made particles such as soot from diesel exhaust.[11–13]

1.5. Nanofibers as anti-bacterial agent

In the last two decades, applications of electrospun nanofibers are extended and nanofiber materials with diversified functionalities are introduced. The electrospun nanofibers incorporated with functional additives such as antibacterial agents have been fabricated for antimicrobial applications. These electrospun nanofibers show enhanced antimicrobial performance compared to traditional antimicrobial materials, and have a wide range of applications in filtration, wound-dressing materials, protective textiles, tissue scaffolds, and biomedical devices.[1,4,6,7,14–16]

References

(1) Bie, X.; Khan, M. Q.; Ullah, A.; Malik, S.; Kharaghani, D.; Duy, P. N.; Tamada, Y.; Kim, I. S. Fabrication and Characterization of Wound Dressings Containing Gentamicin/Silver for Wounds in Diabetes Mellitus Patients. *Mater. Res. Express* **2020**.

(2) Song, K.; Wu, Q.; Qi, Y.; Kärki, T. Electrospun Nanofibers with Antimicrobial Properties. *Electrospun Nanofibers* **2017**, No. October, 551–569. https://doi.org/10.1016/B978-0-08-100907-9.00020-9.

(3) Hashmi, M.; Ullah, S.; Kim, I. S. Electrospun Momordica Charantia Incorporated Polyvinyl Alcohol (PVA) Nanofibers for Antibacterial Applications. *Mater. Today Commun.* **2020**, 101161. https://doi.org/https://doi.org/10.1016/j.mtcomm.2020.101161.

(4) Hashmi, M.; Ullah, S.; Kim, I. S. Electrospun Momordica Charantia Incorporated Polyvinyl Alcohol (PVA) Nanofibers for Antibacterial Applications. *Mater. Today Commun.* **2020**, *24* (January), 101161. https://doi.org/10.1016/j.mtcomm.2020.101161.

(5) Ambekar, R. S.; Kandasubramanian, B. Advancements in Nanofibers for Wound Dressing: A Review. *Eur. Polym. J.* **2019**, *117* (May), 304–336. https://doi.org/10.1016/j.eurpolymj.2019.05.020.

(6) Bie, X.; Khan, M. Q.; Ullah, A.; Ullah, S.; Kharaghani, D.; Phan, D.-N.; Tamada, Y.; Kim, I. S. Fabrication and Characterization of Wound Dressings Containing Gentamicin/Silver for Wounds in Diabetes Mellitus Patients. *Mater. Res. Express* **2020**, *7* (4), 045004. https://doi.org/10.1088/2053-1591/ab8337.

(7) Ullah, S.; Hashmi, M.; Kharaghani, D.; Khan, M. Q.; Saito, Y.; Yamamoto, T.; Lee, J.; Kim, I. S. Antibacterial Properties of in Situ and Surface Functionalized Impregnation of Silver Sulfadiazine in Polyacrylonitrile Nanofiber Mats. *Int. J. Nanomedicine* **2019**, *14*, 2693–2703. https://doi.org/10.2147/IJN.S197665.

(8) Ullah, S.; Hashmi, M.; Khan, M. Q.; Kharaghani, D.; Saito, Y.; Yamamoto, T.; Kim, I. S. Silver Sulfadiazine Loaded Zein Nanofiber Mats as a Novel Wound Dressing. *RSC Adv.* **2019**, *9* (1), 268–277. https://doi.org/10.1039/C8RA09082C.

(9) Kajdič, S.; Planinšek, O.; Gašperlin, M.; Kocbek, P. Electrospun Nanofibers for Customized Drug-Delivery Systems. *J. Drug Deliv. Sci. Technol.* **2019**, *51* (March), 672–681. https://doi.org/10.1016/j.jddst.2019.03.038.

(10) Kharaghani, D.; Gitigard, P.; Ohtani, H.; Kim, K. O.; Ullah, S.; Saito, Y.; Khan, M. Q.; Kim, I. S. Design and Characterization of Dual Drug Delivery Based on In-Situ Assembled PVA/PAN Core-Shell Nanofibers for Wound Dressing Application. *Sci. Rep.* **2019**, *9* (1), 1–11. https://doi.org/10.1038/s41598-019-49132-x.

(11) Akduman, C.; Akcakoca Kumbasar, E. P. Nanofibers in Face Masks and Respirators to Provide Better Protection. *IOP Conf. Ser. Mater. Sci. Eng.* **2018**, *460* (1). https://doi.org/10.1088/1757-899X/460/1/012013.

(12) Ullah, S.; Ullah, A.; Lee, J.; Jeong, Y.; Hashmi, M.; Zhu, C.; Joo, K. Il; Cha, H. J.; Kim, I.-S. Reusability Comparison of Melt-Blown vs. Nanofiber Face Mask Filters for Use in the Coronavirus Pandemic. *ACS Appl. Nano Mater.* **2020**. https://doi.org/10.1021/acsanm.0c01562.

(13) Hashmi, M.; Ullah, S.; Kim, I. S. Copper Oxide (CuO) Loaded Polyacrylonitrile (PAN) Nanofiber Membranes for Antimicrobial Breath Mask Applications. *Curr. Res. Biotechnol.* **2019**, *1* (1), 1–10. https://doi.org/10.1016/j.crbiot.2019.07.001.

(14) Khan, M. Q.; Kharaghani, D.; Sanaullah; Shahzad, A.; Duy, N. P.; Hasegawa, Y.; Azeemullah; Lee, J.; Kim, I. S. Fabrication of Antibacterial Nanofibers Composites by Functionalizing the Surface of Cellulose Acetate Nanofibers. *ChemistrySelect* **2020**, *5* (4), 1315–1321. https://doi.org/10.1002/slct.201901106.

(15) Khan, M. Q.; Kharaghani, D.; Sanaullah; Shahzad, A.; Saito, Y.; Yamamoto, T.; Ogasawara, H.; Kim, I. S. Fabrication of Antibacterial Electrospun Cellulose Acetate/ Silver-Sulfadiazine Nanofibers Composites for Wound Dressings Applications. *Polym. Test.* **2019**, *74* (December), 39–44. https://doi.org/10.1016/j.polymertesting.2018.12.015.

(16) Ullah, A.; Ullah, S.; Khan, M. Q.; Hashmi, M.; Nam, P. D.; Kato, Y.; Tamada, Y.; Kim, I. S. Manuka Honey Incorporated Cellulose Acetate Nanofibrous Mats: Fabrication and in Vitro Evaluation as a Potential Wound Dressing. *Int. J. Biol. Macromol.* **2020**, *155*, 479–489.

https://doi.org/10.1016/j.ijbiomac.2020.03.237.

Chapter 2

Copper Oxide (CuO) loaded polyacrylonitrile (PAN) nanofiber membranes for antimicrobial breath mask applications

2 Introduction

Water and air pollution are two main areas of concerns of modern science and technology. Development in technology especially industrial revolution has changed life style of human being extremely positive but on other hand it has imparted a few negative impacts too, and one the most effected field is health. Meanwhile biotechnology is also improved to overcome the lethal diseases but still a lot of work is to be done by researchers. It is stated in literature that about 60% of total nanofibers production is used for biomedical purpose only. It can be wound air filtration [1], water purification, drug delivery, tumor therapy, or implants [2]–[5].

Polyacrylonitrile (PAN) is synthetic polymer having white color, hydrophobicity, and semi-crystalline structure. The chemical formula of PAN is C_3H_3N. PAN is among few polymers which synthesized in early 20^{th} century. PAN is thermally stable polymer usually degrades over 300℃ [6]. PAN nanofibers fibers of diameter less than 1 micrometer were prepared early 1970s, study also included the influence of flow rate on final properties of fibers [7]. PAN and polyaniline both are hydrophobic polymer, so combining the hydrophobicity of PAN and polyaniline super hydrophobic nonwoven webs were electrospun which were reversible to hydrophilicity in a short time [8]. AgNPs have been widely used with different polymers for antibacterial applications. Dependence of size of AgNPs was also studied by adding TiO_2 in PAN nanofiber mats [9]. PAN nonwoven webs for hydrolysis of soybean oil were also successfully characterized and it was concluded that PAN webs are suitable as a membrane for hydrolysis process [10]. Production of biodiesel from soybean oil was also studied by using PAN membranes immobilized with lipase (similar technique as for hydrolysis of soybean oil) [11]. PAN is an emerging material for healthcare applications such as skin care, wound dressing, and others as well. Vitamins (C & E) extracts have been incorporated with PAN nanofiber mats for skin care using core and shell nanofiber production method [12]. Surface modification of PAN/PVDF nonwoven webs for water treatment application was also done using plasma treatment (at low vacuum conditions). [13] PAN nanofibers are not only useful in medical applications but these cover other fields of science as well. Surface modified PAN nanofibers have been also used as substrate for identification

of small molecules by Surface Enhanced Raman Scattering (SERS) [14]. PAN nanofibers, incorporation with antibacterial agents especially metallic nanoparticles,[15], [16] have been useful in a number of applications like air filters and mask,[17] membranes for water purification, wound care, tissue engineering, hydrolysis, and others[3], [18]–[24]. Copper nanoparticles have potential for antibacterial applications. Copper nanoparticles have been used as antimicrobial agent for breath mask and 2nd degree burn management.[15]

Electrospinning is not new technology in nonwoven production system but it is still one of simple and easiest production technique being used for non-woven textiles. Electrospun nanofibers have major applications in antibacterial food packaging [25]–[28], biomedical, environmental, and electronics industries [3], [18], [19], [29]–[32].

Our research is mainly focused on utilization of copper oxide for antibacterial applications. Copper (II) oxide is one the two stable oxides of copper. It is hydrophilic and has potential applications in magnetic storage. We have used copper oxide nanoparticles for the first time for antimicrobial breath mask applications. Our research is unique as we considered all possible parameters which are required for production of copper oxide nanoparticles loaded nonwoven webs on commercial scale.

2.1 Experimental work

2.1.1 Materials

Polyacrylonitrile in powder form with average molecular weight 150,000 was purchased from the Sigma-Aldrich Corporation (Saint Louis, MO 63103, USA). N, N-Dimethylformamide (DMF) was purchased from FUJIFILM Wako Pure Chemical Corporation (Osaka, Japan). Copper (II) Oxide (nanopowder, <50 nm particle size) was purchased from Sigma-Aldrich Corporation (Saint Louis, MO 63103, USA). Distilled water was used from laboratory.

2.1.2 Method

PAN (8% by weight) was dissolved in DMF. Solution was kept on stirring for 12 hours at room temperature (25±3°C) and copper oxide was added and solution was kept on further stirring for 4 hours. Solution was then loaded to electrospinning for nanofiber production. Electrospinning conditions were as follows: syringe capacity 20ml, nozzle diameter 0.5 mm, Voltage was fixed on 13kv, distance between nozzle and collector

drum was kept on 14cm, and flow rate of solution was 0.5ml/h. Electrospinning conditions were kept same for all samples.

Table 1 Samples concentrations and codes

Serial No.	Weight proportions	Sample Codes
S 1	PAN 100%, CuO 0%	PAN
S 2	PAN 99.75%, CuO 0.25%	0.25% CuO
S 3	PAN 99.50%, CuO 0.50%	0.50% CuO
S 4	PAN 99.25%, CuO 0.75%	0.75% CuO
S 5	PAN 99.00%, CuO 1.00%	1.00% CuO

2.2 Characterizations

Disk diffusion method was adopted for assessment of antibacterial activity of prepared samples. *E-Coli and B. Subtilis* bacteria stains were associated for gram negative and gram positive bacteria stains respectively. Round disks of samples having 8mm diameter were placed in cultured plates (for each type of bacteria stains) and incubated for 12 hours at 37℃ temperature. Drug release (Cu release from PAN nanofibers) was monitored by inductively coupled plasma (ICP) atomic emission spectrometer (SHIMADZU/ICPS, 10000IV, Japan). Scanning Electron Microscope (SEM), *JSM-5300, JEOL Ltd, Japan*, accelerated with 15kV voltage, was used for assessment of morphological properties of neat PAN and PAN/CuO nanofibers. Diameter of prepared nanofibers was measured by taking of average of 50 random readings using Image J software. FTIR (ATR Prestige-21, Shimadzu, Japan) was used to assess chemical reactivity between PAN and CuO. ATR fingerprints were taken from wave number 400 cm^{-1} to 4000 cm^{-1}. Crystal structure was evaluated by Wide angle X-ray diffractions (WAXRD) spectra. XRD spectra were taken at 25℃ using Rotaflex RT300 mA, Rigaku, Osaka, Japan, with angular angle ranging $5 \leq 2\theta \leq 80°$, and measurements were taken by Nickel-filtered Cu. Ka radiation. Thermal degradability of PAN and PAN/CuO nanofibers was evaluated by using thermo-plus TG 8120, Rigaku Corporation, Osaka, Japan. TGA test was performed in static mode under air atmosphere and heating rate of 10 ℃/min. Temperature range was set 0–500℃ using aluminum pans. Hydrophilicity was assessed by water contact angle test using contact angle analyzer (Digidrop, GBX, Whitestone way, France). Elemental composition was analyzed by X-

ray photoelectron spectroscopy (XPS), *Shimadzu-Kratos AXIS-ULTRA HAS SV*, Shimadzu, Kyoto, Japan. Mechanical properties of PAN and PAN/CuO nanofibers were evaluated by using Universal Testing Machine (UTM), Tesilon RTC 250A; A&D Company Ltd., Japan. Five specimens for each model were prepared were prepared following ISO 13634 standard and test was performed under a crosshead speed of 5 mm/min and room temperature. Mechanical properties i.e. Tensile Stress, Tensile strain, and Young's modulus were extracted from UTM data by the following equations (1), (2), and (3) respectively.

$$\varepsilon = \frac{\Delta l}{l} \quad \text{..... Equation 1}$$

$$\sigma = \frac{F}{A} \quad \text{.....Equation 2}$$

$$E = \frac{\sigma}{\varepsilon} \quad \text{..... Equation 3}$$

Where $\varepsilon, \sigma,$ and E are strain, stress, and Young's modulus. Δl is change in length, l is original length of specimen, F is applied force, and A is cross sectional area of specimen. Air permeability test was performed using Air Permeability Tester Kato Tech Co., Ltd. Breathability test was performed using upright cup method (A-2) for breathability measurement. Samples were prepared following ASTM E96. Surface area and pore size distribution of prepared nanofiber mats were measured by Brunauer-Emmett-Teller (BET), (SHIMADZU Tri star II 3020, Japan) using nitrogen adsorption method.

2.3 Results & discussions

2.3.1 Morphological properties

Morphological properties of prepared nanofiber mats were observed by SEM analysis. It can be seen in figure 2.1that prepared nanofibers are bead-free. All nanofiber mats had uniform morphology as well. It means that addition of CuO nanoparticles did not cause any beads formation or non-uniformity in PAN nanofibers.

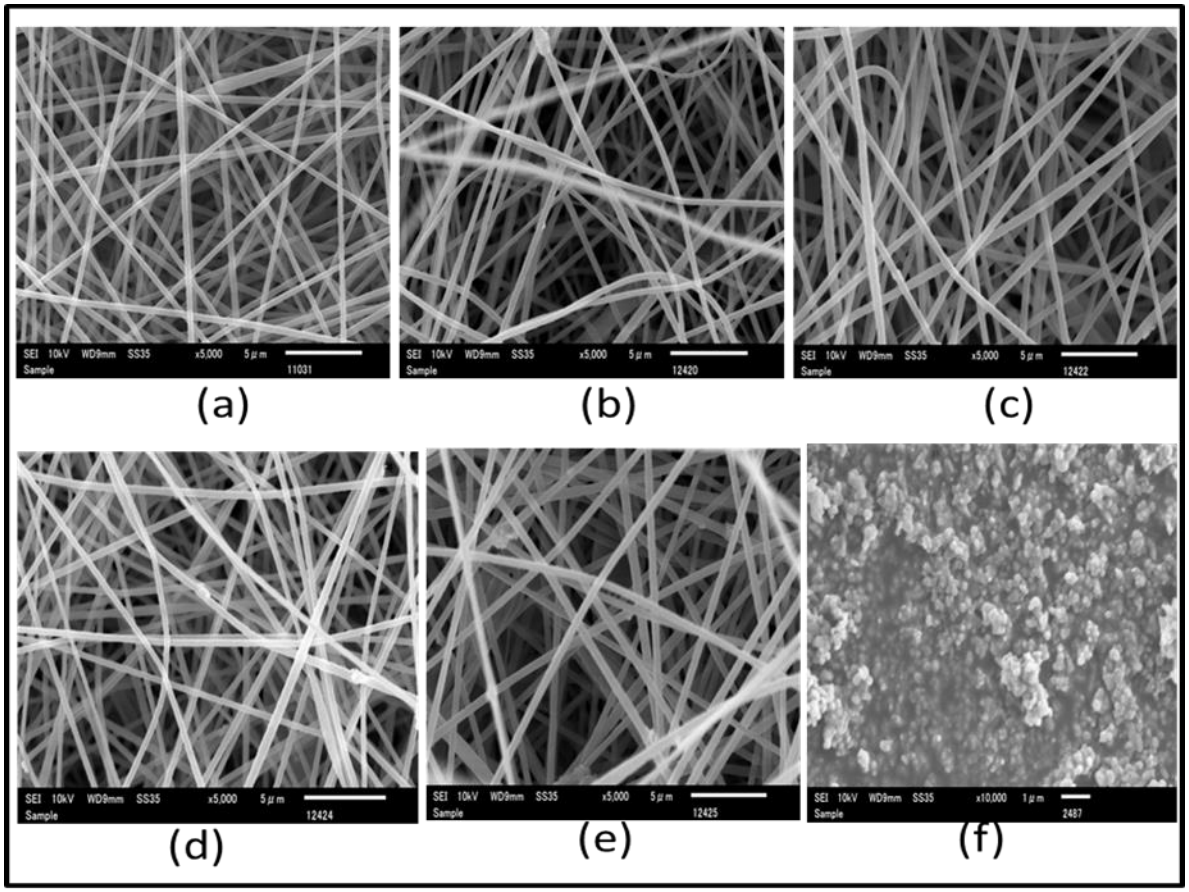

Figure 2.1 SEM images of (a) PAN nanofibers, (b) 0.25% CuO, (c) 0.50% CuO, (d) 0.75% CuO, (e) 1.00% CuO in PAN nanofibers, and (f) CuO nanoparticles

Figure2.1 (f) represents morphology of copper oxide nanoparticles. It was observed that copper nanoparticles were of spherical shape with an average diameter of 37±9 nm. Spherical shape of copper oxide nanoparticles helps to boost antibacterial activity as it provides higher surface area as compared to that of nano-rods or other shapes. Dispersion of spherical nanoparticles is uniform which also exhibited a uniform and smooth release from PAN nanofibers.

2.3.2 Diameter interpretation

Figure 2.2 shows the average diameters of pure PAN nanofibers and PAN nanofibers with varying concentration of copper oxide. Slight increment in diameters of nanofibers with increasing concentrations of copper oxide was observed for all samples. It is fact that addition of nanoparticles especially metallic nanoparticles causes increase in diameter of nanofibers. Average diameter of pure PAN nanofiber was 141nm while PAN nanofibers having 0.25%, 0.50%, 0.75%, 1.00% copper oxide exhibited diameters of 161nm, 169nm, 184nm, 197nm respectively.

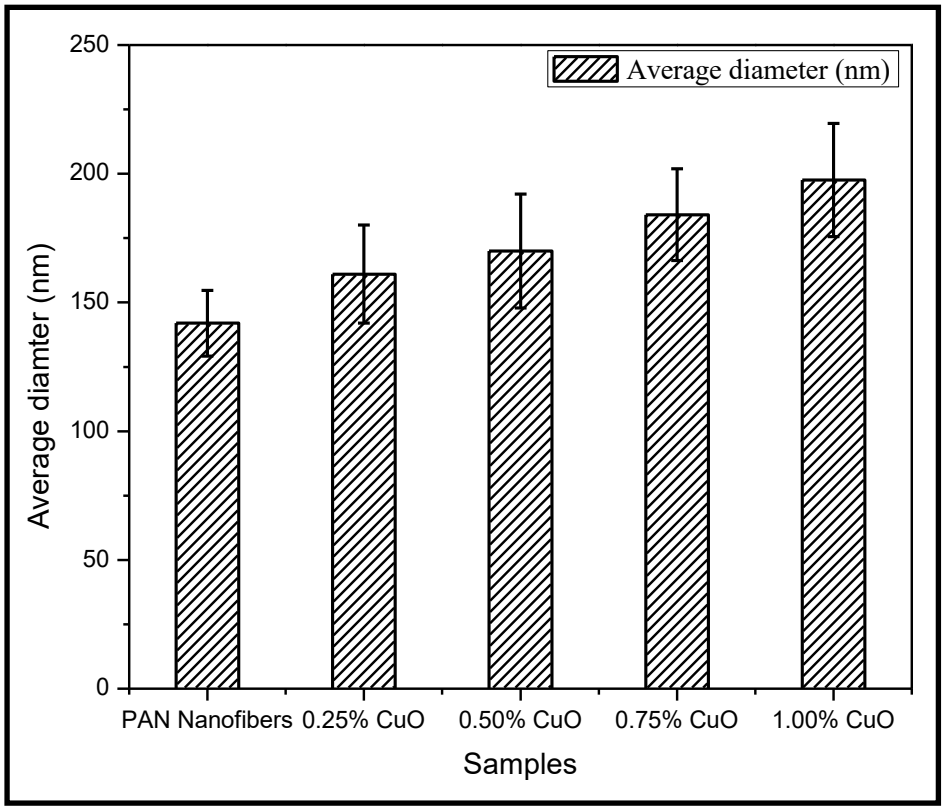

Figure 2.2 Average diameters of PAN/CuO nanofibers

2.3.3 EDX analysis

EDX analysis was done to confirm availability copper oxide encapsulated within PAN nanofibers. It was observed that Cu and O peaks were prominent in all samples having copper oxide content in nanofiber mats. In figure 2.3 it can be observed that higher counts were found in specimen having higher concentration of copper oxide and vice versa. These values are not exact representation of copper oxide added in sample but these values represented direct relation of copper oxide in the nanofibers. Exact concentrations of CuO nanoparticles in PAN nanofibers are shown in figure 2.3.

.

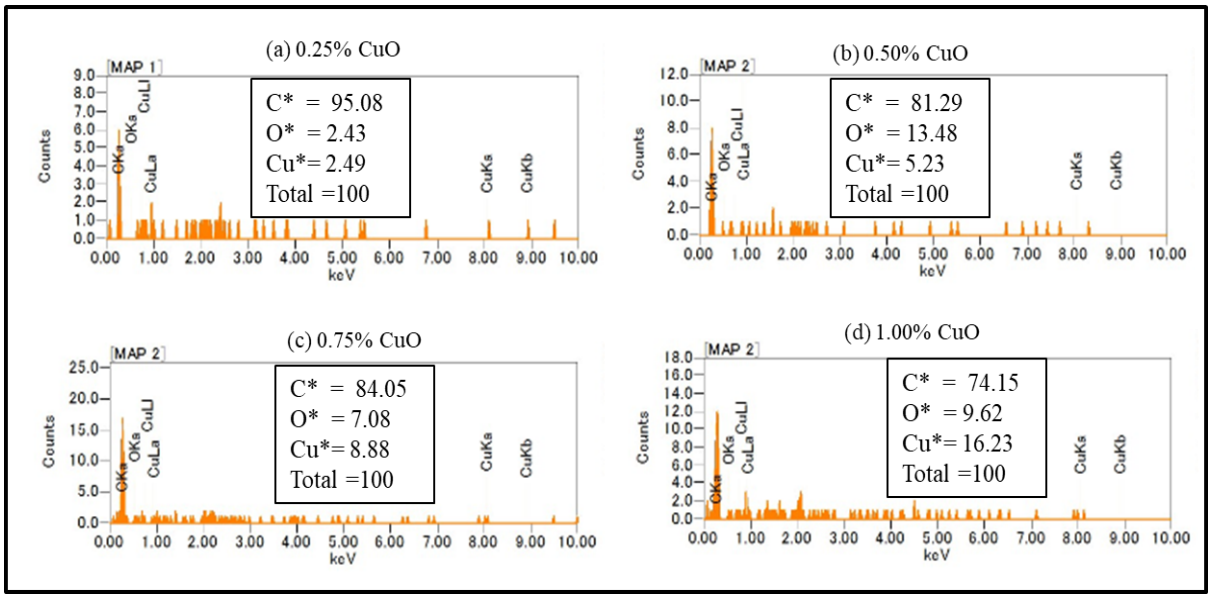

Figure 2.3 EDX analysis of PAN/CuO nanofibers (composition insight)

2.3.4 X-Ray diffraction (XRD)

XRD was done to confirm crystalline structure of nanofiber mats. Pure PAN nanofibers (4) showed a sharp peak at 2θ = 17˚, and a small peak at 2θ = 30˚.while PAN did not exhibit any peak up to 2θ = 80˚. PAN nanofibers showed characteristic peaks of pure PAN. First peak (17˚) could be associated with hexagonal lattice of PAN. It was observed that characteristic peak of PAN was decreased after addition of copper oxide in to PAN nanofibers which clears that crystallinity of pure PAN was decreased and hexagonal lattice of PAN was broken meanwhile CuO exhibited its characteristic peaks at 2θ = 36˚ and 2θ = 38˚, interestingly peaks intensity was increased with increasing copper oxide concentration in PAN nanofibers. Occurrence of CuO characteristic peaks imparted crystallinity to PAN/CuO nanofiber mats. It was also observed by tensile test that tensile strength of PAN/CuO nanofibers was increased with increasing amount of CuO in PAN nanofibers. Tensile strength has direct relation with crystallinity of polymers.

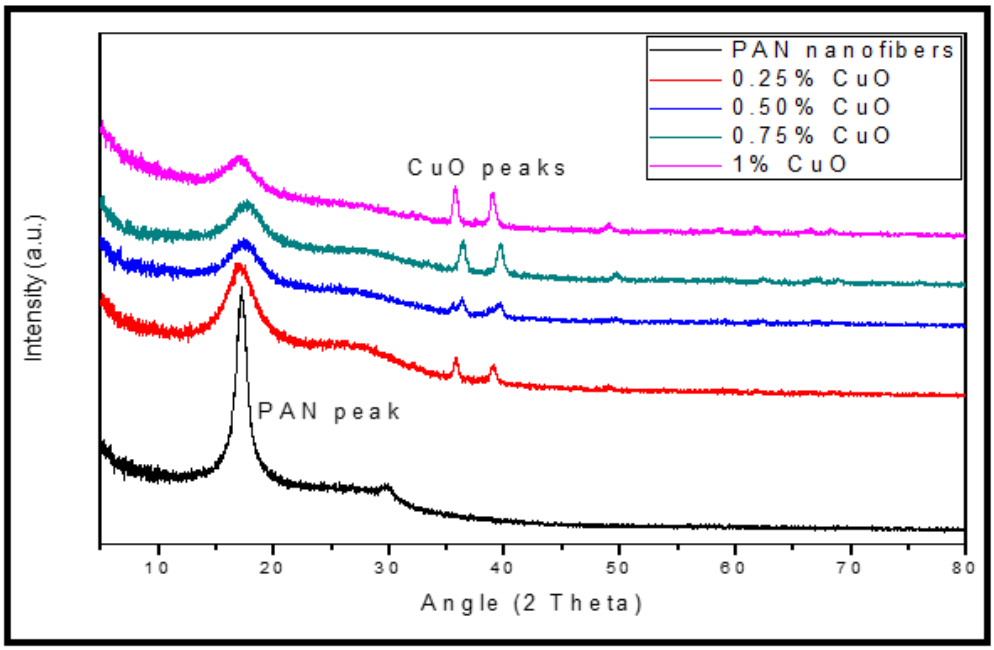

Figure 2. 4 XRD analysis of PAN/CuO nanofibers

2.3.5 XPS analysis

Elemental analysis was done by X-ray photoelectron spectroscopic study. Presence of copper oxide (CuO) was observed. As copper oxide consists of two elements copper and oxygen so XPS spectra for Cu 2p, Cu 3p, and O 2s was obtained. Figure 2.5 shows spectra of PAN/CuO nanofibers. It can be observed in Figure (a) that all samples exhibited O 2s peak at binding energy of 25eV, and intensity of peak was in increasing trend with increasing concentration of CuO in PAN nanofibers. Figure 2.5 (b) shows Cu 2p characteristic peaks at binding energies 934eV and 955eV with gap of 21eV, while Cu 3p characteristic peak was found at binding energy of 75eV. Intensities of Cu characteristic peaks were also in increasing trend with increasing concentration of CuO in PAN nanofibers. Figure 2.5(d) represents XPS spectra of pure PAN nanofibers. PAN was characterized for its basic characteristic elements C, N, and O. it can be shown in XPS spectra that PAN nanofibers exhibited C-1s peak at binding energy 290 eV, N-1s at 400 eV, and O-1s at 550 eV. It can be also observed that carbon peak is sharp and possess higher intensity as compared to oxygen and nitrogen peaks, which is clear indication of chemical composition of PAN, as PAN contains about 80% carbon of its total chemical composition. Atomic composition of PAN was precisely described by Bing Cao et al [33]

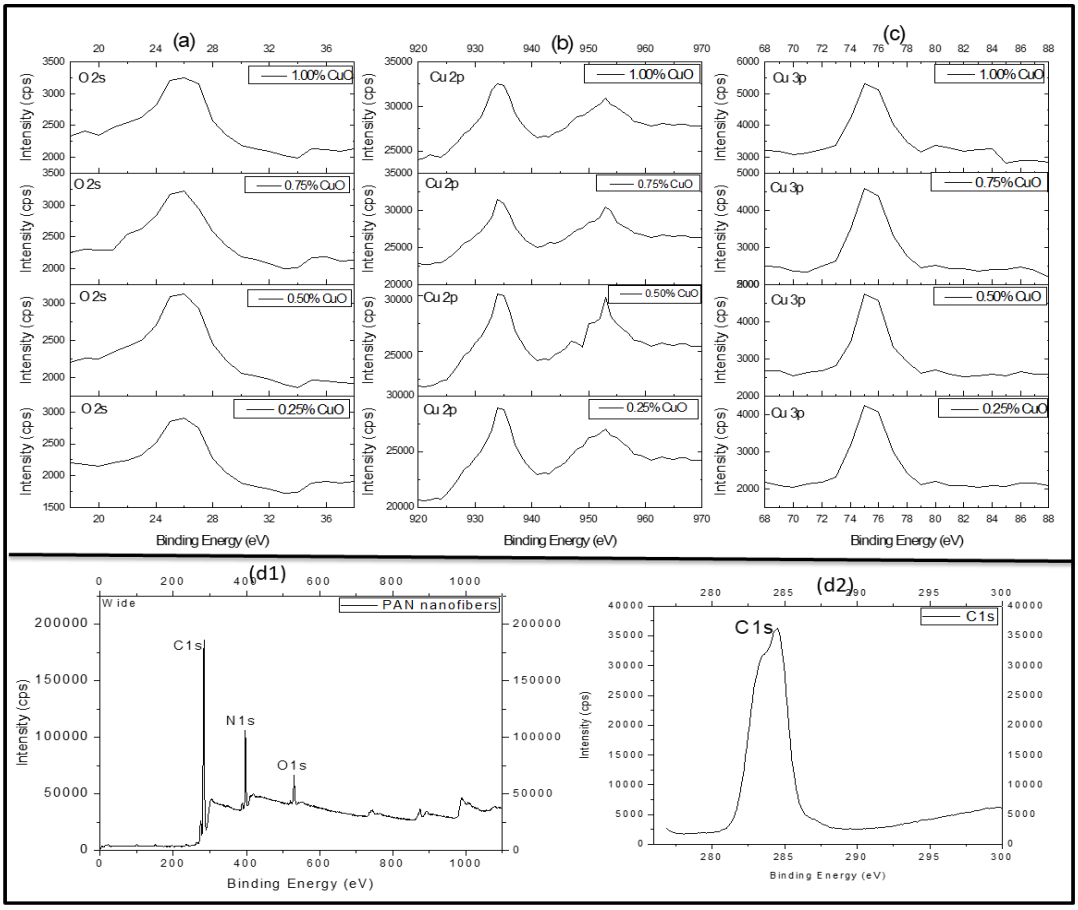

Figure 2.5 XPS analysis of PAN/CuO nanofibers

2.3.6 Mechanical properties

Mechanical properties of PAN/CuO nanofibers was analyzed by universal testing machine. Tensile strength, elongation at break, and tensile modulus were calculated from stress strain data. It can be observed in 6 that neat PAN nanofiber mats presented tensile strength of 4.00 MPa. Prominent increment in tensile strength PAN/CuO nanofibers was observed. Tensile strength of 0.25% CuO, 0.50% CuO, 0.75% CuO, 1.00% CuO were 5.50 MPa, 6.98 MPa, 7.28 MPa, and 8.43 MPa respectively which is clear indication that addition of metallic nanoparticles imparted tensile strength to the nanofiber mats. By XPS study it was also concluded that overall crystallinity of PAN/CuO nanofibers was increased by addition of CuO nanoparticles. Elongation at break was slightly decreased by addition of copper oxide nanoparticles up to lower concentration (0.75% CuO), but it was observed that elongation of sample having 1.00% CuO was almost same as that of neat PAN nanofiber mats. Figure 2.6 represents trend of tensile strength (with standard deviation) by addition of copper oxide. It can be concluded that tensile strength has direct and linear relationship with copper oxide concentration in PAN nanofibers.

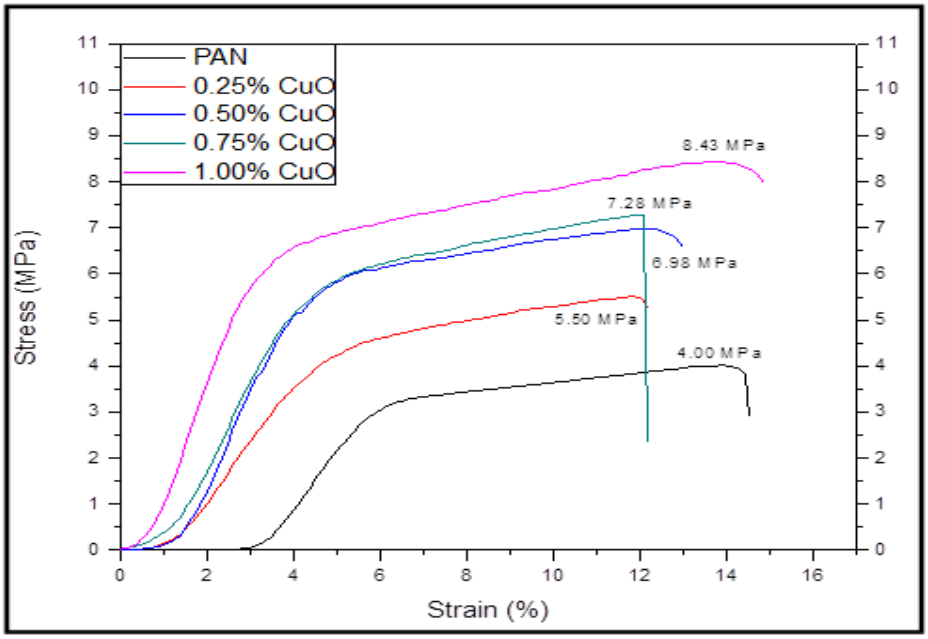

Figure 2.6 Stress - Strain plot of neat PAN and PAN/CuO nanofibers

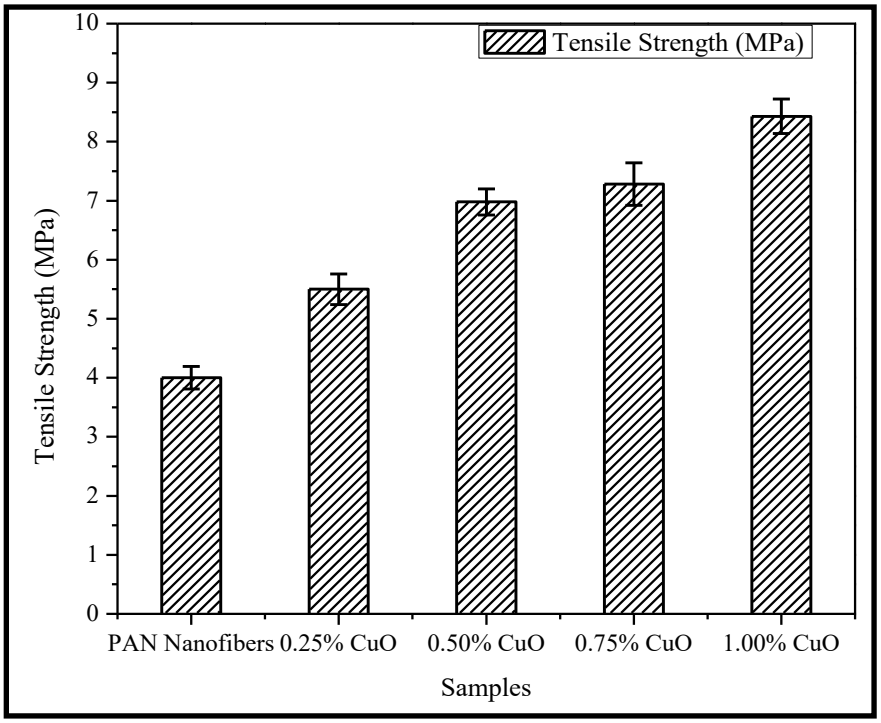

Figure 2.7 Interpretation of tensile strength of PAN and PAN/CuO nanofibers

2.3.7 Thermal analysis

Behavior of material under thermal circumstances was confirmed by thermal gravimetric analysis. TGA graph is usually divided in three major zones. 1st zone of graph is limited to 100°C which represents removal of moisture or low boiling impurities. In Figure 2.8 it can be observed that all specimen exhibited almost similar trend up to 100°C which shows that there was not any moisture uptake by the samples. 2nd zone represents thermal degradation zone which is considered significant part of TGA graph. It can be observed in graph that onset of all specimen is in the range of 290 to 340 degree Celsius. Onset temperatures for samples having higher concentration of copper oxide was gradually decreased with increasing copper oxide content. It is fact that PAN is thermally stable polymer (as studied by H. Onishi et al) [34] so it represented the same trend but addition of copper oxide made it low thermally stable and combustion zone (3rd zone of graph) for PAN/CuO started over 340°C. Residual content for PAN/CuO nanofiber samples reached lowest value around 400°C having higher concentration of copper oxide. Evaluating the TGA graph, it can be concluded that copper oxide lowered thermal stability of PAN nanofibers but still stable enough to be used for environmental or biomedical engineering.

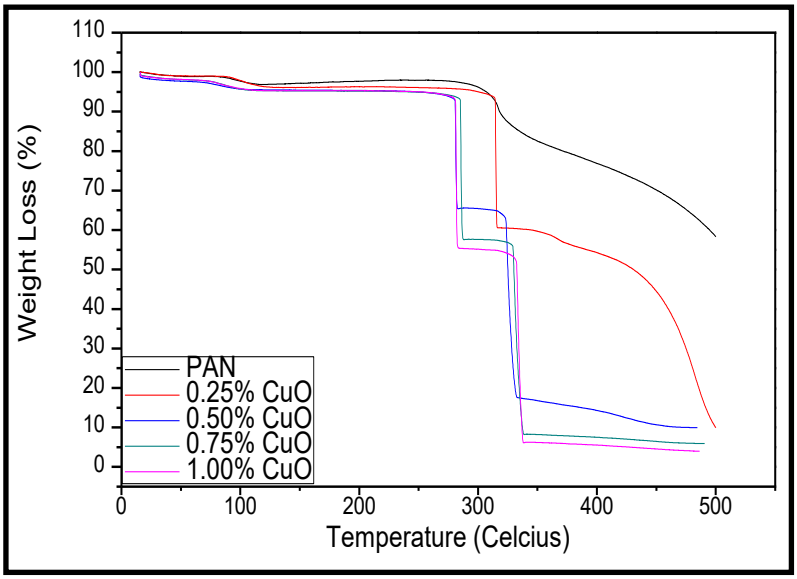

Figure 2.8 Thermal degradation analysis (TGA Plot) of PAN and PAN/CuO nanofiber

2.3.8 Air permeability test

Air permeability of prepared nanofiber mats was analyzed to check the effect of CuO loading in PAN

nanofibers. Figure 2.9 shows the air resistivity which was exhibited by prepared specimen. PAN nanofibers showed higher resistance to air flow while samples having CuO were less resistant against air flow. Values of air resistivity (R) of PAN, 0.25% CuO, 0.50% CuO, 0.75% CuO, 1.00% CuO were 24.05, 23.13, 17.69, 14.38, and 10.08 respectively. It may be due to compact and dense structure of neat PAN nanofibers while presence of copper oxide increased porosity of nanofiber mats that's why air flow was increased. As our target application is air filter/ breath mask, lower air resistance is supportive tool for PAN/CuO nanofibers for such applications.

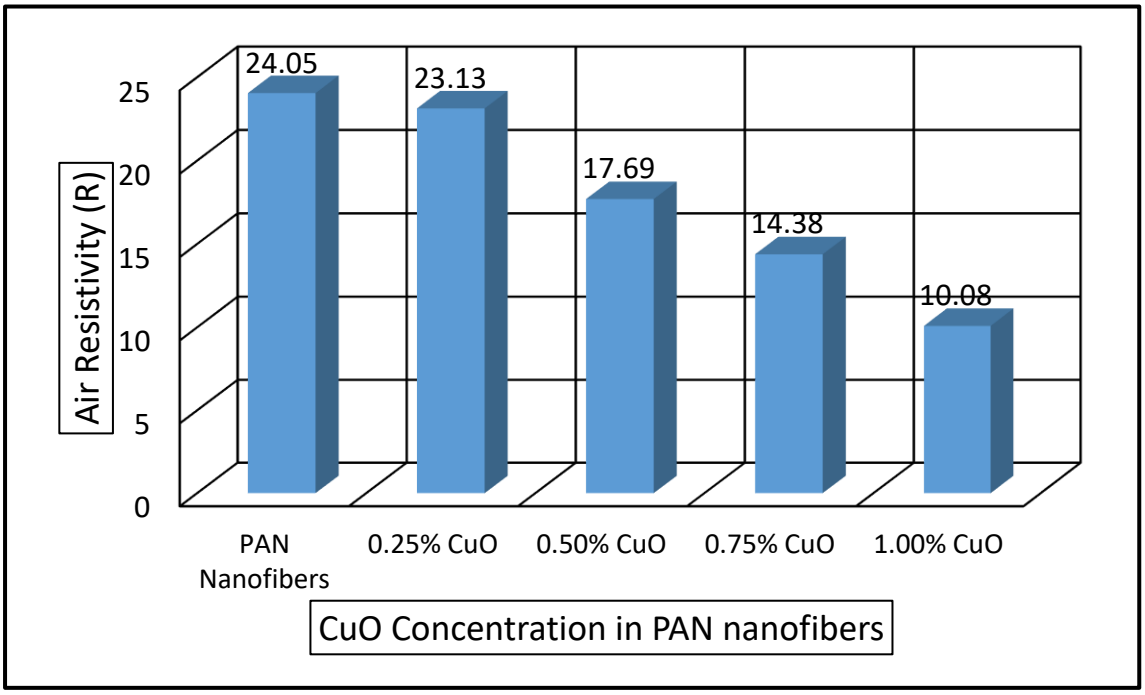

Figure 2.9 Air permeability of PAN and PAN/CuO nanofiber mats

2.3.9 BET surface area & pore size distribution

BET surface area and average pore diameter of prepared nanofiber specimen were analyzed by nitrogen adsorption method. 1 gram of each specimen was filled in a standard bulb with internal diameter of 3/8 inches. All samples were degassed using degasser accessory (Helium gas was used for degassing of samples). Figure 2.10 represents quantity of nitrogen adsorption with respect to relative pressure. It can be observed that adsorption of nitrogen increased with increasing concentration of copper oxide nanoparticles in PAN nanofibers. Figure 3D view, and Figure (2D view) show nitrogen adsorption for neat PAN nanofiber mat,

0.25% CuO, 0.50% CuO, 0.75% CuO, and 1.00% CuO were 11 cm^3/g STP, 44 cm^3/g STP, 53 cm^3/g STP, 58 cm^3/g STP, and 69 cm^3/g STP. Table 2 shows surface area of specimen. Surface area of prepared specimen was found to be directly proportional to the concentration of copper oxide in PAN nanofibers. Usually PAN nanofibers have low surface area, it also reflected in our test result as neat PAN nanofibers showed 8.09 ± 0.012 m^2/g. nanofiber mats containing copper oxide presented higher surface areas as compared to that of neat NBR nanofibers. Specimen 0.25% CuO, 0.50% CuO, 0.75% CuO, and 1.00% CuO had surface areas of 11.58 ± 0.0076 m^2/g, 14.05 ± 0.0091 m^2/g, 17.99 ± 0.010 m^2/g, and 20.63 ± 0.087 m^2/g respectively. Average pore size of neat PAN nanofibers, 0.25% CuO, 0.50% CuO, 0.75% CuO, and 1.00% CuO was 18.44 Å, 19.24 Å, 17.39 Å, 18.02 Å, and 17.54 Å respectively.

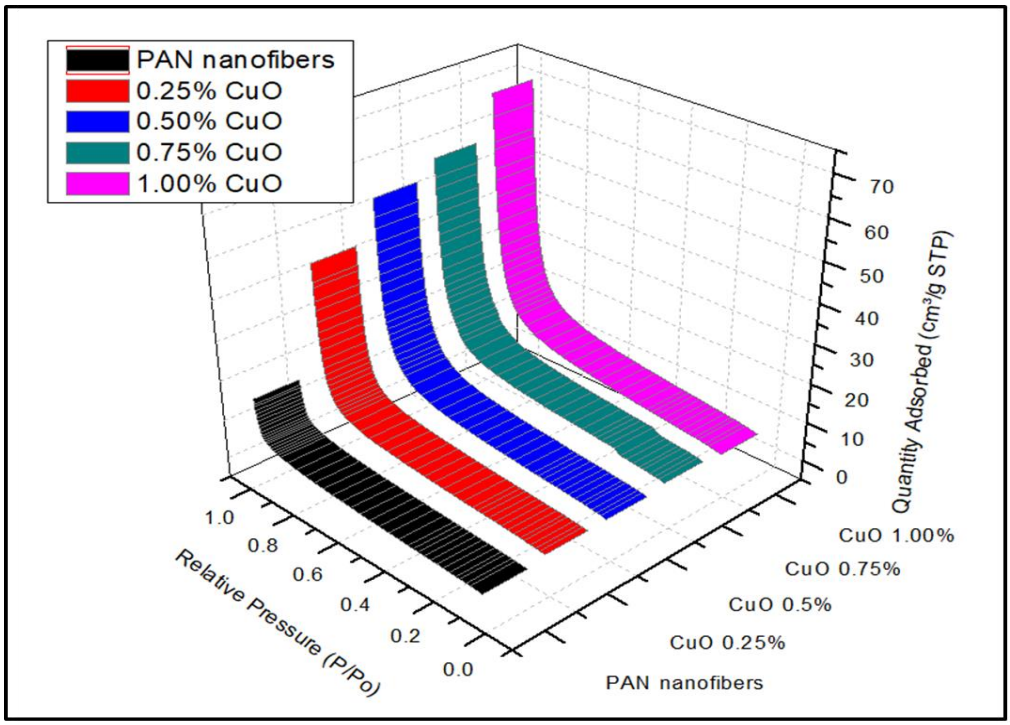

Figure 2.10 Plot of relative pressure vs quantity of nitrogen gas adsorbed by PAN/CuO nanofibers

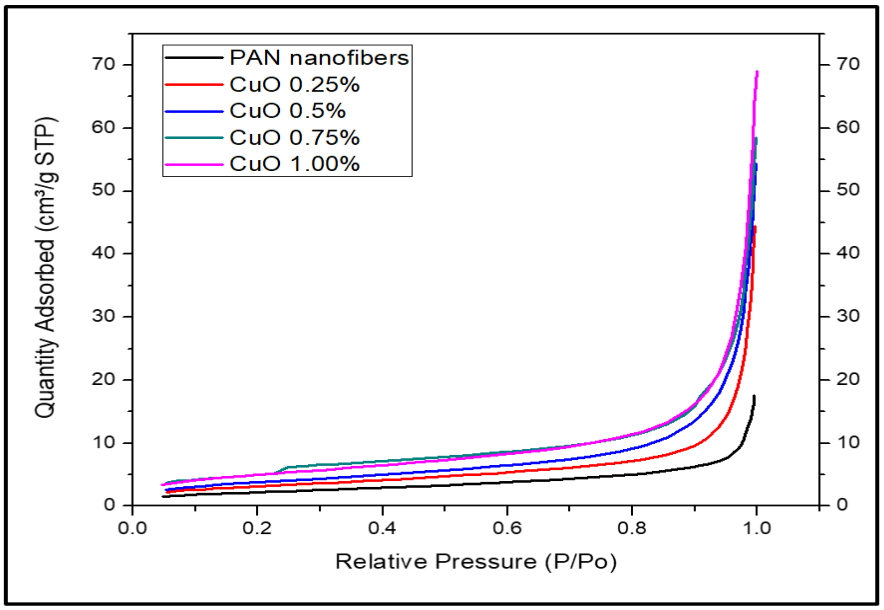

Figure 2.11 BET surface area and porosity study using nitrogen adsorption method

	PAN Nanofibers	0.25% CuO	0.50% CuO	0.75% CuO	1.00% CuO
BET Surface Area (m^2/g)	8.09±0.012	11.58±0.0076	14.05±0.0091	17.99±0.010	20.63±0.087
Average Pore Diameter (Å)	18.44	19.24	17.39	18.02	17.54

Table 2 BET surface area and average pore diameters of PAN and PAN/CuO nanofibers

2.3.10 Breathability test

Breathability test was performed by upright cup method. Round shaped samples having diamter of 6 cm were cut for each specimen. Test was performed according to ASTM E96 at 40°C and 50% humidity level. A cup was filled with warm water (40°C) to a certain level and samples were placed open side of cup and fixed with bolts. Samples were gripped strongly to avoid any leakage. Weight of all cups (with samples and water) was noted down, and samples were placed in controlled chamber. Weight change was noted after 24 hours and moisture intake of nanofibers was calculted from values of initial and final weights of samples. It was observed that water uptake was increased in samples having higher concentrations of copper oxide as compared to that of neat PAN nanofiber mat. Figure 2.12 represents graphical interpretation of water uptake values of all specimen. It can be observed that values of water uptake for neat PAN, 0.25% CuO, 0.50% CuO, 0.75% CuO, and 1.00% CuO were 4729 gr/m^2/day, 5163 gr/m^2/day, 5708 gr/m^2/day, 6497 gr/m^2/day, and 6839 gr/m^2/day. It was concluded that nanofiber based nonwoven webs presented medium performance, and breathability was improved with addition of copper oxide nanoparticles.

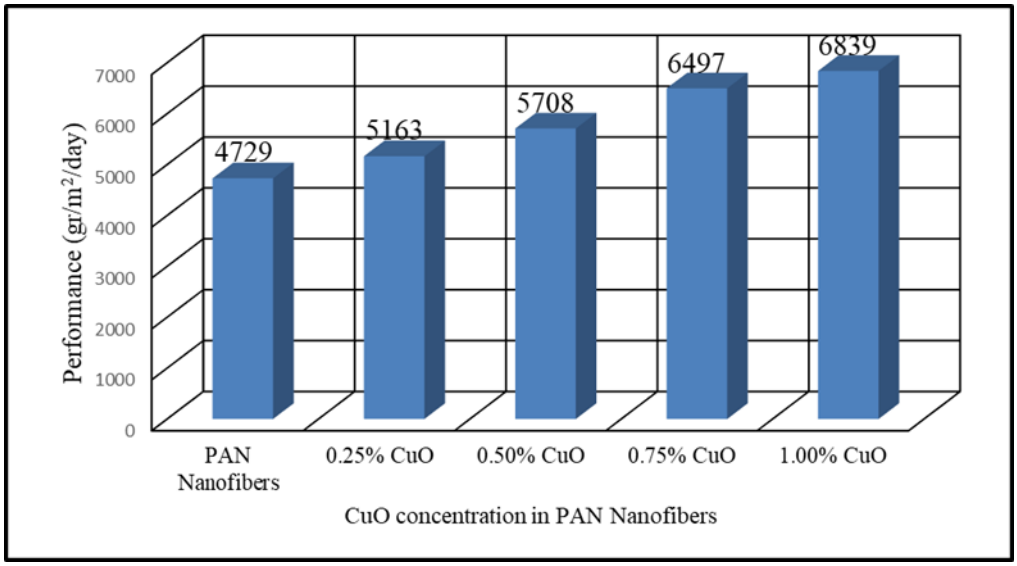

Figure 2.12 Breathability performance using upright cup method

2.3.11 Water contact angle

Hydrophilicity of neat PAN and PAN/CuO nanofibers was analyzed by water contact angle measurement. PAN is hydrophobic in nature but PAN nanofibers vary from hydrophobic to hydrophilic depending upon the percentage of PAN in electrospinning solution. It can be observed in that water contact angle for neat PAN nanofiber is 124° which reflected hydrophobic nature of pure PAN, while contact angle became smaller

as concentration of copper oxide increased in PAN nanofibers. Values of contact angles for 0.25% CuO, 0.50% CuO, 0.75% CuO, and 1.00% CuO were 78°, 57°, 3°, and 0° respectively. Water contact angle for samples having 1.00& CuO took less than 3 seconds to reach 0°. It can be concluded that addition of copper oxide imparted hydrophilicity to PAN nanofiber mats.

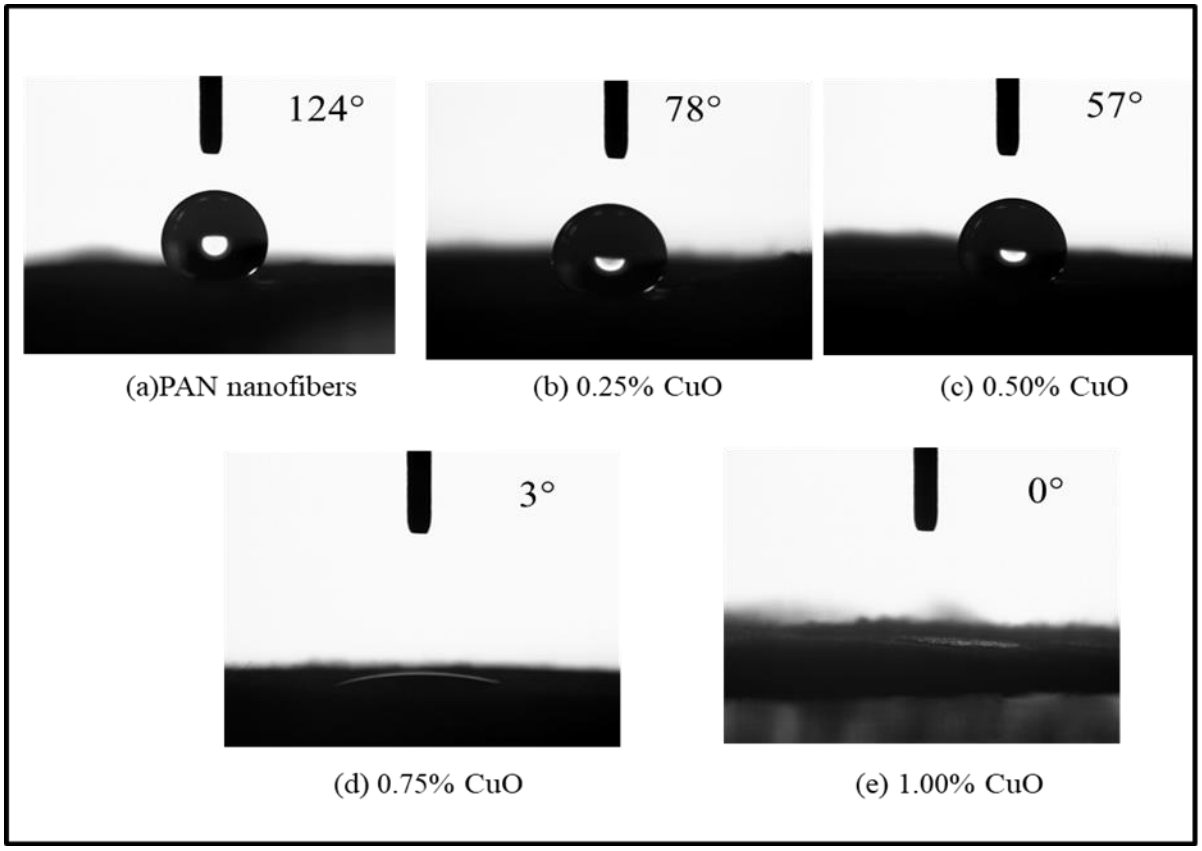

Figure 2.13 Analysis of hydrophilicity by water contact angle test

2.3.12 Antibacterial activity test

Antimicrobial properties was investigated using disk diffusion method. As shown in figure 2.14 (A) *E-Coli, (B) B. Subtilis.* B. Subtilis and E-Coli bacteria stains were associated for gram-positive bacteria stain and gram-negative bacteria stain respectively. The effectiveness of Cu released from PAN nanofibers was determined from the zone inhibition of the bacteria. The zone inhibition by antibacterial activity of both stains was compared with control. In figure 2.14 it can be observed that inhibition zone was gradually increased with increasing concentration of CuO in PAN nanofibers. It can be also observed that copper oxide was effective for both type (gram positive and gram negative) of bacteria which represented excellent antimicrobial feature of copper oxide. Excellent antibacterial efficacy was observed for samples with 1.00%

CuO concentration, while sample having lower concentration of CuO also showed consistent results as compared to that of control for both types of bacteria.

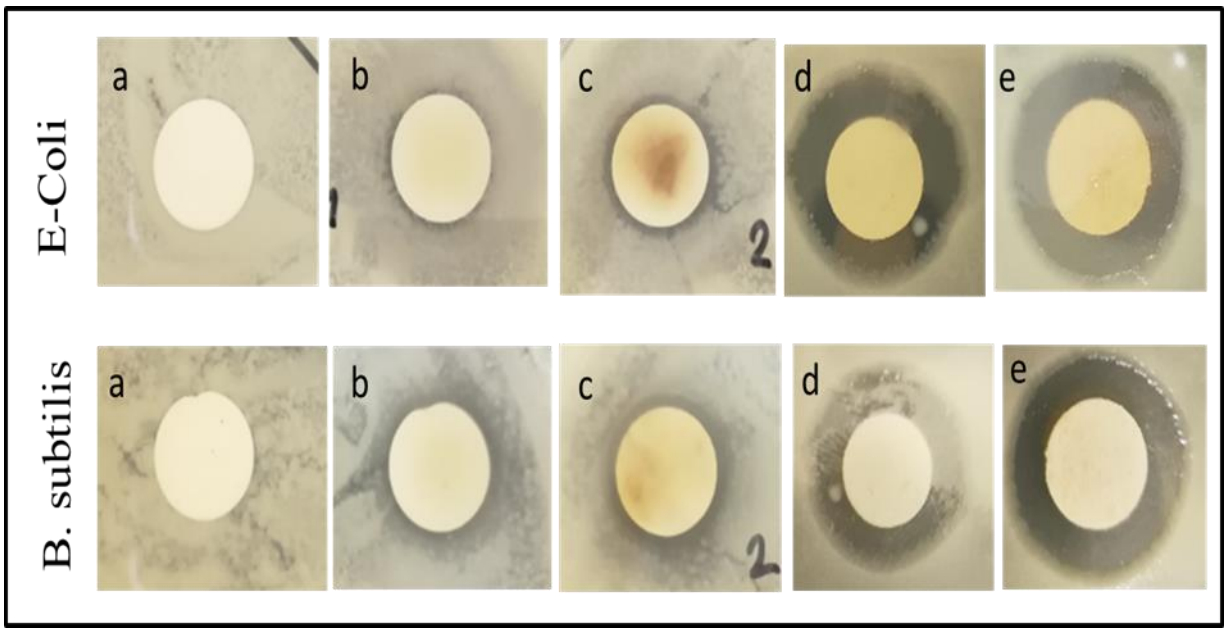

Figure 2.14 Antimicrobial activity test by disk diffusion method (for gram negative and gram positive stains)

2.3.13 Release properties

Effectiveness of antimicrobial activity was also confirmed by monitoring drug release from PAN nanofibers. In order to investigate Cu nanoparticles release, 0.02 g of PAN/CuO nanofibers was dissolved in copper sulphate ($CuSO_4$) as standard samples. 1 gram of each sample was soaked in 50 ml of deionized water for 72 hours. 1 ml of each sample was taken after 30min, 1h, 2h, 4h, 8h, 24h, 48h, and 72h.

Figure 2.15 shows that Cu release from 0.25% CuO, 0.50% CuO, 0.75% CuO, and 1.00% CuO were 5.51 ppm, 12.97 ppm, 21.12 ppm, and 33.98 ppm after 72h. It was also observed that PAN/CuO nanofibers were not dissolved in water even after 72 hours, and nanofiber structure was retained. Released quantity of Cu from nanofibers was observed to be directly proportional to the concentration of CuO in PAN nanofibers.

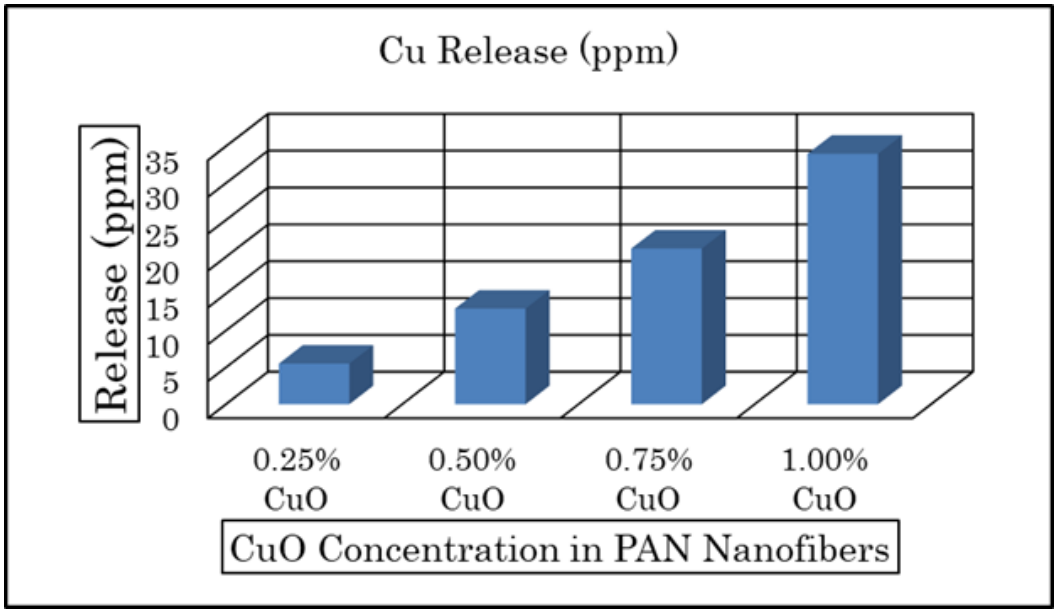

Figure 2.15 Investigation of drug release using ICP

2.3.14 Toxicity test

Toxicity test was performed to confirm the toxic effect of released CuO on human body in case of direct inhaling. 15 round specimen of diameter 3mm were cut for each sample and all specimen were sterilized by washing with 70% ethanol and Phosphate buffered saline (PBS) reagent. Using clean bench, Cells (NIH3T3) were cultured in trypsin reagent. Sterilized samples were placed in 96 well microplate (microplate was also sterilized prior to use). 200 µL cell solution was added in each sample's well and 1 well for each specimen as a control. Trypsin reagent was added in 1 for each specimen as a medium. Sample assay was incubated at 37°C for 5 days. After 5 days WST-1 was added in each well and incubated for 2 hours. Absorbance was measured using Thermo Scientific, Multiskan FC instrument. Figure 2.16 represents the results of absorbance of each sample in comparison with respective control. It was observed that pure PAN nanofibers exhibited excellent absorption (88% of that of control) and it can be concluded that PAN has good biocompatibility and less toxicity. While addition of CuO decreased the absorption. Absorption values for 0.25% CuO, 0.50% CuO, 0.75% CuO, and 1.00% CuO were recorded as 77.88%, 74.91%, 67.84%, and 59.38% respectively as compared to their respective control samples. It can be concluded that increasing amount of CuO in PAN nanofibers are leading towards toxic nature but until addition of 1.00% CuO the absorption is not lower than 50% of control, so it is in safe limits [35]–[37]. Cell survival rate for all specimen

were above 50%. But we recommend that no more than 1.00% of copper oxide nanoparticles should be used for practical applications.

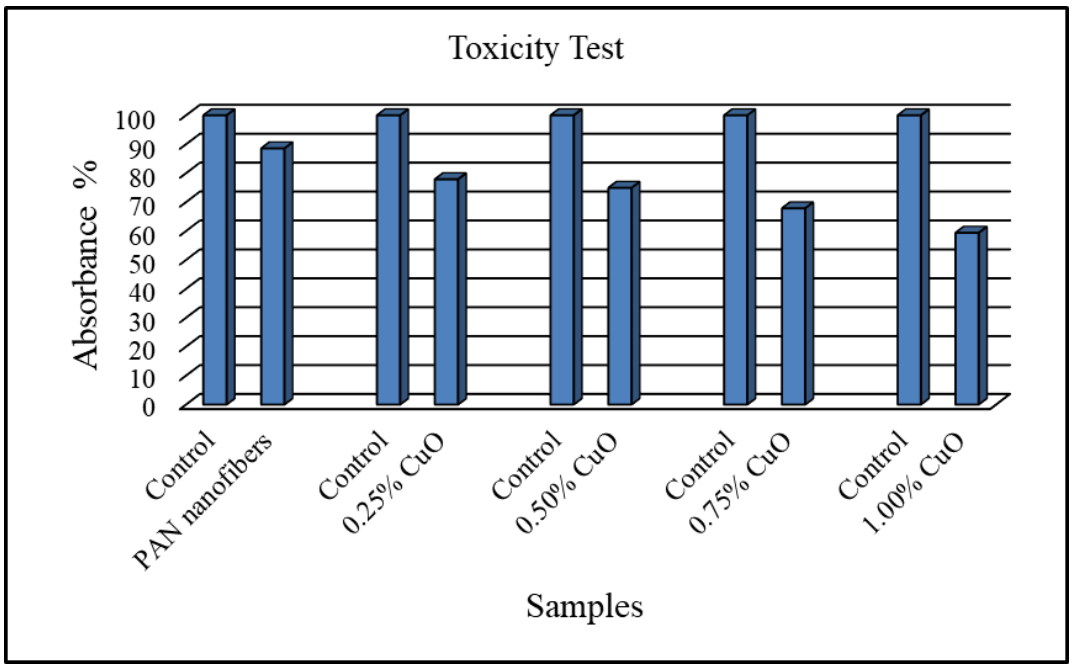

Figure 2.16 Absorbance of each sample in comparison with control

2.4 Conclusion

PAN/CuO nanofibers were successfully electrospun with varying concentrations of CuO in PAN nanofibers. Addition of copper oxide nanoparticles imparted strength to PAN nanofibers. Tensile strength of PAN/CuO nanofibers having 1.00% CuO nanoparticles was significantly increased (8.43 MPa). Morphological properties also exhibited uniformity and smooth production of nanofibers (beads free nanofibers). Prepared nanofiber mats presented excellent antimicrobial activity and release properties. Breathability test was performed which also resulted in significant breathability (performance of nanofibers was in medium range). MTT analysis also represented that more than 50% of total cells were survived after 120 hours of incubation. Air permeability of nanofiber mats was improved by addition of copper oxide nanoparticles. Analyzing above mentioned properties which include antimicrobial, drug release behavior, mechanical properties, thermal properties, breathability, air permeability, surface and structural properties, it can be concluded that copper oxide nanoparticles have significant potential for antimicrobial and structural applications. We recommend PAN/CuO nanoparticles for antimicrobial breath mask applications on the basis of above described results.

References

[1] X. Zhao *et al.*, "Cleanable Air Filter Transferring Moisture and Effectively Capturing PM2.5," *Small*, vol. 13, no. 11, pp. 1–11, 2017.

[2] D. Kharaghani, Y. Kee Jo, M. Q. Khan, Y. Jeong, H. J. Cha, and I. S. Kim, "Electrospun antibacterial polyacrylonitrile nanofiber membranes functionalized with silver nanoparticles by a facile wetting method," *Eur. Polym. J.*, vol. 108, no. August, pp. 69–75, 2018.

[3] M. Q. Khan *et al.*, "The development of nanofiber tubes based on nanocomposites of polyvinylpyrrolidone incorporated gold nanoparticles as scaffolds for neuroscience application in axons," *Text. Res. J.*, p. 004051751880118, 2018.

[4] H. Lee *et al.*, "Electrospun tri-layered zein/PVP-GO/zein nanofiber mats for providing biphasic drug release profiles," *Int. J. Pharm.*, vol. 531, no. 1, pp. 101–107, 2017.

[5] U. Dashdorj *et al.*, "Fabrication and characterization of electrospun zein/Ag nanocomposite mats for wound dressing applications," *Int. J. Biol. Macromol.*, vol. 80, pp. 1–7, 2015.

[6] a. K. Gupta, D. K. Paliwal, and P. Bajaj, "Melting behavior of acrylonitrile polymers," *J. Appl. Polym. Sci.*, vol. 70, no. 13, pp. 2703–2709, 1998.

[7] T. Subbiah, G. Bhat, R. Tock, S. Parameswaran, and S. Ramkumar, "Electrospinning of nanofibers.," *J. Appl. Polym. Sci.*, vol. 96, no. 2, pp. 557–569, 2005.

[8] Y. Zhu, L. Feng, F. Xia, J. Zhai, M. Wan, and L. Jiang, "Chemical dual-responsive wettability of superhydrophobic PANI-PAN coaxial nanofibers," *Macromol. Rapid Commun.*, vol. 28, no. 10, pp. 1135–1141, 2007.

[9] S. K. Lim, S. K. Lee, S. H. Hwang, and H. Kim, "Photocatalytic deposition of silver nanoparticles onto organic/inorganic composite nanofibers," *Macromol. Mater. Eng.*, vol. 291, no. 10, pp. 1265–1270, 2006.

[10] S. F. Li and W. T. Wu, "Lipase-immobilized electrospun PAN nanofibrous membranes for soybean oil hydrolysis," *Biochem. Eng. J.*, vol. 45, no. 1, pp. 48–53, 2009.

[11] S.-F. Li, Y.-H. Fan, R.-F. Hu, and W.-T. Wu, "Pseudomonas cepacia lipase immobilized onto the electrospun PAN nanofibrous membranes for biodiesel production from soybean oil," *J. Mol. Catal. B Enzym.*, vol. 72, no. 1–2, pp. 40–45, 2011.

[12] X. M. Wu, C. J. Branford-White, D. G. Yu, N. P. Chatterton, and L. M. Zhu, "Preparation of core-shell PAN nanofibers encapsulated α-tocopherol acetate and ascorbic acid 2-phosphate for photoprotection," *Colloids Surfaces B Biointerfaces*, vol. 82, no. 1, pp. 247–252, 2011.

[13] F. Yalcinkaya, B. Yalcinkaya, A. Pazourek, J. Mullerova, M. Stuchlik, and J. Maryska, "Surface Modification of Electrospun PVDF/PAN Nanofibrous Layers by Low Vacuum Plasma Treatment," *Int. J. Polym. Sci.*, vol. 2016, 2016.

[14] S. Ren *et al.*, "Electrospun nanofibers made of silver nanoparticles, cellulose nanocrystals, and polyacrylonitrile as substrates for surface-enhanced raman scattering," *Materials (Basel).*, vol. 10, no. 1, 2017.

[15] D. Kharaghani *et al.*, "Fabrication of electrospun antibacterial PVA/Cs nanofibers loaded with CuNPs and AgNPs by an in-situ method," *Polym. Test.*, vol. 72, no. October, pp. 315–321, 2018.

[16] D. Kharaghani, Y. Kee Jo, M. Q. Khan, Y. Jeong, H. J. Cha, and I. S. Kim, "Electrospun antibacterial polyacrylonitrile nanofiber membranes functionalized with silver nanoparticles by a facile wetting method," *Eur. Polym. J.*, vol. 108, no. July, pp. 69–75, 2018.

[17] D. Kharaghani *et al.*, "Preparation and In-Vitro Assessment of Hierarchal Organized Antibacterial Breath Mask Based on Polyacrylonitrile/Silver (PAN/AgNPs) Nanofiber," *Nanomaterials*, vol. 8, no. 7, p. 461, 2018.

[18] M. Q. Khan *et al.*, "*In vitro* assessment of dual-network electrospun tubes from poly(1,4 cyclohexane dimethylene isosorbide terephthalate)/PVA hydrogel for blood vessel application," *J. Appl. Polym. Sci.*, vol. 47222, p. 47222, 2018.

[19] M. Khan *et al.*, "Self-Cleaning Properties of Electrospun PVA/TiO2 and PVA/ZnO Nanofibers Composites," *Nanomaterials*, vol. 8, no. 9, p. 644, 2018.

[20] A. Haider, S. Haider, and I. K. Kang, “A comprehensive review summarizing the effect of electrospinning parameters and potential applications of nanofibers in biomedical and biotechnology,” *Arab. J. Chem.*, 2015.

[21] R. Khajavi and M. Abbasipour, “Electrospinning as a versatile method for fabricating coreshell, hollow and porous nanofibers,” *Sci. Iran.*, vol. 19, no. 6, pp. 2029–2034, 2012.

[22] T. Pan and W. Wang, “From cleanroom to desktop: Emerging micro-nanofabrication technology for biomedical applications,” *Ann. Biomed. Eng.*, vol. 39, no. 2, pp. 600–620, 2011.

[23] J. Gunn and M. Zhang, “Polyblend nanofibers for biomedical applications: Perspectives and challenges,” *Trends Biotechnol.*, vol. 28, no. 4, pp. 189–197, 2010.

[24] J. Xie, X. Li, and Y. Xia, “Putting electrospun nanofibers to work for biomedical research,” *Macromol. Rapid Commun.*, vol. 29, no. 22, pp. 1775–1792, 2008.

[25] L. Lin, X. Liao, and H. Cui, “Cold plasma treated thyme essential oil/silk fibroin nanofibers against Salmonella Typhimurium in poultry meat,” *Food Packag. Shelf Life*, vol. 21, no. March, p. 100337, 2019.

[26] Y. Zhu, H. Cui, C. Li, and L. Lin, “A novel polyethylene oxide/Dendrobium officinale nanofiber: Preparation, characterization and application in pork packaging,” *Food Packag. Shelf Life*, vol. 21, no. December 2018, p. 100329, 2019.

[27] D. Surendhiran, H. Cui, and L. Lin, “Encapsulation of Phlorotannin in Alginate/PEO blended nanofibers to preserve chicken meat from Salmonella contaminations,” *Food Packag. Shelf Life*, vol. 21, no. October 2018, p. 100346, 2019.

[28] H. Cui, J. Wu, C. Li, and L. Lin, “Improving anti-listeria activity of cheese packaging via nanofiber containing nisin-loaded nanoparticles,” *LWT - Food Sci. Technol.*, vol. 81, pp. 233–242, 2017.

[29] J. Sana Ullah, Motahira Hashmi, Lee and I. S. Kim, “Antibacterial properties of in situ and surface functionalized impregnation of silver sulfadiazine in polyacrylonitrile nanofiber mats,” pp. 2693–2703, 2019.

[30] M. Q. Khan *et al.*, “Fabrication of antibacterial electrospun cellulose acetate/ silver-sulfadiazine nanofibers composites for wound dressings applications,” *Polym. Test.*, vol. 74, no. December, pp. 39–44, 2019.

[31] S. Ullah *et al.*, “Silver sulfadiazine loaded zein nanofiber mats as a novel wound dressing,” *RSC Adv.*, vol. 9, no. 1, pp. 268–277, 2019.

[32] M. Q. Khan *et al.*, “The fabrications and characterizations of antibacterial {PVA}/Cu nanofibers composite membranes by synthesis of Cu nanoparticles from solution reduction, nanofibers reduction and immersion methods,” *Mater. Res. Express*, vol. 6, no. 7, p. 75051, Apr. 2019.

[33] J. Wang, P. Jia, K. Pan, and B. Cao, “Functionalization of polyacrylonitrile nanofiber mat via surface-initiated atom transfer radical polymerization for copper ions removal from aqueous solution,” *Desalin. Water Treat.*, vol. 54, no. 10, pp. 2856–2867, 2015.

[34] T. H. Cho *et al.*, “Battery performances and thermal stability of polyacrylonitrile nano-fiber-based nonwoven separators for Li-ion battery,” *J. Power Sources*, vol. 181, no. 1, pp. 155–160, 2008.

[35] E. O. Erhirhie, C. P. Ihekwereme, and E. E. Ilodigwe, “Advances in acute toxicity testing: strengths, weaknesses and regulatory acceptance,” *Interdiscip. Toxicol.*, vol. 11, no. 1, pp. 5–12, 2018.

[36] A. Bahuguna, I. Khan, V. K. Bajpai, and S. C. Kang, “MTT assay to evaluate the cytotoxic potential of a drug,” *Bangladesh J. Pharmacol.*, vol. 12, no. 2, pp. 115–118, 2017.

[37] G. Manley, “Public Access NIH Public Access,” vol. 71, no. 2, pp. 233–236, 2013.

Chapter 3

Electrospun momordica charantia incorporated polyvinyl alcohol (PVA) nanofibers for antibacterial applications

3. Introduction

Momordica charantia (MC), Cucurbitaceae family, also called bitter melon or bitter gourd, which is a well-known vegetable found in Africa, Asia and the Caribbean. As a medicinal plant, Momordica charantia (MC) having medicinal characteristic, is used in the treatment of number of diseases which include viral infections, diabetes, HIV, inflammation, cancer, and ulcers [1]. Bitter gourd is an emerging material for biomedical applications. It was also used for green synthesis of sliver nanoparticles for wound care applications [2]. Anti-inflammatory effects in mice were also studied using bitter gourd as an anti-inflammatory material [3]. Natural products have excellent medicinal properties, green chemistry, and biocompatibility which makes them suitable for many applications in biomedical and environmental engineering. Momordica charantia is being used for biosynthesis of metallic nanoparticles for improved biocompatibility [4][5]. K. D. Mwambete studied antibacterial activity of methanolic and petroleum ether crude extracts of MC in 2009. They extracted crude extracts of MC fruit, analyzed yield percentage, and its antibacterial results by zone inhibition method [6]. An in-vivo study was also held on anticancer properties of MC extract on Fisher 344 male rats. It was concluded that MC extract has potential against cancer cells [7]. Leaves, roots, and seeds extract of momordica charantia fruit was extracted and studied for anti-inflammatory properties by M. Ullah et al [8]. Momordica charantia extract has potential in anti-inflammatory, anti-cancer, diabetes, and other antimicrobial applications in health care sector [2], [9], [18], [10]–[17]. Electrospinning is simple and one of the oldest technique to fabricate nano-scaled fibers with smooth and homogenous morphology. These nanofibers can be electrospun by natural polymers and synthetic polymers as well depending on required application [19]–[22]. Electrospun nanofibers have potential applications in biomedical, environmental, and structural applications including wound dressings[23]–[25] [20], [26], tissue engineering, bio implants [27] [28], bio sensors, air filters [22], water purification, super capacitors and others [29]–[33].

Polymer can be natural, semi synthetic, or fully synthetic. There are several limitations for polymers depending on applications. A number of natural and synthetic polymers are used for biomedical applications due to their extraordinary biocompatibility, drug delivery properties, inherent antibacterial properties,

biodegradability, and self-healing. Polyvinyl Alcohol (PVA) is one of biocompatible polymers which is widely used for biomedical and environmental applications including wound dressings, self-cleaning surgical gowns. Bio-sensors, waste-water treatment [34]–[39]. We have selected momordica charantia (MC) water soluble extract for its excellent

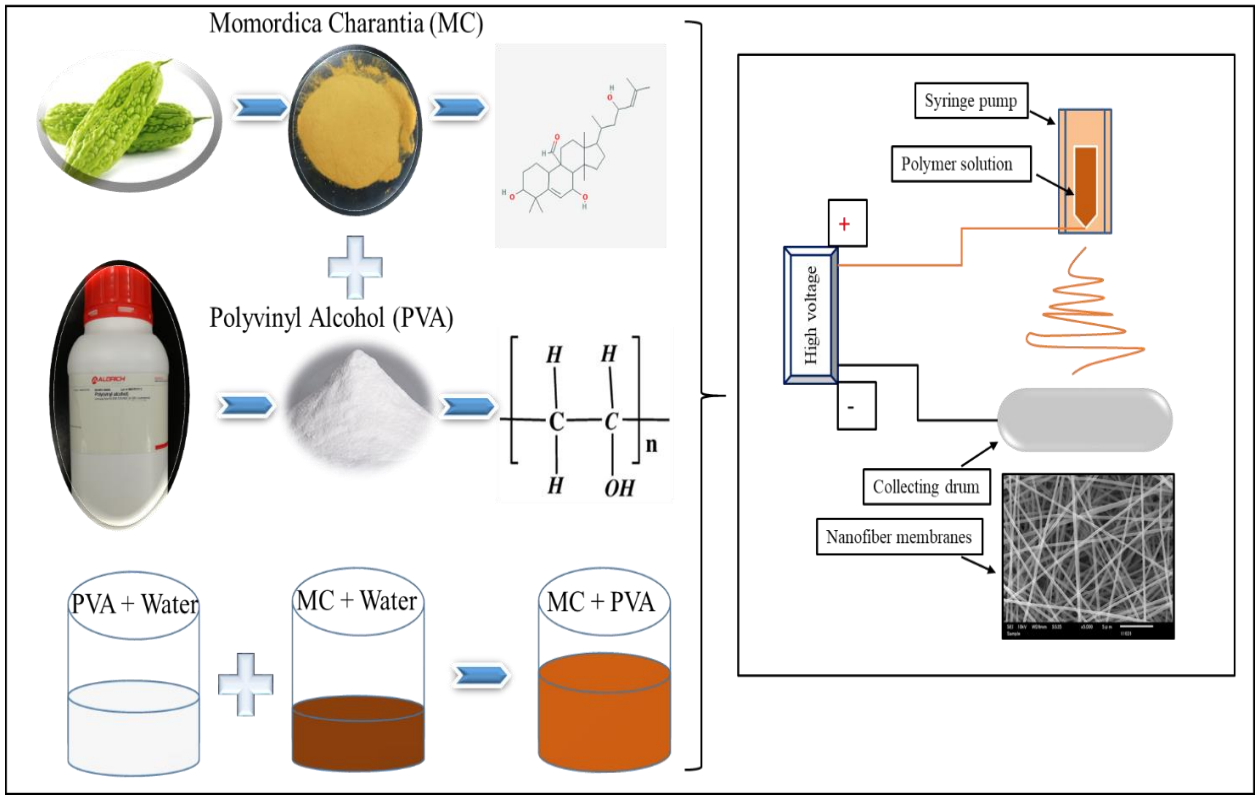

Figure 3.1 Graphical presentation of PVA/MC nanofibers fabrication process

Antibacterial properties, and PVA for its wider range of biomedical applications. Momordica Charantia (MC) water soluble extract was loaded on electrospinning for the first time, to fabricate a nano-scaled nonwoven web of fibers. This research is unique due to following reasons; (a) momordica charantia (MC) extract was loaded on electrospinning for the first time, (b) PVA was selected core material as it is also water soluble (to obtain a homogeneous solution of PVA, and MC), (c) Antibacterial, surface morphology, mechanical & thermal characterizations were performed to assess potential of electrospun momordica charantia extract in combination with PVA nanofibers, (d) utilization of natural extract will lead towards sustainable and eco-friendly solution in healthcare system.

3.1 Experimental setup

3.1.1 Materials & methods

Momordica charantia (MC) water soluble extract was purchased from water soluble proteins, Shanghai, China. Hydrolyzed (87-89%) polyvinyl alcohol (PVA) polymer, in powder form (molecular weight 80000-120000), was purchased from Sigma Aldrich Corporation, USA. 25% solution of glutaraldehyde (GA) was also supplied by Sigma Aldrich (USA). While, Hydrochloric acid (HCL) with (99% purity) was supplied by Wako chemicals (Japan). Distilled water and other required accessories were used from laboratory.

Neat PVA nanofibers were electrospun as per our recent research work [40]. For all samples containing different concentrations of MC extract, firstly PVA was dissolved in distilled water (8% W/W) at 60°C for 12 hours. When, PVA was fully dissolved different proportions of momordica charantia (MC) extract was added in solution and kept for stirring for 2 hours approximately (until homogeneous solution was formed). Resultant solution was then electrospun at a voltage of 12 kV, distance of 15 cm between tip and collector and flow rate of 1 ml/h. Nanofiber mats were crosslinked by HCL fume method following traditional crosslinking technique as done in our previous research [41].

3.3.2 Characterization

Antibacterial activity and cytotoxicity test (WST-1 Assay)

Antibacterial properties of momordica charantia extract were analyzed by disk diffusion method. *B. Subtilis* (B-Sub 168 - *gram positive) and E. coli* (BUU25113 - *gram negative)* bacteria strains were cultured in separate plates for each type of bacteria and round disks of 13 mm diameter were placed over the cultured bacteria stains. Cultured plates with samples were incubated for 24 hours at 37°C temperature.

WST-1 assay was carried out to confirm any toxic effect of MC extract in human body [42]. Fibroblast cells (NIH3T3) were used for cytotoxicity test. 5 disks of diameter 3 mm (for each specimen and for each day) were sterilized by washing with 70% ethanol and Phosphate buffered saline (PBS) reagent. NIH3T3 cells were firstly cultured in trypsin, cells were counted under microscope, and cell dilution was prepared for adding in sterilized 96 wells microplate. 5000 cells (200 μL cell solution) were added in each well (sample wells and control as well). Microplate was incubated at 37°C for 1 day, 3 days, 5 days, and 7 days. After 1,

3, 5, and 7 days, 10 µL of WST-1 was added in each well and incubated for 2 hours respectively. Absorbance was measured using refractometer Thermo Scientific, Multiskan FC instrument.

Scanning electron microscopy (SEM)

PVA and PVA/MC composite nanofibers' morphology was observed by SEM images taken by using Scanning Electron Microscopy, *JSM-5300, JEOL Ltd, Japan*, (accelerated by a voltage of 20 kV). Average diameter of all nanofiber mats was measured by Image J. software (50 readings were taken from each image and average is presented in results section).

Fourier transform infrared spectroscopy- Attenuated total refraction (FTIR-ATR)

Possibility of any chemical interaction between PVA and momordica charantia (MC) was observed using FTIR, "ATR Prestige-21, Shimadzu, Japan". Different wave number ranges were set for taking FTIR and FTIR-ATR spectra as follows; wavenumber of 600 cm^{-1} to 4000 cm^{-1} for ATR while 400 cm^{-1} to 4000 cm^{-1} for FTIR (for momordica charantia extract).

X-ray diffraction (XRD)

Crystallinity of PVA and PVA/MC composite nanofibers was observed by XRD spectra which was taken at 25℃ by using x-ray diffraction "Rotaflex RT300 mA, Rigaku, Osaka, Japan", with an angular angle of $5 \leq 2\theta \leq 70°$, and measurements were taken by Nickel-filtered Cu. Ka radiation.

X-ray photoelectron spectroscopy (XPS)

X-ray photoelectron spectroscopy (XPS), "*Shimadzu-Kratos AXIS-ULTRA HAS SV*, Shimadzu, Kyoto, Japan" was used to analyze elemental composition of PVA and MC extract in PVA/MC composite nanofibers. Wide spectra was obtained in set range of 0-1100 eV while narrow spectra were also obtained for O-1s and C-1s.

Thermogravimetric Analysis (TGA)

Effect of momordica charantia loading on thermal properties of final composite nanofibers was studied using TGA "Thermo-plus TG 8120, Rigaku Corporation, Osaka, Japan". Test was conducted under normal atmosphere (ambient conditions under air), and heating rate of 10℃/min. temperature range for all specimen were set from 25℃ to 500℃.

Universal Testing Machine (UTM)

Mechanical properties is one of the essential parameters to analyze the performance and practical aspect of any material. Universal Testing Machine (UTM), "Tensilon RTC 250A; A&D Company Ltd., Japan" was used to assess mechanical properties of PVA and PVA/MC nanofibers ISO 13634 was followed for specimen preparation. Crosshead speed was adjusted at 5 mm/min while experiment was performed at room temperature 25℃ ± 3℃. Tensile stress and strain were calculated from available data (UTM data).

3.2 Results and discussions

3.2.1 Morphological properties

Figure 3.2 represents SEM images of neat PVA and PVA/MC nanofibers with varying loading of MC extract up to 50% (w/w). It can be observed that neat PVA nanofibers presented smooth morphology and no bead can be seen in neat PVA nanofibers (Fig. 2 (a)). While a few beads were observed in PVA/MC (20% MC) sample, and beads formation was gradually increased with increasing MC quantity in PVA solution. It can be said that momordica charantia has no tendency to be converted in to nanofibers, that's the reason that MC was only encapsulated in PVA nanofibers while some of the MC extract was still electro-sprayed in beads form. Figure 2(b-e) shows an increasing trend of beads formation but there was almost no effect on PVA nanofibers' production as PVA/MC solution was homogenously mixed.

Figure 3.2 (f) represents average diameter of nanofibers. It can be observed that neat PVA nanofibers had uniform diameter distribution (lower value of standard deviation), while PVA/MC nanofibers exhibited a wide range of diameters. Diameter range was increased with increasing MC extract but at 50% MC loading, diameter was drastically decreased. It can be associated with a reason that MC was encapsulated with in the nanofibers for samples (b-d) while sample e (50% MC), there were separate nanofibers of PVA and MC was on the surface of PVA nanofibers. Which indicates that 40% loading of MC was optimum to get MC encapsulated in to PVA nanofibers, increasing quantity to 50% caused a phase separation between PVA and

MC. That's why there were only PVA nanofibers in the matrix. Morphological changes in PVA nanofibers before and after crosslinking were also studied in our recent research [40]

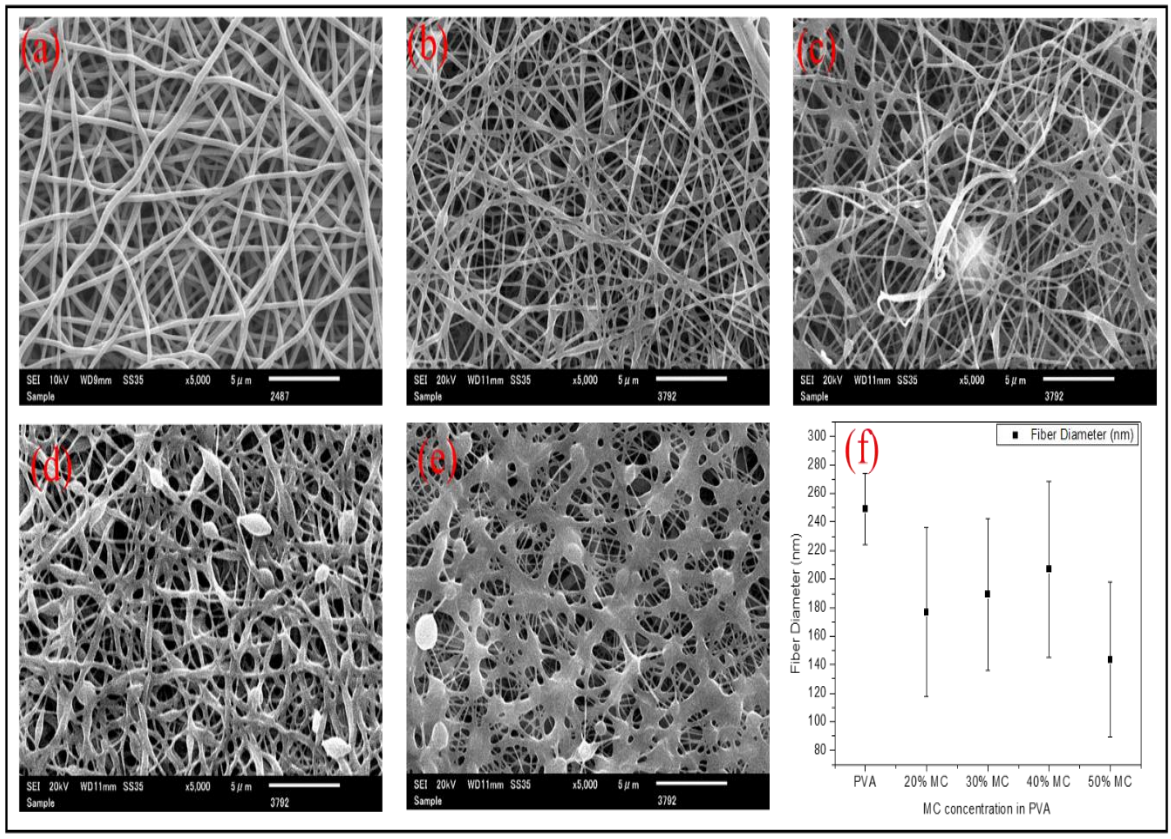

Figure 3.2 SEM images of (a) pure PVA nanofibers, (b) 20% MC, (c) 30% MC, (d) 40% MC, (e) 50% MC in PVA/MC nanofibers, and (f) Average diameter of nanofibers

3.2.2 FTIR and X-ray photoelectron spectroscopy (XPS)

PVA is hydrophilic polymer because of abundant hydroxyl groups. That's one of the main reasons that PVA nanofibers are not stable in water or aqueous mixtures. PVA nanofibers are crosslinked prior to practical applications where there is any direct contact with water or aqueous mixtures. Crosslinking of PVA nanofibers by HCL and glutaraldehyde fumes interlocked hydroxyl functional groups of PVA [41]. Figure 3.3 represents FTIR-ATR spectra of neat PVA, MC extract, and PVA/MC nanofibers. Spectra of neat PVA represents a strong peak in range of 3000 cm^{-1} to 3500 cm^{-1} (precisely at 3239 cm^{-1}) which is generally associated with –OH stretching. It is clear indication that there are still hydroxyl groups in main chain of PVA despite crosslinking. However, crosslinked PVA nanofibers are far better for applications where there is moisture or water contact. A peak at 2900 cm^{-1} was also observed which referred to ($–CH_2–$) asymmetric

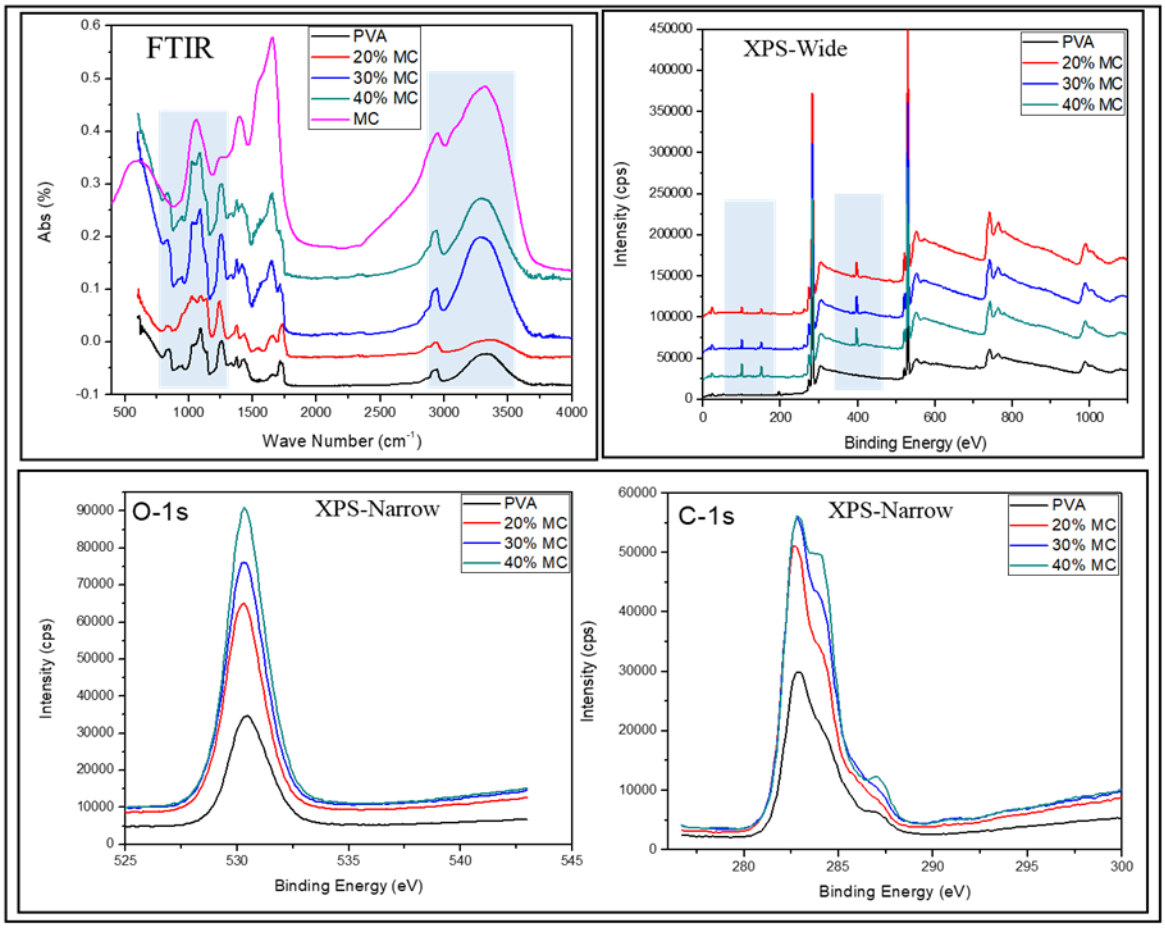

Figure 3.3 FTIR-ATR spectra of pure PVA nanofibers, pure MC extract, and PVA/MC nanofibers with varying MC concentration, XPS spectra (wide) of pure PVA nanofibers and PVA/MC nanofibers, and XPS spectra (Narrow, C-1s, and O-1s) of pure PVA nanofibers and PVA/MC nanofibers

and symmetric band. Momordica charantia mainly contains different components which include triterpenes, steroids, proteins, and alkaloids along with some of the phenolic compounds. A sharp peak was observed in the wavenumber range of 1500 cm^{-1} - 1600 cm^{-1} in all spectra of PVA/MC and pure MC extract. It can be also observed that above mentioned peak was more prominent in samples having higher concentrations of MC extract. Figure 3.3 also represents XPS spectra (wide and narrow respectively) of neat PVA nanofibers and PVA/MC nanofibers. Neat PVA nanofibers exhibited C-1s and O-1s peaks at binding energy 282.5 eV and 531 eV. It can be observed in figure 4 that carbon and oxygen peaks of neat PVA nanofibers are smaller than that of PVA/MC nanofibers. XPS spectra (wide) clearly shows a sharp peak at binding energy of 400 eV, which is associated with nitrogen. It can be concluded that PVA/MC nanofibers contain nitrogen, oxygen, and carbon. While PVA/MC also exhibited peaks at binding energy of 100 eV and 150 eV (can be seen in

XPS wide spectra), which are associated with MC only. As neat PVA nanofibers did not show any of above mentioned peaks.

3.2.3 Thermal degradation study

TGA was used to carry on investigation of behavior of PVA and PVA/MC composite nanofibers under high temperature conditions. Figure 3.4 presents TGA plot of PVA, MC, and PVA/MC composite nanofibers.

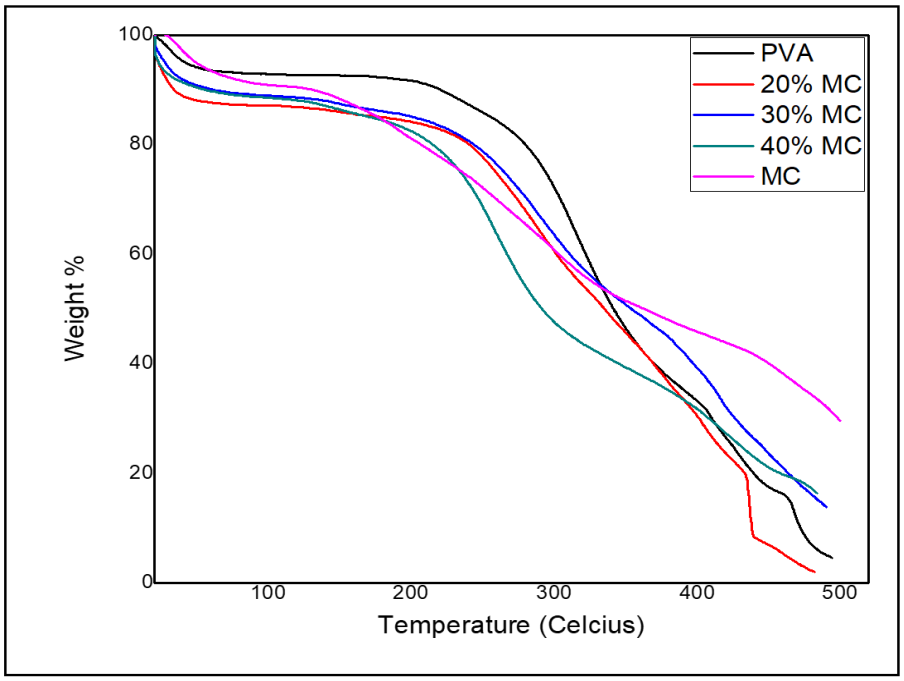

Figure 3.4 Thermal degradation study of PVA nanofibers, MC extract, and PVA/MC nanofibers

It can be observed that in temperature range of 25 °C to 100 °C, all samples exhibited almost similar trend which shows that moisture or high volatile components were present in same amount in all samples [22], [43], [44]. But onset temperature for MC extract occurred at lower temperature (150 °C) while onset of PVA/MC composite nanofibers occurred at higher temperature ranges as compared to that of neat MC. Residual contents also increased as MC concentration increased in PVA/MC composite nanofibers. It can be observed that neat PVA nanofibers were thermally stable up to 220 °C and exhibited uniform degradation until 480 °C where it reached combustion stage. Low thermal stability of MC can be associated with its amorphousness. However, thermal stability of PVA nanofibers is still enough to be used for practical applications as antibacterial nanofiber mats.

3.2.4 Crystallinity and mechanical properties

Crystallinity of PVA and PVA/MC nanofibers was assessed XRD. Figure 3.5 represents XRD spectra of neat PVA nanofibers and PVA with varying concentrations of MC extract. It can be observed that PVA nanofibers presented a characteristic peak at an angle (2θ) of 19.6 which is generally associated with amorphous structure of PVA. Momordica charantia is considered to be amorphous in nature. It can be observed in XRD spectra that addition of momordica charantia extract in to PVA nanofibers affected crystalline structure at large. Peak at 2θ = 19.6 was drastically decreased with increasing concentration of momordica charantia. Decreased crystallinity also affects mechanical properties of material. It was confirmed from UTM results that tensile strength of PVA/MC composite nanofibers was decreased to 1/4th of tensile strength of neat PVA nanofibers when 40% MC extract was loaded with PVA. Herein, we conclude that momordica charantia does not act as reinforcement rather it decreases mechanical properties of partner material.

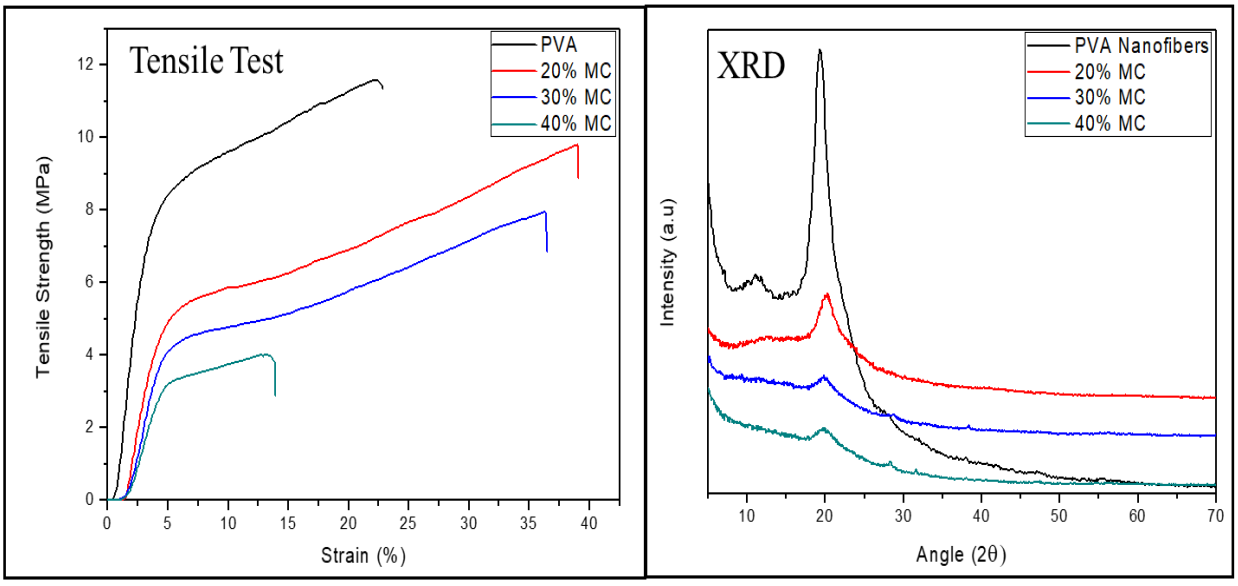

Figure 3.5 X-Ray Diffraction of pure PVA, and PVA/MC nanofibers

3.2.5 Antibacterial and cytotoxicity assay

Antibacterial activity was measured by disk diffusion method [44]–[46] against gram positive and gram negative bacteria. Bacillus subtilis (B. subtilis) and Escherichia coli (E. coli) bacteria stains were selected as gram positive and gram negative bacteria stains. Each bacteria stain were cultured on separated plates and

samples were placed on disks. Disks having samples were then incubated for 12 hours (overnight) at 37°C temperature. Pictures were taken and zone of inhibition was measured using Image J. software. It can be observed in figure 3.6 that neat PVA nanofibers did not show any antibacterial activity against both types of bacteria stains while PVA/MC composite nanofibers exhibited excellent antibacterial properties. Antimicrobial properties were prominent when proportion of MC extract was higher as compared to that of lower loading of MC extract. It was also observed that bioactive components in MC extract were found to be more effective against gram positive bacteria stain as compared to that of gram negative stain. Inhibited zone for neat PVA, 20% MC, 30% MC, and 40% MC samples were recorded as 0mm, 4.282 mm, 14.036 mm, and 16.811 mm for gram positive (B. Sub) bacteria stains while 0 mm, 4.214 mm, 5.357 mm, and 14.685 mm for gram negative (E. Coli) respectively. PVA is biocompatible polymer which is also a good carrier of drugs for wound dressings, that can be one of the reasons that PVA/MC extract exhibited excellent antibacterial properties due to controlled released of MC extract from PVA nanofibers [47]. WST-1 assay was used to assess cell proliferation and effect of MC extract on cell growth. It was observed that neat PVA nanofibers exhibited better results as compared to that of PVA/MC composite nanofibers for 1, 3, 5, and 7 days. However, cell growth was also observed on samples having MC extract, and it can be observed in Figure 3.6 that minimum absorption of WST-1 (day 7) was recorded at 140%, which is clear indication that cell growth was supported by MC extract. Furthermore it can concluded that MC extract is not toxic to human body and supports cell proliferation.

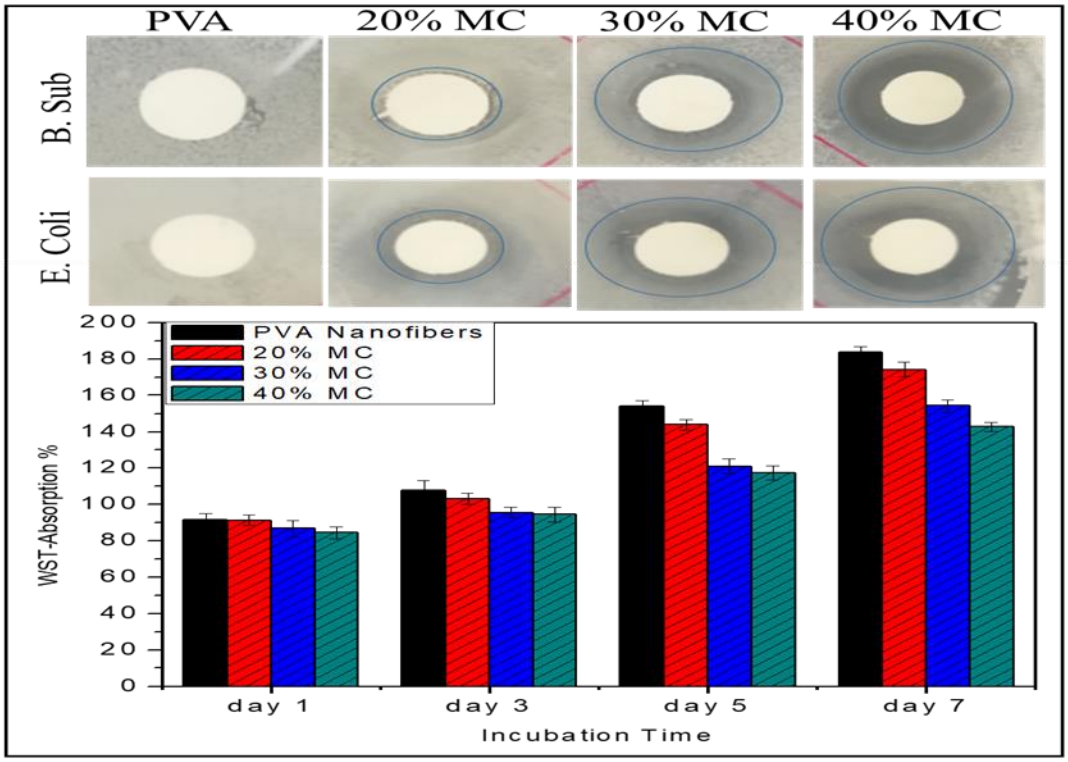

Figure 3.6 Antibacterial activity test (upper), and cytotoxicity analysis (lower) of PVA, and PVA/MC nanofibers

3.3 Conclusion

Momordica charantia (MC) extract (water soluble) was loaded on electrospinning in combination with PVA which is well known biocompatible polymer. PVA nanofibers are generally beads-free and more uniform in morphology. Addition of MC extract in PVA solution caused beads formation, and beads occurrence was increased with increasing MC concentration in PVA. Maximum of 50% (w/w) MC loading was run on electrospinning which resulted electro-sprayed PVA/MC nanofibers (less nanofibers, more beads). Samples having 40% MC was considered better as these samples presented better morphological, antibacterial, surface, and thermal properties, hence recommended for further production of nanofibers. Satisfactory results were obtained from toxicity test. But mechanical properties (tensile strength) were suppressed with increasing MC extract concentration in PVA/MC solution. However, our target application is more focused on antibacterial and biocompatibility of prepared nanofiber mats which both are satisfactory. It can be concluded that MC extract is suitable and sustainable replacement of antibacterial drug due to its excellent antibacterial activity against both gram positive and gram negative bacteria. WST-1 assay also showed that MC extract is suitable in applications such as wound dressings.

References

[1] D. M. Cuong *et al.*, "Medically important carotenoids from Momordica charantia and their gene expressions in different organs," *Saudi J. Biol. Sci.*, vol. 24, no. 8, pp. 1913–1919, 2017, doi: 10.1016/j.sjbs.2017.11.039.

[2] S. Alippilakkotte, S. Kumar, and L. Sreejith, "Fabrication of PLA/Ag nanofibers by green synthesis method using Momordica charantia fruit extract for wound dressing applications," *Colloids Surfaces A Physicochem. Eng. Asp.*, vol. 529, no. May, pp. 771–782, 2017, doi: 10.1016/j.colsurfa.2017.06.066.

[3] C. Y. Chao, P. J. Sung, W. H. Wang, and Y. H. Kuo, "Anti-inflammatory effect of momordica charantia in sepsis mice," *Molecules*, vol. 19, no. 8, pp. 12777–12788, 2014, doi: 10.3390/molecules190812777.

[4] B. Ajitha, Y. A. K. Reddy, and P. S. Reddy, "Biosynthesis of silver nanoparticles using Momordica charantia leaf broth: Evaluation of their innate antimicrobial and catalytic activities," *J. Photochem. Photobiol. B Biol.*, vol. 146, pp. 1–9, 2015, doi: 10.1016/j.jphotobiol.2015.02.017.

[5] S. A. David, S. I. Rajadurai, and S. V. Kumar, "Biosynthesis of copper oxide nanoparticles using Momordica charantia leaf extract and their characterization," vol. 31, no. December, pp. 333–340, 2017.

[6] K. D. Mwambete, "The in vitro antimicrobial activity of fruit and leaf crude extracts of Momordica charantia: A Tanzania medicinal plant," *Afr. Health Sci.*, vol. 9, no. 1, pp. 34–39, 2009.

[7] D. Asiamah, "Chemopreventive Potential of Bitter Melon (Momordica Charantia) against Precancerous Lesions in the Colon of Fisher 344 Male Rats," *Int. J. Cancer Res.*, vol. 7, no. 1, pp. 36–46, 2011.

[8] M. Ullah, M. Showkat, N. U. Ahmed, S. Islam, and N. Absar, "Evaluation of Momordica charantia L. fruit extract for analgesic and anti-inflammatory activities using in vivo assay," *Research Journal of Medicinal Plant*, vol. 6, no. 3. pp. 236–244, 2012, doi: 10.3923/rjmp.2012.236.244.

[9] G. Manoharan, E. Cummings, and J. Singh, "Effects of crude water-soluble extract of Momordica

charantia on viability, caspase activity, cytochrome c release and on cytosolic calcium levels in different cancer cell lines," *Cancer Cell Microenviron.*, pp. 1–10, 2014, doi: 10.14800/ccm.273.

[10] G. T. Zhao *et al.*, "Cucurbitane-type triterpenoids from the stems and leaves of Momordica charantia," *Fitoterapia*, vol. 95, pp. 75–82, 2014, doi: 10.1016/j.fitote.2014.03.005.

[11] A. Upadhyay, P. Agrahari, and D. K. Singh, "A review on salient pharmacological features of momordica charantia," *Int. J. Pharmacol.*, vol. 11, no. 5, pp. 405–413, 2015, doi: 10.3923/ijp.2015.405.413.

[12] F. Zhang, L. Lin, and J. Xie, "A mini-review of chemical and biological properties of polysaccharides from Momordica charantia," *Int. J. Biol. Macromol.*, vol. 92, no. 235, pp. 246–253, 2016, doi: 10.1016/j.ijbiomac.2016.06.101.

[13] M. Raish *et al.*, "Momordica charantia polysaccharides mitigate the progression of STZ induced diabetic nephropathy in rats," *Int. J. Biol. Macromol.*, vol. 91, pp. 394–399, 2016, doi: 10.1016/j.ijbiomac.2016.05.090.

[14] K. Raina, D. Kumar, and R. Agarwal, "Promise of bitter melon (Momordica charantia) bioactives in cancer prevention and therapy," *Semin. Cancer Biol.*, vol. 40_41, pp. 116–129, 2016, doi: 10.1016/j.semcancer.2016.07.002.

[15] N. M. Aruan, I. Sriyanti, D. Edikresnha, T. Suciati, M. M. Munir, and K. Khairurrijal, "Polyvinyl Alcohol/Soursop Leaves Extract Composite Nanofibers Synthesized Using Electrospinning Technique and their Potential as Antibacterial Wound Dressing," *Procedia Eng.*, vol. 170, pp. 31–35, 2017, doi: 10.1016/j.proeng.2017.03.006.

[16] J. Ahamad, S. Amin, and S. R. Mir, "Momordica charantia Linn. (Cucurbitaceae): Review on Phytochemistry and Pharmacology," *Res. J. Phytochem.*, vol. 11, no. 2, pp. 53–65, 2017, doi: 10.3923/rjphyto.2017.53.65.

[17] G. Perumal, S. Pappuru, D. Chakraborty, A. Maya Nandkumar, D. K. Chand, and M. Doble, "Synthesis and characterization of curcumin loaded PLA—Hyperbranched polyglycerol electrospun blend for wound dressing applications," *Mater. Sci. Eng. C*, vol. 76, pp. 1196–1204, 2017, doi:

10.1016/j.msec.2017.03.200.

[18] F. Saeed *et al.*, "Bitter melon (Momordica charantia): A natural healthy vegetable," *Int. J. Food Prop.*, vol. 21, no. 1, pp. 1270–1290, 2018, doi: 10.1080/10942912.2018.1446023.

[19] S. Ullah *et al.*, "Antibacterial properties of in situ and surface functionalized impregnation of silver sulfadiazine in polyacrylonitrile nanofiber mats," *Int. J. Nanomedicine*, vol. 14, pp. 2693–2703, 2019, doi: 10.2147/IJN.S197665.

[20] S. Ullah *et al.*, "Silver sulfadiazine loaded zein nanofiber mats as a novel wound dressing," *RSC Adv.*, vol. 9, no. 1, pp. 268–277, 2019, doi: 10.1039/C8RA09082C.

[21] M. Q. Khan *et al.*, "*In vitro* assessment of dual-network electrospun tubes from poly(1,4 cyclohexane dimethylene isosorbide terephthalate)/PVA hydrogel for blood vessel application," *J. Appl. Polym. Sci.*, vol. 47222, p. 47222, 2018, doi: 10.1002/app.47222.

[22] M. Hashmi, S. Ullah, and I. S. Kim, "Copper oxide (CuO) loaded polyacrylonitrile (PAN) nanofiber membranes for antimicrobial breath mask applications," *Curr. Res. Biotechnol.*, vol. 1, no. 1, pp. 1–10, Nov. 2019, doi: 10.1016/j.crbiot.2019.07.001.

[23] A. Bahramzadeh, P. Zahedi, and M. Abdouss, "Acrylamide-plasma treated electrospun polystyrene nanofibrous adsorbents for cadmium and nickel ions removal from aqueous solutions," *J. Appl. Polym. Sci.*, vol. 133, no. 5, pp. 1–9, 2016, doi: 10.1002/app.42944.

[24] B. Motealleh, P. Zahedi, I. Rezaeian, M. Moghimi, A. H. Abdolghaffari, and M. A. Zarandi, "Morphology, drug release, antibacterial, cell proliferation, and histology studies of chamomile-loaded wound dressing mats based on electrospun nanofibrous poly(ε-caprolactone)/polystyrene blends," *J. Biomed. Mater. Res. - Part B Appl. Biomater.*, vol. 102, no. 5, pp. 977–987, 2014, doi: 10.1002/jbm.b.33078.

[25] P. Zahedi, I. Rezaeian, and S. H. Jafari, "In vitro and in vivo evaluations of phenytoin sodium-loaded electrospun PVA, PCL, and their hybrid nanofibrous mats for use as active wound dressings," *J. Mater. Sci.*, vol. 48, no. 8, pp. 3147–3159, 2013, doi: 10.1007/s10853-012-7092-9.

[26] D. Kharaghani *et al.*, "Design and characterization of dual drug delivery based on in-situ assembled

PVA/PAN core-shell nanofibers for wound dressing application," *Sci. Rep.*, vol. 9, no. 1, pp. 1–11, 2019, doi: 10.1038/s41598-019-49132-x.

[27] I. Rezaeian, B. Motealleh, M. Gholami, P. Zahedi, A. Salehpour, and M. A. Zarandi, "Drug release, cell adhesion and wound healing evaluations of electrospun carboxymethyl chitosan/polyethylene oxide nanofibres containing phenytoin sodium and vitamin C," *IET Nanobiotechnology*, vol. 9, no. 4, pp. 191–200, Aug. 2015, doi: 10.1049/iet-nbt.2014.0030.

[28] M. Q. Khan *et al.*, "The development of nanofiber tubes based on nanocomposites of polyvinylpyrrolidone incorporated gold nanoparticles as scaffolds for neuroscience application in axons," *Text. Res. J.*, p. 004051751880118, 2018, doi: 10.1177/0040517518801185.

[29] C. Ye *et al.*, "Preparation of Poly(lactic-co-glycolic acid)-Based Composite Microfibers for Postoperative Treatment of Tumor in NIR I and NIR II Biowindows," *Macromol. Biosci.*, vol. 18, no. 10, pp. 1–13, 2018, doi: 10.1002/mabi.201800206.

[30] X. M. Wu, C. J. Branford-White, D. G. Yu, N. P. Chatterton, and L. M. Zhu, "Preparation of core-shell PAN nanofibers encapsulated α-tocopherol acetate and ascorbic acid 2-phosphate for photoprotection," *Colloids Surfaces B Biointerfaces*, vol. 82, no. 1, pp. 247–252, 2011, doi: 10.1016/j.colsurfb.2010.08.049.

[31] S.-F. Li, Y.-H. Fan, R.-F. Hu, and W.-T. Wu, "Pseudomonas cepacia lipase immobilized onto the electrospun PAN nanofibrous membranes for biodiesel production from soybean oil," *J. Mol. Catal. B Enzym.*, vol. 72, no. 1–2, pp. 40–45, 2011, doi: 10.1016/j.molcatb.2011.04.022.

[32] L. Lin, Y. Dai, and H. Cui, "Antibacterial poly(ethylene oxide) electrospun nanofibers containing cinnamon essential oil/beta-cyclodextrin proteoliposomes," *Carbohydr. Polym.*, vol. 178, no. June, pp. 131–140, 2017, doi: 10.1016/j.carbpol.2017.09.043.

[33] H. Cui, M. Bai, M. M. A. Rashed, and L. Lin, "The antibacterial activity of clove oil/chitosan nanoparticles embedded gelatin nanofibers against Escherichia coli O157:H7 biofilms on cucumber," *Int. J. Food Microbiol.*, vol. 266, no. November 2017, pp. 69–78, 2018, doi: 10.1016/j.ijfoodmicro.2017.11.019.

[34] J. Kim, T. Kang, H. Kim, H. J. Shin, and S. G. Oh, "Preparation of PVA/PAA nanofibers containing thiol-modified silica particles by electrospinning as an eco-friendly Cu (II) adsorbent," *J. Ind. Eng. Chem.*, vol. 77, pp. 273–279, 2019, doi: 10.1016/j.jiec.2019.04.048.

[35] P. Kampalanonwat and P. Supaphol, "The study of competitive adsorption of heavy metal ions from aqueous solution by aminated polyacrylonitrile nanofiber mats," *Energy Procedia*, vol. 56, no. C. pp. 142–151, 2014, doi: 10.1016/j.egypro.2014.07.142.

[36] D. Morillo Martín, M. Faccini, M. A. García, and D. Amantia, "Highly efficient removal of heavy metal ions from polluted water using ion-selective polyacrylonitrile nanofibers," *Journal of Environmental Chemical Engineering*, vol. 6, no. 1. pp. 236–245, 2018, doi: 10.1016/j.jece.2017.11.073.

[37] M. Zhu *et al.*, "Electrospun Nanofibers Membranes for Effective Air Filtration," *Macromol. Mater. Eng.*, vol. 302, no. 1, pp. 1–27, 2017, doi: 10.1002/mame.201600353.

[38] S. Deng, X. Liu, J. Liao, H. Lin, and F. Liu, "PEI modified multiwalled carbon nanotube as a novel additive in PAN nanofiber membrane for enhanced removal of heavy metal ions," *Chemical Engineering Journal*, vol. 375. 2019, doi: 10.1016/j.cej.2019.122086.

[39] T. J. Alwan, Z. A. Toma, M. A. Kudhier, and K. M. Ziadan, "Preparation and Characterization of the PVA Nanofibers Produced By Electrospinning Article Madridge Journal of Nanotechnology & Nanoscience Preparation and Characterization of the PVA Nanofibers Produced By Electrospinning," *Madridge J. Nanotechnol. Nanosci.*, vol. 1, no. January, pp. 1–3, 2016, doi: 10.18689/mjnn.2016-101.

[40] S. Ullah *et al.*, "Stabilized nanofibers of polyvinyl alcohol (PVA) crosslinked by unique method for efficient removal of heavy metal ions," *J. Water Process Eng.*, vol. 33, no. December 2019, p. 101111, Feb. 2020, doi: 10.1016/j.jwpe.2019.101111.

[41] M. Khan *et al.*, "Self-Cleaning Properties of Electrospun PVA/TiO2 and PVA/ZnO Nanofibers Composites," *Nanomaterials*, vol. 8, no. 9, p. 644, 2018, doi: 10.3390/nano8090644.

[42] A. Ullah *et al.*, "Manuka honey incorporated cellulose acetate Nanofibrous Mats: Fabrication and In

Vitro evaluation as a potential wound dressing.," *Int. J. Biol. Macromol.*, 2020, doi: https://doi.org/10.1016/j.ijbiomac.2020.03.237.

[43] M. S. Irfan, Y. Q. Gill, S. Ullah, M. T. Naeem, F. Saeed, and M. Hashmi, "Polyaniline-NBR blends by in situ polymerization: Application as stretchable strain sensors," *Smart Mater. Struct.*, vol. 28, no. 9, 2019, doi: 10.1088/1361-665X/ab1df3.

[44] M. Q. Khan *et al.*, "The fabrications and characterizations of antibacterial PVA/Cu nanofibers composite membranes by synthesis of Cu nanoparticles from solution reduction, nanofibers reduction and immersion methods," *Mater. Res. Express*, vol. 6, no. 7, 2019, doi: 10.1088/2053-1591/ab1688.

[45] M. Q. Khan *et al.*, "Fabrication of Antibacterial Nanofibers Composites by Functionalizing the Surface of Cellulose Acetate Nanofibers," *ChemistrySelect*, vol. 5, no. 4, pp. 1315–1321, 2020, doi: 10.1002/slct.201901106.

[46] X. Bie *et al.*, "Fabrication and characterization of wound dressings containing gentamicin/silver for wounds in diabetes mellitus patients," *Mater. Res. Express*, 2020, [Online]. Available: http://iopscience.iop.org/10.1088/2053-1591/ab8337.

[47] J. Santiago-Morales, G. Amariei, P. Letón, and R. Rosal, "Antimicrobial activity of poly(vinyl alcohol)-poly(acrylic acid) electrospun nanofibers," *Colloids Surfaces B Biointerfaces*, vol. 146, pp. 144–151, 2016, doi: 10.1016/j.colsurfb.2016.04.052.

Chapter 4

Antibacterial properties of in situ and surface functionalize impregnation of silver sulfadiazine (AgSD) in PAN nanofiber mats

4. Introduction

Advancement in technology has been beneficial for human being, meanwhile it has imparted some negative impacts on some of the major areas, and health is one of the most affected area among all of them. Biotechnology is also improving day by day by using advanced machinery as well as emerging materials which have better antibacterial,[1–6] biodegradability, and biocompatibility. Nanofiber mats have been used in biomedical applications since few decades. Nanofibers are important part of biomedical technology as 60% of total nanofibers production is specifically used in biomedical applications. It can be tumor therapy,[7] wound dressing, drug delivery, self-healing of wounds, or implants.[8–11]

Silver, incorporation with natural or synthetic polymers, has been used as an effective antibacterial agent since decades. Silver has potential applications in healthcare especially in nanoparticles form. Silver Sulfadiazine (AgSD) has been used for treatment of second order burns for the in early 1970's.[12] By that time, it was considered at lower concentration, sulfadiazine group in AgSD was not effective for antibacterial activity but it was effective either in combination with silver or at higher concentrations.[13] Several studies were carried out to investigate the effect of cerium salt on inactivation of silver sulfadiazine and it was observed that addition of cerium salts made inhibition zone closer which was associated to inactivation of silver sulfadiazine.[14] At first, silver nano-particles were not accepted as an effective antimicrobial agent because of availability of other good due to emerging antibacterial agents which were available in market, but. The use of AgNPs as antibacterial agent went up due electrospinning method because electrospinning provides efficient use of metallic nano-particles.[15] Nylon/silver based composite membranes were analyzed for structural applications, and it resulted in improved mechanical properties of composite membranes as compared to that of nylon membranes.[16] Higher antibacterial activity was also observed in electrospun Polyvinyl Alcohol (PVA) and Chitosan (Cs) incorporation with Sliver nitrate ($AgNO_3$).[17] Silver nano-particles (AgNPs) impregnation in Nylon 6 by one step direct electrospinning of have also been characterized for surface, morphological, and antimicrobial activity as well.[18]

AgNPs have broad applications when incorporated with natural or synthetic polymers, i.e., Zein, Poly methyl methacrylate (PMMA), Chitosan, Polyvinylpyrrolidone (PVP), Polyacrylonitrile (PAN), and other polymers as well. [11,19–21]

Polyacrylonitrile (PAN) is a white, semi-crystalline organic synthetic polymer with chemical formula of C_3H_3N. PAN was synthesized in 1930 for the first time. It degrades above 300°C.[22] PAN fibers having diameter less than 1 micron were successfully prepared in 1971, and effect of flow rate of polymer on final properties was studies in detail.[23] Effect of loading proportions of Ag nanoparticles (Ag nanoparticles were embedded by photocatalytic reduction of silver nitrate under UV irradiation) on PAN/TiO_2 was studied and it was concluded that Ag nanoparticles (~2nm size) were greatly affected by the amount of TiO_2 present in nanofibers.[24] PAN-PANI super-hydrophobic nanofibers mats were fabricated by in-situ polymerization method which had water contact angle of 164.5˚. Prepared nanofibers were also reversible to hydrophilic within a short time.[25] PAN nanofiber membrane was successfully prepared and characterized for soybean oil hydrolysis process. It was done by immobilization of lipase by covalent bonding.[26] Similar technique was also used for biodiesel production from soybean oil.[27] PAN (core & shell) nanofiber mats have been used in skin care applications incorporation with vitamin C and vitamin E extracts. Concerned application area for such products is protection against damage by UV rays.[28] PAN/PVDF nanofibers were surface modified by low vacuum plasma treatment for water remediation application.[29] PAN nanofibers are not only useful in medical applications but these cover other fields of science as well. Surface modified PAN nanofibers have been also used as substrate for identification of small molecules by Surface Enhanced Raman Scattering (SERS).[30] Electrospinning is a useful technique to fabricate nanofibers having diameters ranging from tens of nanometer to microns.[31,32] Since electrospinning is not new method for fabrication of nanofibers, it was started from 1931 but proper setup for producing nanofibers from electrospinning became practical and popular in early 21st century. From then it has been used for production of nanofibers for different applications including water filtration, wound care, breath masks, and other biomedical applications too. Natural and synthetic fibers have been electrospun either in single form or blends of different types of polymers to get desired features.[33–40] Figure 4. *1* briefly illustrate process of electrospinning.

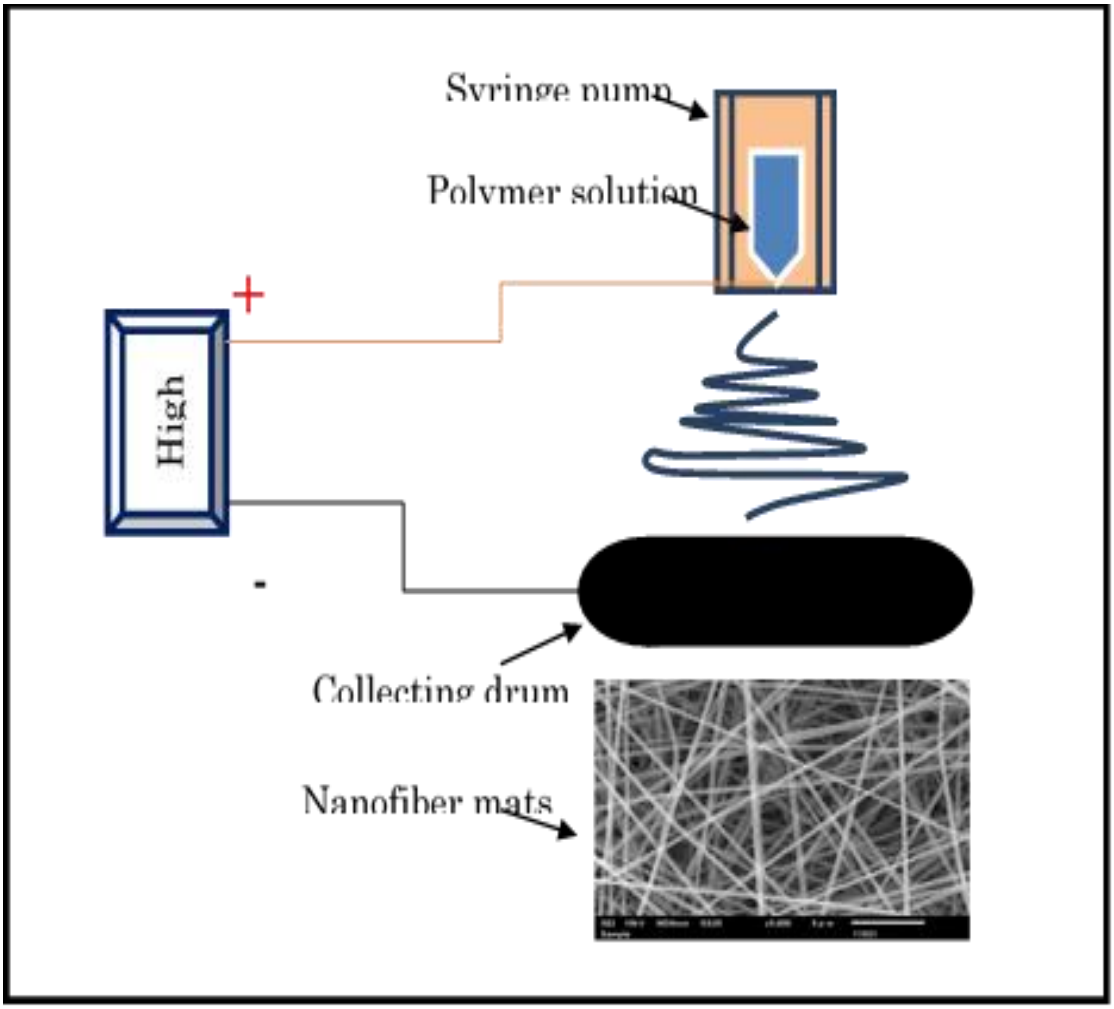

Figure 4. 1 Schematic illustration of electrospinning process

Keeping in view of applications of PAN and AgSD in biomedical field, we prepared PAN/AgSD nanofiber mats for wound dressing. We are first to load AgSD on electrospun nanofiber mats as well as fabrication of AgSD on nanofiber mats by immersion method. This research will be beneficial for other researchers as well as industries to produce PAN nanofiber with better antimicrobial properties either by in situ loading of AgSD or deposition of AgSD on nanofiber mats by immersion method. Combination of mechanical & thermal properties of PAN nanofibers and antibacterial properties of AgSD would be effective for biomedical applications.

4.1 Experimental work

4.1.1 Materials

PAN polymer was purchased from the Sigma-Aldrich Corporation (Saint Louis, MO 63103, USA), that was in powder form and had average molecular weight of 150,000 (typical). Sulfadiazine sodium salt

(analytical standard, ≥98%) was purchased from Sigma-Aldrich Corporation (Saint Louis, MO 63103, USA). Silver Nitrate ($AgNO_3$), with purity 99.8%, was purchased from FUJIFILM Wako Pure Chemical Corporation (Osaka, Japan). N,N-Dimethylformamide (DMF) was purchased from FUJIFILM Wako Pure Chemical Corporation (Osaka, Japan). Silver (I) sulfadiazine (AgSD) was purchased from Sigma-Aldrich Corporation (Saint Louis, MO 63103, USA) in powder form with 98% purity. Sodium Hydroxide (NaOH) (in pallets form) was purchased from FUJIFILM Wako Pure Chemical Corporation (Osaka, Japan). Distilled water was used from laboratory.

4.1.2 Methods

Samples were prepared by following 3 methods.

1. Pure PAN nanofiber mats

PAN (8% by weight) was dissolved in DMF. Solution was kept on stirring for 12 hours at room temperature (25±3℃) and solution was then loaded to electrospinning for nanofiber production. Electrospinning conditions were as follows: syringe capacity 20ml, nozzle diameter 0.5 mm, Voltage was fixed on 15kv, distance between nozzle and collector drum was kept on 14cm, and flow rate of solution was 0.5ml/h. Electrospinning conditions remained same for all samples.

2. PAN/AgSD in-situ Electrospun ((PAN/AgSD (E.S))

For PAN/AgSD (E.S) samples, firstly PAN (8% by weight) was dissolved in DMF for 12 hours and then AgSD (0.6% by weight) was added to the PAN/DMF solution and kept on stirring for 2 hours. Then solution was loaded to electrospinning on the same parameters as that of for sample 1.

3. Self-synthesized AgSD on PAN nanofibers (PAN/AgSD Immersion)

For PAN/AgSD Immersion samples, in first step pure PAN nanofiber mats were electrospun as per all parameters of sample 1 and then samples were placed in glass tray which contained aqueous solution of Sulfadiazine sodium salt (0.2% by weight) and Silver nitrate (0.1% by weight). Tray was placed in controlled stirring chamber for 24 hours and then samples were removed from solution of SD and $AgNO_3$ and were placed in (0.1% by weight) aqueous solution of sodium hydroxide (NaOH) for 4 hours for reduction of

AgNO3. Samples were then dried in vacuum oven at 30℃ for 12 hours. Samples were kept in air-tight bags for further testing.

4.2 Characterizations

Antibacterial properties were determined by disc diffusion method where *E.coli* (BUU25113) and *Bacillus* (B-sub 168) bacteria strains were used as gram negative and gram positive bacteria respectively. The nanofiber mats were cut in to discs having 8mm diameter and were placed on top of two different plates, which were cultured with each bacteria strain and incubated overnight for 12h at 37^{o}C. The morphological properties of prepared nanofiber mats were determined by using Scanning Electron Microscope (SEM) (JSM-5300, JEOL Ltd, Japan), which was accelerated with the voltage of 10 kV, and TEM (JEM-2100 JEOL Japan), accelerated with 200 kV and an image analysis software (Image J, version 1.4.3) was used to calculate the average diameters of nanofibers by taking 50 readings randomly for each sample. Wide angle X-ray diffractions (WAXRD) was performed for the determination of the crystal structure (at 25°C) of nanofiber mats using Nickel-filtered Cu. Ka radiation assisted Rotaflex RT300 mA (Rigaku manufacturer, Osaka, Japan), with an angular angle of $5 \leq 2\theta \leq 80°$. The chemical reactivity among PAN and AgSD functional groups was characterized by using FTIR with an attenuated total reflectance (ATR) Prestige-21 (Shimadzu, Japan) and wavelength for ATR spectra was set in the range of 400cm^{-1} to 4000cm^{-1}. Thermal degradation of PAN, PAN/AgSD (E.S), and PAN/AgSD (Immersion) was studied thermogravimetric analysis (TGA) using thermo-plus TG 8120 (Rigaku Corporation, Osaka, Japan) which was run under ambient conditions (room temperature) at heating rate of 10 °C/min and temperature range was set 0–500°C for all samples. The XPS analysis was performed by using Shimadzu-Kratos AXIS-ULTRA HAS SV (Shimadzu, Kyoto, Japan). Mechanical properties (tensile strength, strain, and modulus) of PAN and PAN/AgSD nanofibers was determined by using the Universal Testing Machine (Tesilon RTC 250A; A&D Company Ltd., Japan). Five specimen for each sample were prepared, according to ISO 13634. Test was run at room temperature and crosshead speed was kept as 5 mm/min. From UTM data, values of strain, stress, and Young's modulus were calculated by the following equations (1), (2), and (3) respectively.

$$\varepsilon = \frac{\Delta l}{l} \quad \text{..... Equation 4}$$

$$\sigma = \frac{F}{A} \quad \text{.....Equation 5}$$

$$E = \frac{\sigma}{\varepsilon}$$ ……. Equation 6

Where ε, σ, and E are strain, stress, and Young's modulus. Δl is change in length, l is original length of specimen, F is applied force, and A is cross sectional area of specimen.

4.3 Results & discussions

4.3.1 Antibacterial activity test

Disc diffusion method was opted to investigate antibacterial properties of prepared nanofiber mats as shown in Figure *4.* (A) E.coli. (B) Bacillus. *E.coli. and Bacillus* bacteria strain were associated to gram-negative and gram-positive bacteria respectively. Zone inhibition around the disc was determined to evaluate the effectiveness of antibacterial property of nanofibers (due to AgSD released from PAN nanofibers). The antibacterial activity of AgSD loaded PAN nanofiber mats was taken into account for both bacteria strains compared with control sample. Excellent antibacterial efficiency was observed for both samples while sample having AgSD by immersion method ((PAN/AgSD (Immersion)) showed consistent results for both types of bacteria. It was detected that as amount of AgSD In samples was increased, it had a significant influence on antibacterial property of nanofiber mats. Herein, from the results it was concluded that self-synthesized AgSD on PAN nanofibers had better antibacterial activity as compared to in situ added AgSD in PAN nanofibers.

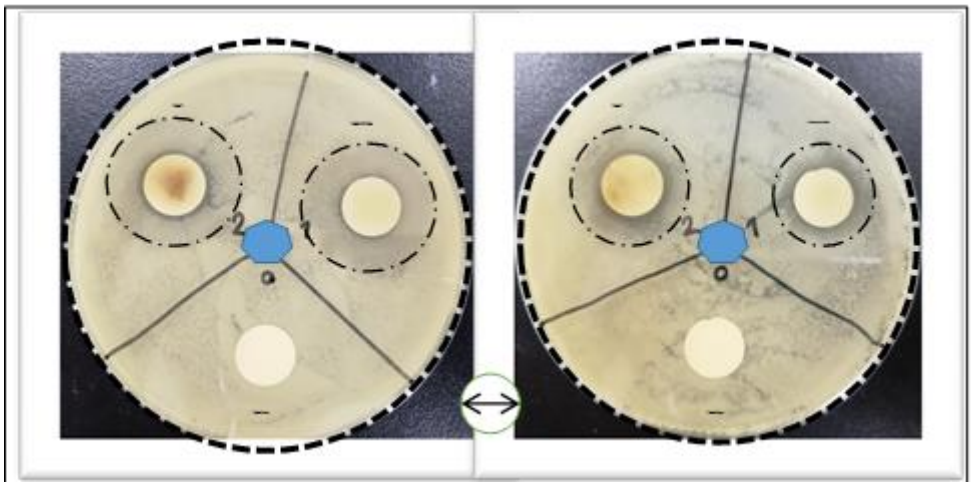

Figure 4.2 Antibacterial activity test (A) E.coli (B) Bacillus

4.3.2 Morphological properties

Morphological properties of prepared nanofiber mats were determined by SEM. The SEM images in Figure 4. Show that nanofibers of pure PAN were smooth without any bead formation on specified conditions. Addition of AgSD by in situ method affected smoothness of electrospun fibers as they became slightly rough and slight increment in diameter was also noted. SEM image of samples having AgSD by immersion method showed that AgSD got entangled in between PAN nanofibers as well AgSD nanocrystal were also observed on the surface of nanofibers. Diameter of PAN/AgSD Immersion samples was also slightly greater than both of the previous samples.

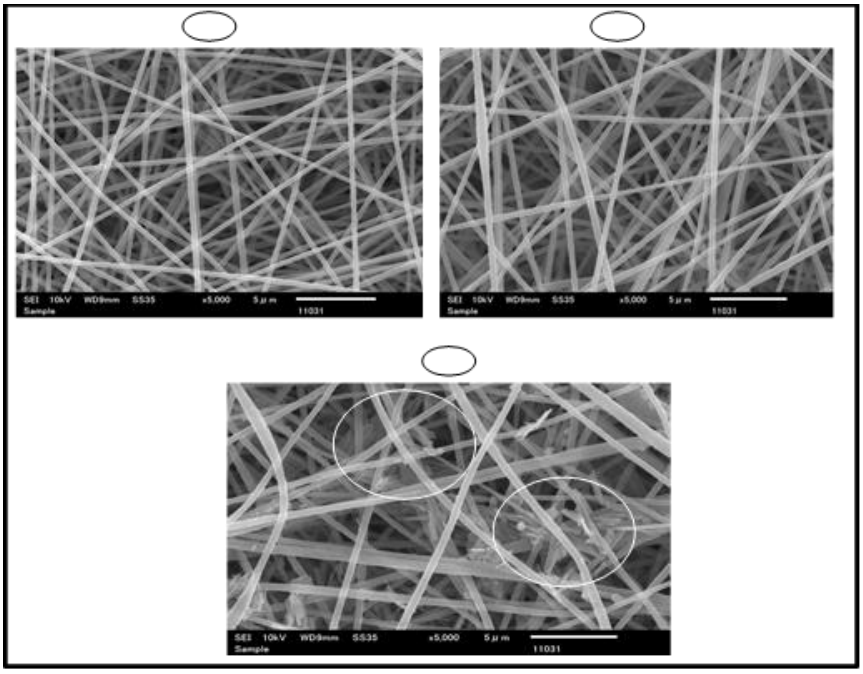

Figure 4.3 SEM images of (a) PAN nanofibers, (b) PAN/AgSD (E.S) nanofibers, (c) PAN/AgSD (Immersion) nanofibers

Figure 4. shows nanoparticles distribution on the nanofibers. It can be observed that AgSD nanoparticles were evenly distributed on the surface of nanofibers which were prepared by direct in situ method. While, AgSD synthesized by immersion method showed nanoparticles in the form of grafts. Surface of nanofibers was also covered by AgSD grafts.

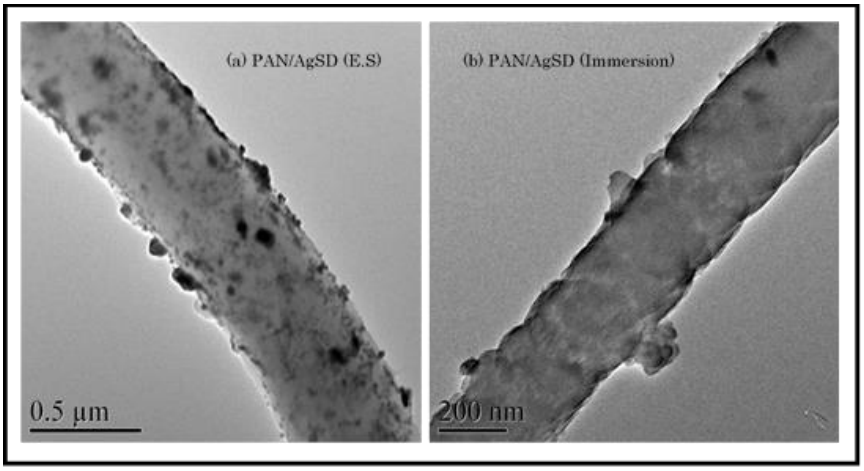

Figure 4.4 TEM images of (a) PAN/AgSD (E.S) nanofiber mats, (b) PAN/AgSD (Immersion) nanofiber mats

4.3.2.1 Nanofiber's diameter

As we mentioned above that diameter of nanofibers was altered with impregnation of AgSD in to the PAN either by in situ method or immersion method. Figure 4. shows quantitative explanation of average diameters of nanofibers. The average of 50 nanofibers from each sample exhibited slight variation in diameters. In Figure 4., it can be noticed that average diameters of PAN, PAN/AgSD (E.S), PAN/AgSD (Immersion) were 141.94, 145.02, and 146.94 respectively. Although there is slight increment in diameters with addition of AgSD in PAN nanofibers but these diameters are within the range of standard deviation of all samples. So, we can conclude that there was slight or no effect of AgSD on the diameter of PAN nanofibers.

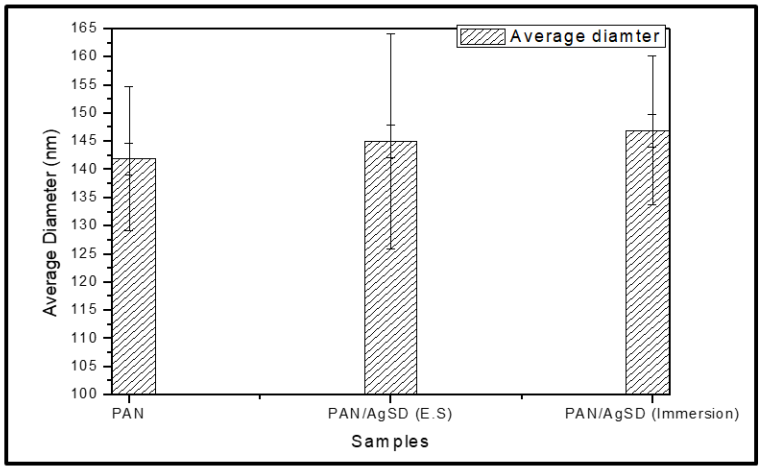

Figure 4.5 Diameter interpretation of PAN and PAN/AgSD nanofibers

4.3.3 EDX analysis

EDX study was carried out for the quantitative assessment of Sulfur and Ag contents in the nanofibers. It can be shown in Figure 4. that sample (a) has lower values of Ag and S as compared to that of sample (b). It was concluded that samples having self-synthesized AgSD by immersion method had higher values of both Ag as well as S. further it was also proven by antibacterial activity test where self-synthesized AgSD on PAN nanofibers had shown excellent results.

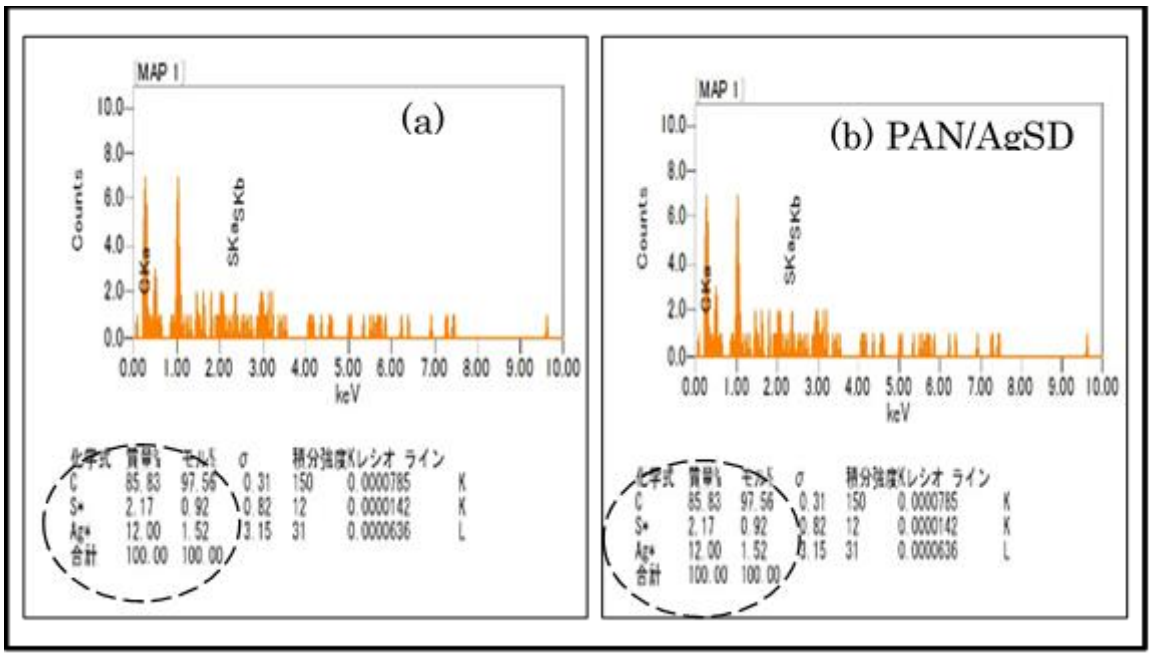

Figure 4.6 EDX analysis of PAN/AgSD (E.S) and PAN/AgSD (Immersion) nanofibers

4.3.4 FTIR Interpretation

FTIR spectra of pure PAN and composite nanofibers of PAN/AgSD are shown in Figure 4.. It was observed that AgSD had shown sharp peaks at 1203 and 1231.6 cm^{-1} which can be associated with the main functionality of AgSD that is SO_2 asymmetric stretching. AgSD loaded nanofibers had also represented peaks on 1561 cm^{-1}, 1583 cm^{-1} and 3410 cm^{-1} which can be associated with stretching band of amine (NH_2) group. It was interesting to observe that the spectra of pure PAN nanofibers was not affected by impregnation of AgSD in PAN nanofibers, which leads towards indication that there may be no chemical reaction between PAN and AgSD [29,30]. PAN showed prominent peaks at 1452 cm^{-1}, 1664 cm^{-1}, 2240 cm^{-1}, and 2923cm^{-1}. Peaks at 1664 cm^{-1}, 2240 cm^{-1}, and 2923cm^{-1} represent stretching vibrations of –C=N, –C≡N, and –CH

groups respectively while peak at 1452 cm^{-1} represents bending vibration of –CH2 group. It was observed that characteristic peak of PAN nanofibers at wavelength of 1664 cm^{-1} slightly decreased with in situ addition of AgSD in PAN while same peak becomes shorter with addition of AgSD by immersion method. It was also observed that PAN/AgSD (Immersion) samples showed higher intensity and sharper peaks than PAN/AgSD (E.S) samples.

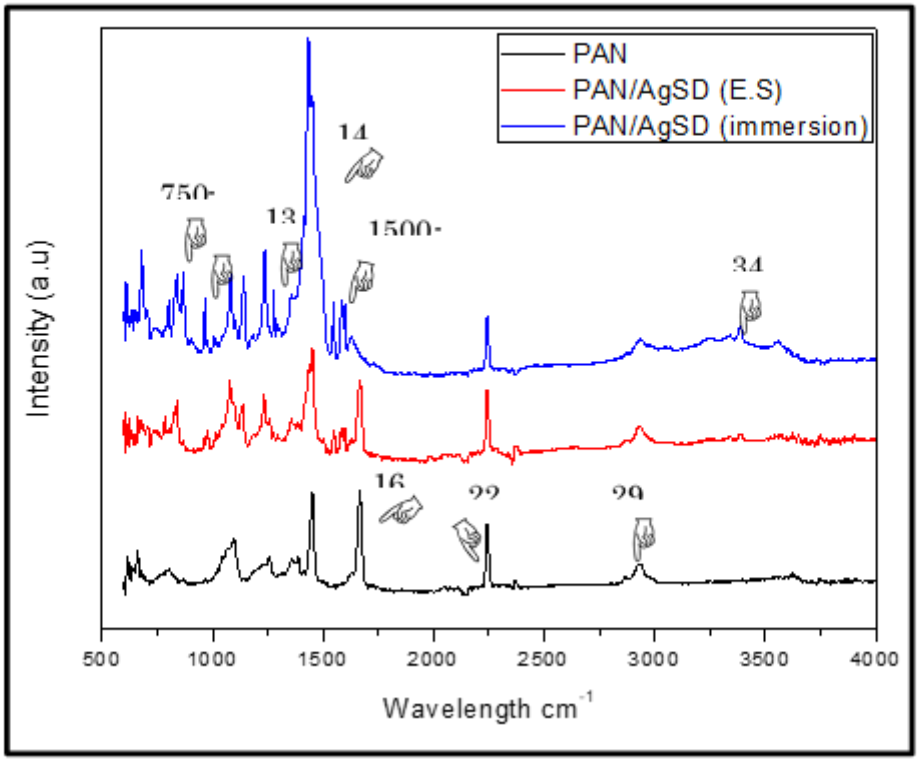

Figure 4.7 FTIR-ATR Spectra of PAN and PAN/AgSD nanofiber mats

4.3.5 X-Ray diffraction (XRD)

XRD was studied to check crystalline structure of nanofiber mats. Pure PAN nanofibers (Figure 4.) showed a sharp peak at 2θ = 17˚, and a small peak at 2θ = 30˚.while PAN did not exhibit any peak up to 2θ = 80˚. PAN nanofibers showed characteristic peaks of pure PAN. First peak (17˚) could be associated with hexagonal lattice of PAN. Impregnation of AgSD in PAN exhibited sharp peaks at 2θ = 9˚, 2θ = 11˚, 2θ = 21˚, and many shorter peaks from 2θ = 30˚ to 2θ = 60˚. All other peaks, except from the two peaks (2θ = 17˚and 2θ = 30˚), represented the occurrence of AgSD and all those were linked with AgSD. XRD plot also

revealed that stability of PAN was altered by the impregnation of AgSD, as intensity of characteristic peak (2θ = 17˚) decreased with addition of AgSD. It was observed that PAN/AgSD (Immersion) sample showed higher intensity peaks than that of PAN/AgSD (E.S) samples. Presence of AgSD in PAN nanofibers were also confirmed by XPS analysis.

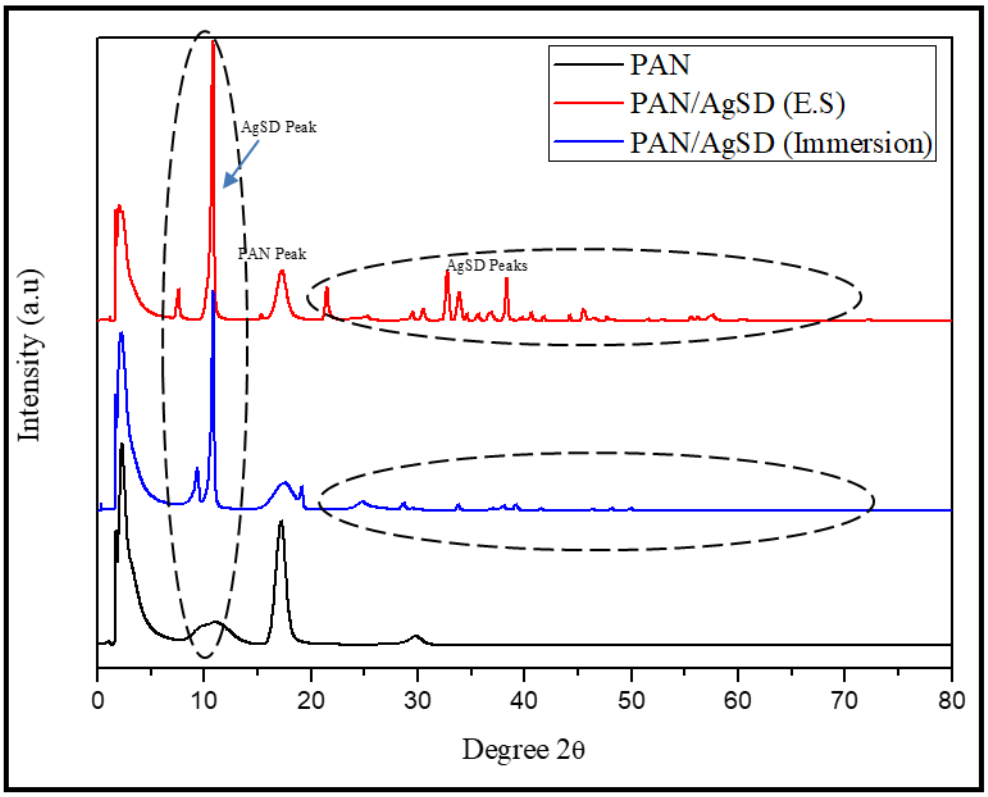

Figure 4.8 XRD analysis of PAN nanofibers and PAN/AgSD nanofibers

4.3.6 Thermogravimetric analysis (TGA)

TGA was performed to analyze the significance of AgSD on thermal properties of PAN. Also, effect of in situ added and self-synthesized AgSD on thermal properties of PAN nanofibers was taken under consideration. TGA curve is generally separated in to three parts. Where 1st part (up to 100°C) declares moisture removal. 2nd part of curve indicates thermal degradation onset and offset as well, and the last part indicates combustion zone where residual amount is measured. It can be observed in Figure 4. that 1st part of TGA curve represented the higher amount of moisture absorbed by PAN/AgSD (Immersion) nanofibers than that of PAN nanofibers and PAN/AgSD (E.S) nanofiber mats. The 2nd part of TGA curve, which

indicates the onset temperature, showed that onset of pure PAN nanofibers was at 320℃. PAN/AgSD (E.S) showed onset at 290℃ and onset of PAN/AgSD (Immersion) occurred at 190℃. PAN/AgSD (E.S) nanofibers showed a sharp onset, while PAN/AgSD (Immersion) showed gradual onset. Residual amounts for PAN nanofibers, PAN/AgSD (E.S), and PAN/AgSD (Immersion) were 58%, 44%, and 32% respectively. From TGA data it was decided that impregnation of AgSD caused low thermal stability to PAN. As PAN has excellent thermal stability so addition of AgSD made it degradable which is taken as good characteristic for biomedical applications.

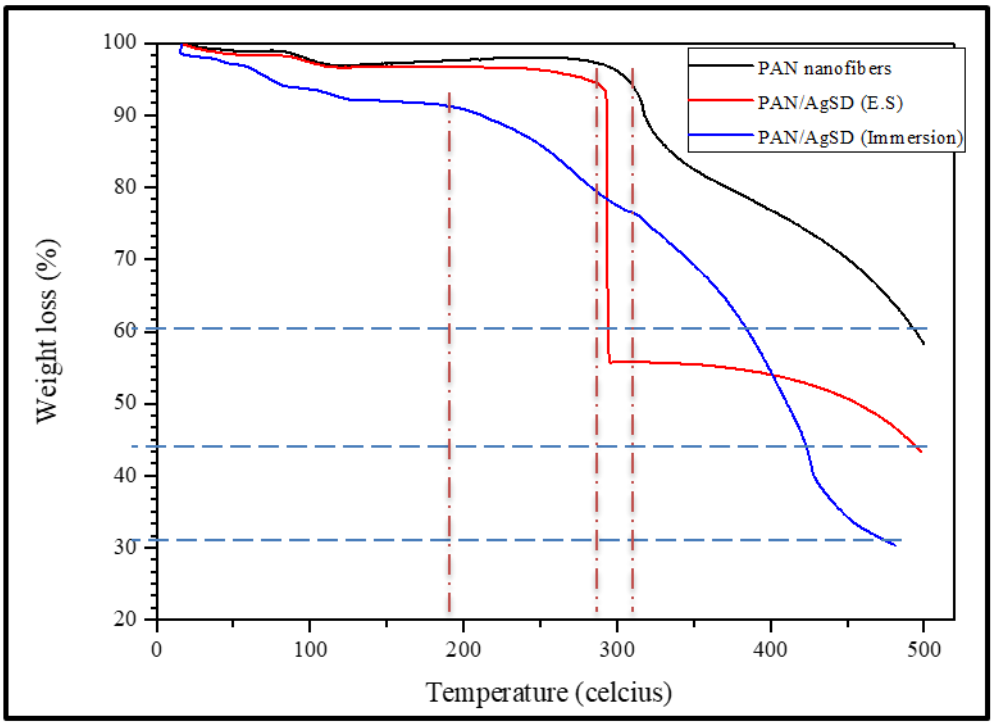

Figure 4.9 Thermal degradation analysis of PAN nanofibers and PAN/AgSD nanofiber

4.3.7 X-Ray spectroscopy (XPS)

XPS was performed to confirm the existence of AgSD in nanofiber mats (Figure 4.). As AgSD consists of Ag (Silver) and S (Sulfur), that's why XPS spectra for Ag (3d and 3p) and Sulfur (2s and 2p) were attained. Ag 3p spectra showed two peaks at 574.0 eV (Ag $3p_{3/2}$) and 606.0 eV (Ag $3p_{1/2}$) with a split of 32eV. Spectra of Ag 3d showed peaks at 370.0 eV and 376.5 eV with a split of 6.5 eV .Those peaks can be correlated to metallic Ag present in nanofibers. The standard peaks for Ag $3p_{3/2}$ and Ag $3p_{1/2}$ were noted at 570.0 eV and

604.0 eV respectively while standard peaks for Ag $3d_{5/2}$ and Ag $3d_{3/2}$ were noted at 368 eV and 374.5 eV. Spectra of S 2s had showed peak at 234.0 eV and that of S 2p at 169.0 eV. But in case of PAN/AgSD (E.S) sample, it was observed that S 2s showed one more peak at 239 eV. While standard peaks for S 2s and S 2p were noted at 231.0 eV and 164.5 eV. It can be seen in Figure 4. that all relevant peaks for Ag and S are sharper and have higher intensity for PAN/AgSD (Immersion) samples as compared to that of PAN/AgSD (E.S) samples. XPS spectra provided clear evidence of presence of silver and sulfur in the nanofiber mats.

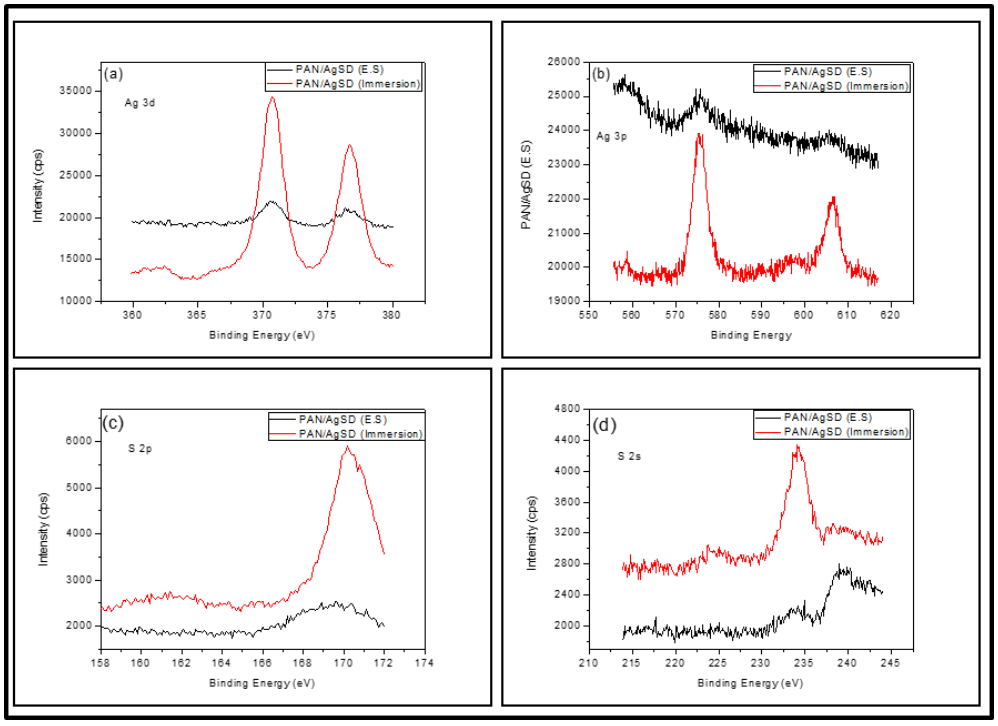

Figure 4.10 XPS analysis of PAN/AgSD (E.S) and PAN/AgSD (Immersion); (a) Ag 3d, (b) Ag 3p, (c) S 2p, and (d) S 2s

4.3.8 Mechanical properties

Mechanical properties (Tensile strength, strain, Young's modulus) of prepared samples were analyzed. Table 4.3 sums up all results obtained from UTM data. It can be also shown in Figure 4. that PAN nanofibers showed higher tensile strength (3.984 MPa) while in situ addition of AgSD decreased the tensile strength of PAN. It can be related with weak physical affection between AgSD and PAN. As from FTIR spectra it was observed that there was no chemical reaction between AgSD and PAN due to retained peaks of PAN in blend form too. It was interesting to observe that tensile strength of PAN/AgSD (Immersion) sample was increased (4.163 MPa) which is indication of stronger physical bonding between AgSD and PAN nanofibers. In SEM

images (Figure 4.) it was observed that PAN/AgSD (Immersion) nanofibers have entangled AgSD in between the joints of nanofibers as well as on the surface of nanofibers, which gives mechanical stability to PAN nanofibers.

Table 4.3 Summary of mechanical properties of PAN nanofibers and PAN/AgSD nanofibers

	PAN Nanofibers	PAN/AgSD (E.S)	PAN/AgSD (Immersion)
Tensile Strength (MPa)	3.984± 0.186	1.728 ± 0.263	4.163 ± 0.314
Elongation at break (%)	11.254 ± 2.317	14.087 ± 1.971	41.004 ± 4.035
Young's Modulus (MPa)	35.400	12.613	10.153

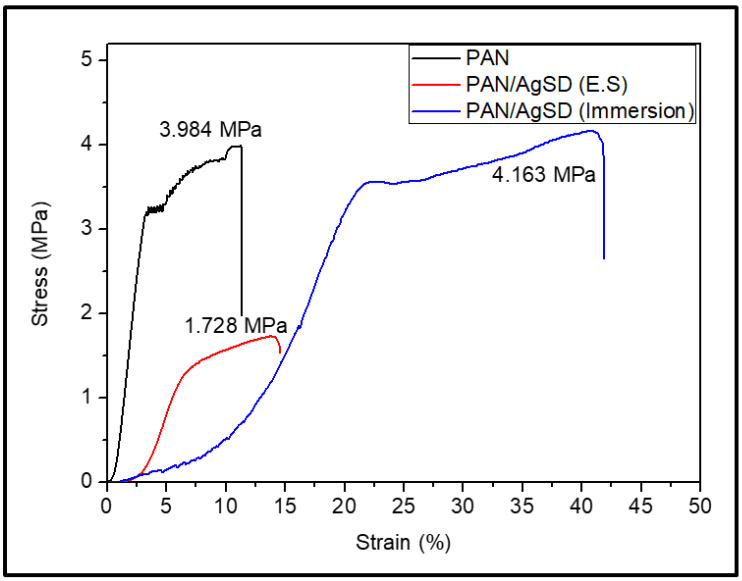

Figure 4.11 Stress-Strain curve of PAN nanofibers and PAN/AgSD nanofibers

As for as elongation at break is concerned, it can be viewed in Figure 4. that elongation at break increased with addition of AgSD either by in situ method or by immersion method. But PAN/AgSD (Immersion) nanofiber mats showed higher value of elongation at break than that of PAN/AgSD (E.S) nanofiber mats.

Figure 4.12 shows bar chart of tensile strength of all samples with standard deviation. Young's modulus is also one of the important performance parameters.

Figure 4.13 shows pictorial analysis and Table 4.3 shows quantitative data of Young's modulus of the samples. It was observed that value of Young's modulus was gradually decreased with addition of AgSD by in situ and immersion methods respectively.

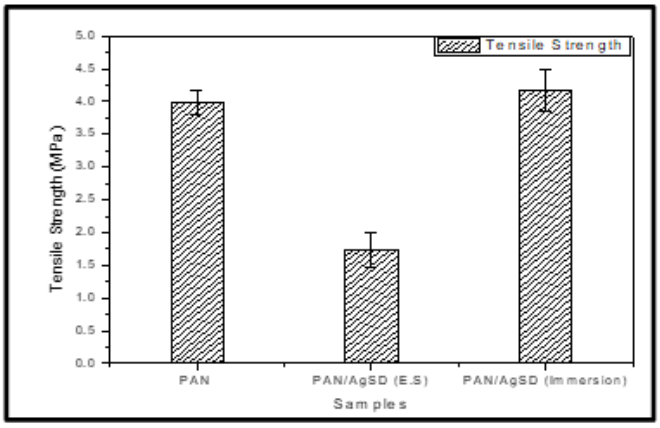

Figure 4.12 Comparison of tensile strength of PAN nanofibers, PAN/AgSD (E.S), and PAN/AgSD (Immersion) nanofibers

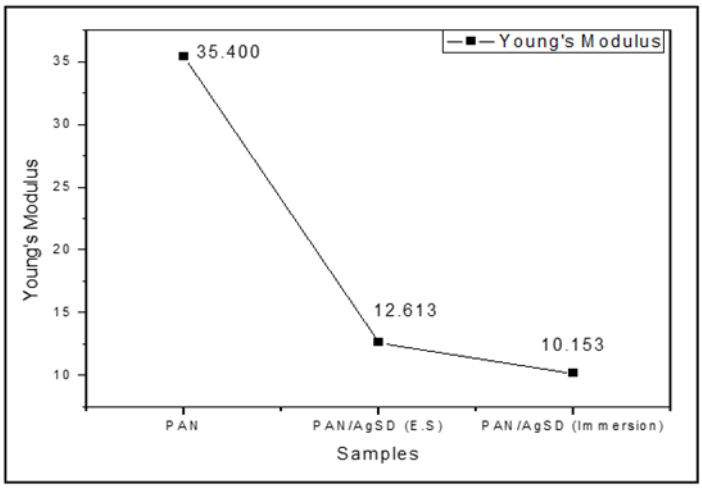

Figure 4.13 Comparison of Young's modulus of PAN nanofibers, PAN/AgSD (E.S), and PAN/AgSD (Immersion)

4.4 Conclusions

Keeping in mind all the results and discussions of prepared specimen, it is concluded that PAN has retained its structure and basic characteristics with addition of AgSD. Antibacterial activity test showed excellent antibacterial results for both PAN/AgSD (E.S) and PAN/AgSD (Immersion) nanofiber mats. From SEM results it is already discussed above that nanofiber structure was not much disturbed by AgSD. Surface of nanofiber became slightly rough which is considered to be helpful for antibacterial activity. FTIR spectra showed characteristic peaks of AgSD and PAN in nanofibers. There was no shift of peak observed so it can be referred to physical bonding between PAN and AgSD. XPS spectra clearly showed presence of Ag and S in nanofiber mats. It was observed that for all above mentioned characterizations, PAN/AgSD (Immersion) nanofibers showed prominent results. XRD analysis showed that crystalline structure of PAN was changes as peak at $2\theta = 17^{\circ}$, which was associated with hexagonal lattice of PAN, was decreased with addition of AgSD which was further observed in TGA study that thermal degradation of PAN/AgSD (E.S) and PAN/AgSD (Immersion) was lower than PAN nanofibers. Tensile strength and elongation at break was increased by addition of AgSD by immersion technique, while tensile strength was decreased with in situ addition of AgSD in PAN nanofibers during electrospinning. From all results it is concluded that PAN/AgSD (Immersion) nanofiber mats have better structural and antibacterial properties than that of PAN/AgSD (In situ) nanofiber mats. So, from our point of view, self-synthesized AgSD is recommended for further production of nanofiber mats for antibacterial applications.

References

1. Lin L, Dai Y, Cui H. Antibacterial poly(ethylene oxide) electrospun nanofibers containing cinnamon essential oil/beta-cyclodextrin proteoliposomes. Carbohydr Polym. 2017;178(June):131-140. doi:10.1016/j.carbpol.2017.09.043

2. Cui H, Bai M, Lin L. Plasma-treated poly(ethylene oxide) nanofibers containing tea tree oil/beta-cyclodextrin inclusion complex for antibacterial packaging. Carbohydr Polym. 2018;179(October 2017):360-369. doi:10.1016/j.carbpol.2017.10.011

3. Lin L, Zhu Y, Li C, Liu L, Surendhiran D, Cui H. Antibacterial activity of PEO nanofibers incorporating polysaccharide from dandelion and its derivative. Carbohydr Polym. 2018;198(February):225-232. doi:10.1016/j.carbpol.2018.06.092

4. Cui H, Bai M, Rashed MMA, Lin L. The antibacterial activity of clove oil/chitosan nanoparticles embedded gelatin nanofibers against Escherichia coli O157:H7 biofilms on cucumber. Int J Food Microbiol. 2018;266(November 2017):69-78. doi:10.1016/j.ijfoodmicro.2017.11.019

5. Lin L, Mao X, Sun Y, Rajivgandhi G, Cui H. Antibacterial properties of nanofibers containing chrysanthemum essential oil and their application as beef packaging. Int J Food Microbiol. 2019;292(May 2018):21-30. doi:10.1016/j.ijfoodmicro.2018.12.007

6. Cui H, Wu J, Li C, Lin L. Improving anti-listeria activity of cheese packaging via nanofiber containing nisin-loaded nanoparticles. LWT - Food Sci Technol. 2017;81:233-242. doi:10.1016/j.lwt.2017.04.003

7. Wu C, Zhao J, Hu F, et al. Design of injectable agar-based composite hydrogel for multi-mode tumor therapy. Carbohydr Polym. 2018;180(August 2017):112-121. doi:10.1016/j.carbpol.2017.10.024

8. Kharaghani D, Kee Jo Y, Khan MQ, Jeong Y, Cha HJ, Kim IS. Electrospun antibacterial polyacrylonitrile nanofiber membranes functionalized with silver nanoparticles by a facile wetting method. Eur Polym J. 2018;108(August):69-75. doi:10.1016/j.eurpolymj.2018.08.021

9. Khan MQ, Kharaghani D, Nishat N, et al. The development of nanofiber tubes based on nanocomposites of polyvinylpyrrolidone incorporated gold nanoparticles as scaffolds for

neuroscience application in axons. Text Res J. 2018;(October):004051751880118. doi:10.1177/0040517518801185

10. Lee H, Xu G, Kharaghani D, et al. Electrospun tri-layered zein/PVP-GO/zein nanofiber mats for providing biphasic drug release profiles. Int J Pharm. 2017;531(1):101-107. doi:10.1016/j.ijpharm.2017.08.081

11. Dashdorj U, Reyes MK, Unnithan AR, et al. Fabrication and characterization of electrospun zein/Ag nanocomposite mats for wound dressing applications. Int J Biol Macromol. 2015;80:1-7. doi:10.1016/j.ijbiomac.2015.06.026

12. Ullah S, Hashmi M, Khan MQ, et al. Silver sulfadiazine loaded zein nanofiber mats as a novel wound dressing. RSC Adv. 2019;9(1):268-277. doi:10.1039/C8RA09082C

13. Fox CL, Modak SM. Mechanism of Silver Sulfadiazine Action on Burn Wound Infections Mechanism of Silver Sulfadiazine Action on Burn Wound Infections. Antimicrob Agents Chemother. 1974;5 (6)(6):582-588. doi:10.1128/AAC.5.6.582.Updated

14. Alan Holder I. In vitro inactivation of silver sulphadiazine by the addition of cerium salts. Burns. 1982;8(4):274-277. doi:10.1016/0305-4179(82)90009-2

15. Rai M, Yadav A, Gade A. Silver nanoparticles as a new generation of antimicrobials. Biotechnol Adv. 2009;27(1):76-83. doi:10.1016/j.biotechadv.2008.09.002

16. Francis L, Giunco F, Balakrishnan A, Marsano E. Synthesis, characterization and mechanical properties of nylon-silver composite nanofibers prepared by electrospinning. Curr Appl Phys. 2010;10(4):1005-1008. doi:10.1016/j.cap.2009.12.025

17. Hang AT, Tae B, Park JS. Non-woven mats of poly(vinyl alcohol)/chitosan blends containing silver nanoparticles: Fabrication and characterization. Carbohydr Polym. 2010;82(2):472-479. doi:10.1016/j.carbpol.2010.05.016

18. Pant B, Pant HR, Pandeya DR, et al. Characterization and antibacterial properties of Ag NPs loaded nylon-6 nanocomposite prepared by one-step electrospinning process. Colloids Surfaces A Physicochem Eng Asp. 2012;395:94-99. doi:10.1016/j.colsurfa.2011.12.011

19. GhavamiNejad A, Rajan Unnithan A, Ramachandra Kurup Sasikala A, et al. Mussel-Inspired Electrospun Nanofibers Functionalized with Size-Controlled Silver Nanoparticles for Wound Dressing Application. ACS Appl Mater Interfaces. 2015;7(22):12176-12183. doi:10.1021/acsami.5b02542

20. Yang CH, Wang LS, Chen SY, et al. Microfluidic assisted synthesis of silver nanoparticle–chitosan composite microparticles for antibacterial applications. Int J Pharm. 2016;510(2):493-500. doi:10.1016/j.ijpharm.2016.01.010

21. Maharjan B, Joshi MK, Tiwari AP, Park CH, Kim CS. In-situ synthesis of AgNPs in the natural/synthetic hybrid nanofibrous scaffolds: Fabrication, characterization and antimicrobial activities. J Mech Behav Biomed Mater. 2017;65:66-76. doi:10.1016/j.jmbbm.2016.07.034

22. Gupta a. K, Paliwal DK, Bajaj P. Melting behavior of acrylonitrile polymers. J Appl Polym Sci. 1998;70(13):2703-2709. doi:10.1002/(SICI)1097-4628(19981226)70:13<2703::AID-APP15>3.0.CO;2-2

23. Subbiah T, Bhat G, Tock R, Parameswaran S, Ramkumar S. Electrospinning of nanofibers. J Appl Polym Sci. 2005;96(2):557-569. doi:10.1002/app.21481

24. Lim SK, Lee SK, Hwang SH, Kim H. Photocatalytic deposition of silver nanoparticles onto organic/inorganic composite nanofibers. Macromol Mater Eng. 2006;291(10):1265-1270. doi:10.1002/mame.200600264

25. Zhu Y, Feng L, Xia F, Zhai J, Wan M, Jiang L. Chemical dual-responsive wettability of superhydrophobic PANI-PAN coaxial nanofibers. Macromol Rapid Commun. 2007;28(10):1135-1141. doi:10.1002/marc.200600902

26. Li SF, Wu WT. Lipase-immobilized electrospun PAN nanofibrous membranes for soybean oil hydrolysis. Biochem Eng J. 2009;45(1):48-53. doi:10.1016/j.bej.2009.02.004

27. Li S-F, Fan Y-H, Hu R-F, Wu W-T. Pseudomonas cepacia lipase immobilized onto the electrospun PAN nanofibrous membranes for biodiesel production from soybean oil. J Mol Catal B Enzym. 2011;72(1-2):40-45. doi:10.1016/j.molcatb.2011.04.022

28. Wu XM, Branford-White CJ, Yu DG, Chatterton NP, Zhu LM. Preparation of core-shell PAN nanofibers encapsulated α-tocopherol acetate and ascorbic acid 2-phosphate for photoprotection. Colloids Surfaces B Biointerfaces. 2011;82(1):247-252. doi:10.1016/j.colsurfb.2010.08.049

29. Yalcinkaya F, Yalcinkaya B, Pazourek A, Mullerova J, Stuchlik M, Maryska J. Surface Modification of Electrospun PVDF/PAN Nanofibrous Layers by Low Vacuum Plasma Treatment. Int J Polym Sci. 2016;2016. doi:10.1155/2016/4671658

30. Ren S, Dong L, Zhang X, et al. Electrospun nanofibers made of silver nanoparticles, cellulose nanocrystals, and polyacrylonitrile as substrates for surface-enhanced raman scattering. Materials (Basel). 2017;10(1). doi:10.3390/ma10010068

31. Wang S, Hu F, Li J, et al. Design of electrospun nanofibrous mats for osteogenic differentiation of mesenchymal stem cells. Nanomedicine Nanotechnology, Biol Med. 2018;14(7):2505-2520. doi:10.1016/j.nano.2016.12.024

32. Ye C, Zhao J, Zheng Y, et al. Preparation of Poly(lactic-co-glycolic acid)-Based Composite Microfibers for Postoperative Treatment of Tumor in NIR I and NIR II Biowindows. Macromol Biosci. 2018;18(10):1-13. doi:10.1002/mabi.201800206

33. Khan MQ, Kharaghani D, Nishat N, et al. The development of nanofiber tubes based on nanocomposites of polyvinylpyrrolidone incorporated gold nanoparticles as scaffolds for neuroscience application in axons. Text Res J. 2018:004051751880118. doi:10.1177/0040517518801185

34. Khan MQ, Kharaghani D, Nishat N, et al. In vitro assessment of dual-network electrospun tubes from poly(1,4 cyclohexane dimethylene isosorbide terephthalate)/PVA hydrogel for blood vessel application. J Appl Polym Sci. 2018;47222:47222. doi:10.1002/app.47222

35. Khan M, Kharaghani D, Ullah S, et al. Self-Cleaning Properties of Electrospun PVA/TiO2 and PVA/ZnO Nanofibers Composites. Nanomaterials. 2018;8(9):644. doi:10.3390/nano8090644

36. Haider A, Haider S, Kang IK. A comprehensive review summarizing the effect of electrospinning parameters and potential applications of nanofibers in biomedical and biotechnology. Arab J Chem. 2015. doi:10.1016/j.arabjc.2015.11.015

37. Khajavi R, Abbasipour M. Electrospinning as a versatile method for fabricating coreshell, hollow and porous nanofibers. Sci Iran. 2012;19(6):2029-2034. doi:10.1016/j.scient.2012.10.037

38. Pan T, Wang W. From cleanroom to desktop: Emerging micro-nanofabrication technology for biomedical applications. Ann Biomed Eng. 2011;39(2):600-620. doi:10.1007/s10439-010-0218-9

39. Gunn J, Zhang M. Polyblend nanofibers for biomedical applications: Perspectives and challenges. Trends Biotechnol. 2010;28(4):189-197. doi:10.1016/j.tibtech.2009.12.006

40. Xie J, Li X, Xia Y. Putting electrospun nanofibers to work for biomedical research. Macromol Rapid Commun. 2008;29(22):1775-1792. doi:10.1002/marc.200800381

Chapter 5

Optimized loading of carboxymethyl cellulose (CMC) in tri-component electrospun nanofibers having uniform morphology

5. Introduction

Advancement in technologies, product, and system design have brought revolution in lifestyle of mankind. However, continuous development is key to sustain in developing society. Nanotechnology is one of the most advanced technologies which covers wide range of applications. [1–3] Electrospinning is a technique to produce the nonwoven mats which offer large surface area to mass ratio. Nanofibers produced by electrospinning have diameter in the range of some nanometers to sub-micron while length of nanofibers can be in the range of some microns to sub-millimeter.[4–10] Due to high surface area, nanofibers from hydrophilic polymers may have best utilization in water adsorption or absorption. However applications of electrospun nanofibers are not limited to water treatment/adsorption only, but cover tissue engineering, biomedical engineering, energy storage, sensors and actuator, food packaging, air filtration, antibacterial, and antiviral nanofibrous products as well.[11–17] Hydrogels are very good in their water absorption properties. They have three dimensional macromolecular networks which swell in the presence of water but do not dissolve in the water. They possess excellent water absorption due to the hydrophilic functional groups which are attached to their backbone chain.[18,19]

Natural, semi-synthetic, and synthetic polymers have wide range of applications in materials science and engineering. However, sustainable development is key consideration for modern research. Cellulose is one of the most useful natural polymers having number of applications in tissue engineering, water treatment, filters, food and packaging industry, and other areas of science as well.[20–24] However, applications of cellulose are limited in the nanofibers based products due to high swelling, gel formation, and processing difficulties. To widen area of applications for cellulose, it is modified in to different semi-synthetics like cellulose acetate, CMC, hydroxyethyl cellulose, and other sub types of cellulose.[25–28] Carboxymethyl cellulose CMC is famous due to its versatile applications in different fields like drug delivery, tissue

engineering, food industry, cosmetics, printing and dying. CMC also gain attention due to its water holding capacity. It possess good water holding capacity even at low temperature. CMC has good water absorption properties in all forms but the absorption rate is higher in film than the fiber. It is reported that the 6000% of water has been absorbed by the CMC film from its initial mass while in fiber form it is 2000%. The water absorbing property of CMC is due to the presence of hydroxyl groups. Hydroxyl groups work as the bonding sites for the water through hydrogen bonding.[29,30] CMC is hydrophilic polymer. It can be easily dissolved in cold water without gel formation. It does not form gel in cold water because unsubstituted sites of backbone chain are not fully active and do not work. While the gel formation rate increase as the temperature of water increase because of unsubstituted sites of cellulose along the backbone chain act as temporary cross linkers between the chains. Viscosity of the CMC increase due to the gel formation and it became very difficult to electrospun.

PVA is a polymer having decreasing trend of viscosity as the temperature increase. The presence of hydroxyl groups on PVA create inter and intra molecular hydrogen bonding. Hydrogen bonding is the reason of the strong interaction between CMC and PVA. The mechanical properties of the blend is also very good. Blend possess smooth morphology with no bead formation. But there is bead formation as the concentration of CMC increase above 5%. Absorption rate of CMC may decrease by adding the PVA. To maintain the good absorption level it is necessary to introduce the strong hydrophilic polymer to the blend.[31–33] PVP is very good hydrophilic polymer with good biocompatibility, excellent film forming properties, non-toxicity, bio degradability and low surface tension.[34,35] PVP also possess electrical conductivity as its intrinsic characteristic and charge storage capacity.[36,37] PVP make strong interaction with both CMC and PVA. Carbonyl groups are present on the backbone chain of the PVP which make inter-chain hydrogen bond with the hydroxyl groups present on the PVA chain.

In this research, PVP and PVA were selected as carriers for CMC. Main objective of this research was to obtain smooth nanofibers with continuous electrospinning. Addition of CMC can enhance some of the characteristic properties of nanofibers which further widened the area of applications for PVA and PVP. CMC having excellent water holding capacity, biocompatibility, biodegradability, and other characteristics can be used in a number of applications such as food packaging (nanofibers based), biomedical and environmental engineering applications. This is a novel idea to load maximum possible amount of CMC on

electrospinning to get uniform nanofibers which can be utilized in practical applications. In future, authors have plan to carry on this idea to further characterize tri-component nanofibers consisting optimized ratios of PVA, PVP, and CMC for mechanical, biodegradability, and water holding capacity to specify application area for betterment of society.

5.1 Materials and methods

Polyvinylpyrrolidone (PVP) with an average molecular weight of 40,000 was purchased from Sigma-Aldrich (USA), Polyvinyl alcohol (PVA) with an average molecular of 85000-124000 and 87-89% hydrolyzed was purchased from Sigma-Aldrich, and sodium carboxymethyl cellulose (Na-CMC) with an average molecular weight of 250,000 and degree of substitution of 1.2 was also purchased from Sigma-Aldrich chemicals (USA). All materials were used as received without chemical or physical modification.

Concentration of PVA in spinning solution was kept constant (6% w/w) while weight percentage of PVP and CMC were varied. PVP was added from 10 weight percent to 14 weight percent while CMC was added as lowest from 1 percent to 3 weight percent as shown in Table . Distilled water was used as solvent for PVA, CMC, and PVP. Stated quantities of polymers were blended and stirred for 8 hours at 60℃ to get homogenous solution. Viscosity of each spinning solution (3 samples for each solution) was measured by a viscometer using 63 number cylinder. Electrospinning was carried out a voltage of 20 kV, distance from tip to collector (cooking sheet was wrapped on collecting drum to get nanofibrous mats) was kept at 18 cm, and flow rate of spinning solution was set to 1.0 ml/h. All samples were prepared following same procedure and conditions. After electrospinning all each sample was kept in air tight plastic bag at room temperature for further characterization.

Table 5.1 Ratio of polymers (w/w) in tri-component composite nanofibrous mats and viscosities of spinning solutions with standard deviation

Sample Code	**Polymers' composition**			**Viscosity**	**Remarks**
	PVA	**PVP**	**CMC**	cps	
PVA/CMC-1	6	0	1	181±7	Nanofiber formation
PVA/CMC-2	6	0	2	238±5	No nanofiber observed
PVA/PVP	6	12	0	157±4	Nanofiber formation
C1P10	6	10	1	141±5	Nanofiber formation

C1P11	6	11	1	161±4	Nanofiber formation
C1P12	6	12	1	187±6	Nanofiber formation
C1P13	6	13	1	201±7	Nanofiber formation
C1P14	6	14	1	218±3	Nanofiber formation
C2P10	6	10	2	197±5	Nanofiber formation
C2P11	6	11	2	204±5	Nanofiber formation
C2P12	6	12	2	215±4	Nanofiber formation
C2P13	6	13	2	237±6	Nanofiber formation
C2P14	6	14	2	249±8	Nanofiber formation
C3P10	6	10	3	236±6	Nanofiber formation
C3P11	6	11	3	247±4	Nanofiber formation
C3P12	6	12	3	252±3	Nanofiber formation
C3P13	6	13	3	277±5	No nanofiber observed
C3P14	6	14	3	286±6	No nanofiber observed

5.2 Characterization

To investigate the chemical reaction between CMC, PVP and PVA, FTIR with an ATR prestige-21 (Shimadzu, Japan) was used. Fingerprints of ATR were recorded from 600 cm^{-1} to 4000 cm^{-1}. Scanning electron microscope (SEM) (JSM-5300, JEOL Ltd, Japan) was used to check the surface properties of nanofiber mats at the voltage of 10 kV. Average diameter was calculated by image analysis software (Image J, version 1.4.3) from 50 readings of random nanofibers of each samples. Water contact angle was investigated by using contact angle analyzer (Digidrop, GBX, Whitestone way, France). Thermal analysis of PVA/CMC, PVA/PVP, and PVA/PVP/CMC composite nanofibers was examined by thermogravimetric analyzer "Thermo-plus TG 8120, Rigaku Corporation, Osaka, Japan". TGA test was performed under ambient (air) atmosphere in static mode and heating rate was set to 10 °C/min and 25°C–500°C temperature range for all specimen. Water contact angle (WCA) was measured using contact angle analyzer (Digidrop,

GBX, Whitestone way, France). Volume of water droplet was set to 2 µL while pictures were captured after 1 second (1000 milli seconds).

5.3 Results & discussions

5.3.1 Fourier transform infrared spectroscopy (FTIR)

All of the three polymers used in this study are highly hydrophilic in nature, and reason behind hydrophilicity is presence of abundant hydroxyl groups in main chains of polymeric structures. FTIR-ATR spectra in Figure 5.1 show the presence of hydroxyl groups (-OH peaks) was found in spectra of PVA, PVA/PVP, PVA/CMC, and PVA/PVP/CMC nanofiber mats. In case of PVA/CMC-1 and PVA/PVP the hydroxyl peak (-OH) was found to be broader as compared to that of composite nanofibers containing all three polymers. In Figure 5.1 , a broader peak was observed at wavenumber of 3150 cm^{-1} – 3450 cm^{-1} which was associated with presence of hydroxyl groups in PVA and PVP main chains, however, same peak was become sharper when concentration of PVP and CMC was increased in composite nanofibers, i.e. a sharp peak was observed at 3402 cm^{-1} which is generic peak of hydroxyl group. Further in results of water contact angle it was also confirmed that increasing percentage of CMC in composite nanofibers imparted super-hydrophilicity to the nanofibrous mats. Characteristic peaks of PVA were observed at 3200 cm^{-1} to 3500 cm^{-1} which indicates presence of hydroxyl group (–OH stretching) in PVA chains. A peak at 2900 cm^{-1} was also observed which referred to ($–CH_2–$) asymmetric and symmetric band.[19] In case of PVP, peak around 1650 cm^{-1} can be associated to stretching vibration of the C=O in the pyrrolidone group, while CH stretching can be assigned to absorption peaks around 2850 cm^{-1} to 2980 cm^{-1}. CH deformation bands can be associated to bands at 1430 cm^{-1} and 1370 cm^{-1} (difference in peaks in red and black in given spectra). C–N bending vibration of pyrrolidone can be associated with the band at 1279 cm^{-1}, however, PVP did not show any significance peak at 3400 cm^{-1} -3500 cm^{-1} which are usually associated with presence of amines.[38] It is highly expected that PVA, PVP, and CMC could form hydrogen bonding among their chains as it helped in uniform processing and homogenous mixing of tri-component blend of three different polymers.

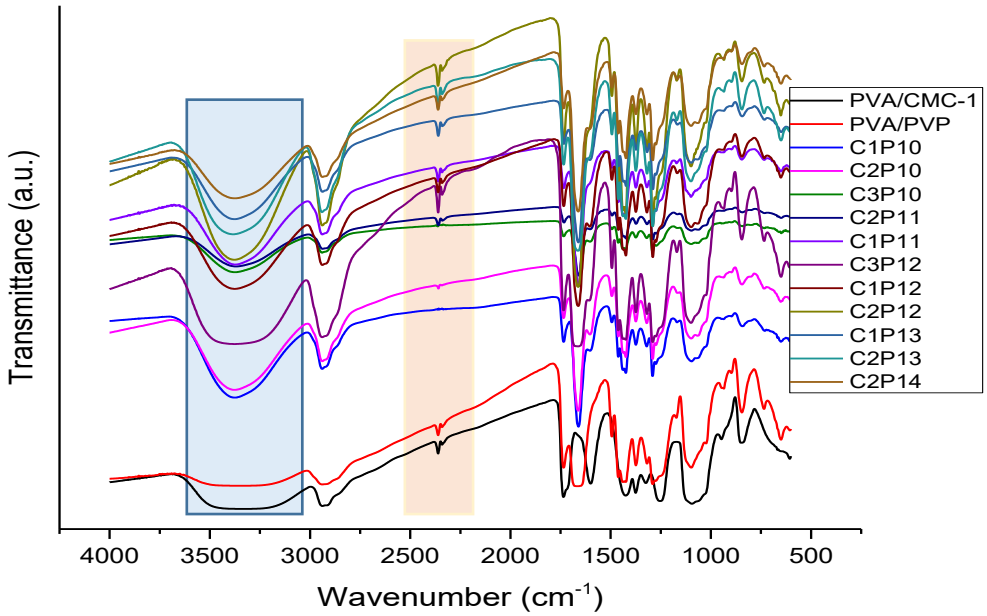

Figure 5.1 FTIR-ATR spectra of PVA/PVP/CMC composite nanofibers with varying weight ratios of PVP and CMC

5.3.2 Morphological properties

Morphological properties like surface structure and nanofibers' diameter were observed by the scanning electron microscope (SEM). As it was also stated in introduction section that CMC cannot be electrospun due to high viscosity and low conductivity. However, PVA is easily electrospun even at varying concentration (6% to 10% is most suitable for smoother nanofibers). PVP is also very difficult to electrospun at lower concentrations due to lower viscosity. Addition of PVP lowers the viscosity of CMC solution as well as imparts conductivity to the spinning solution and makes it electrospunable with good nanofiber formation. Figure *5.* (a & b) represents SEM images of PVA/PVP, PVA/CMC, and PVA/PVP/CMC composite nanofibers with varying concentrations of CMC (1-3 weight ratio) and PVP (10-14 weight ratio). In figure-a it can be observed that PVA/CMC-1 (PVA:CMC = 6:1) exhibited smoother nanofibers while not a single nanofiber was observed by increasing CMC concentration to 6:2 (w/w). PVA/PVP nanofibers were also found to be smoother and finer. Addition of PVP in spinning solution provided with support of conductivity and viscosity, which resulted smoother nanofibers in case of C1P10, C1P11, C1P12, and even C1P14. However, addition of further CMC (weight ratio of 2) did not show the same trend as that of CMC1. Samples C2P10 and C2P11 nanofibers were not uniform and have some beads on the surface, while C2P13

and C2P14 nanofibers had uniform morphology. Ratio of CMC was further increased to weight ratio of 3 to confirm the maximum loading capacity of CMC for smoother nanofibers. It was observed that for CMC-3 only C3P12 sample exhibited smoother morphology while C3P10 and C3P11 samples had beads on the nanofibers' surface, on the other hand, not a single nanofiber was observed in case of C3P13 and C3P14. In conclusion of morphological characterization, it can be stated that maximum and optimum loading capacity for CMC is up to 3 weight ratio with respect to PVA and PVP. While best suitable concentration for smoother and continuous nanofibers production without beads formation is PVA:PVP:CMC = 6:12:3.

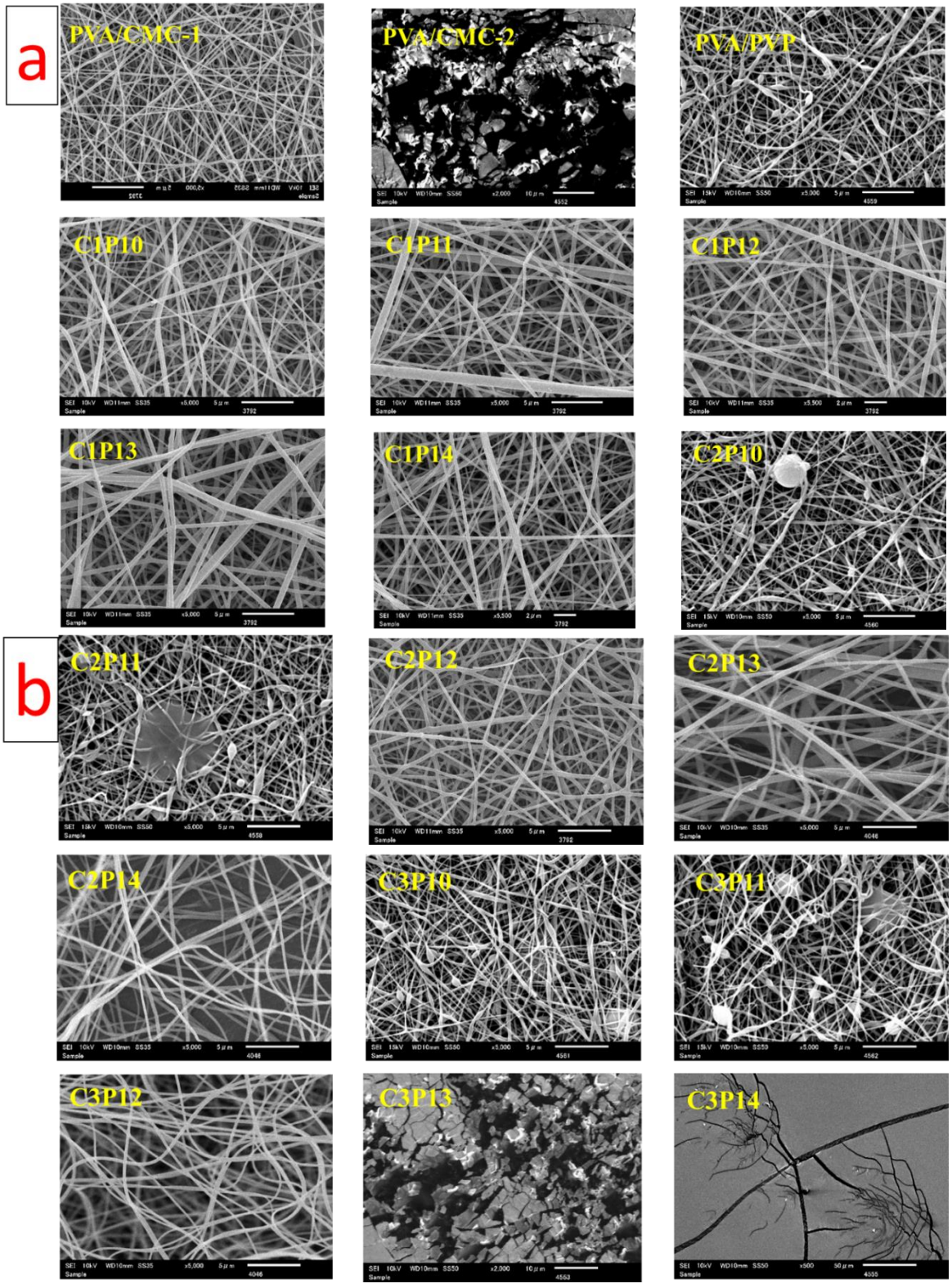

Figure 5.2 (a & b) SEM images of PVA/PVP, PVA/CMC, and PVA/PVP/CMC composite nanofibers: Effect of variation of concentration of PVP and CMC on morphology of nanofibrous mats

5.3.3 Diameter distribution of nanofibers

Diameters of nanofibers were measured by Image J. software by taking 50 random readings of nanofibers for each sample. Figure *5*.3 (a & b) represents diameter distribution trend as shown in histogram of each sample (here samples represent only that polymer compositions that were easily converted to nanofibers on electrospinning). It can be shown that PVA/CMC-1 samples exhibited uniform nanofibers of diameter range 80 nm to 180 nm having an average diameter of 120 nm which indicates successful conversion of polymers in to nanofibers.

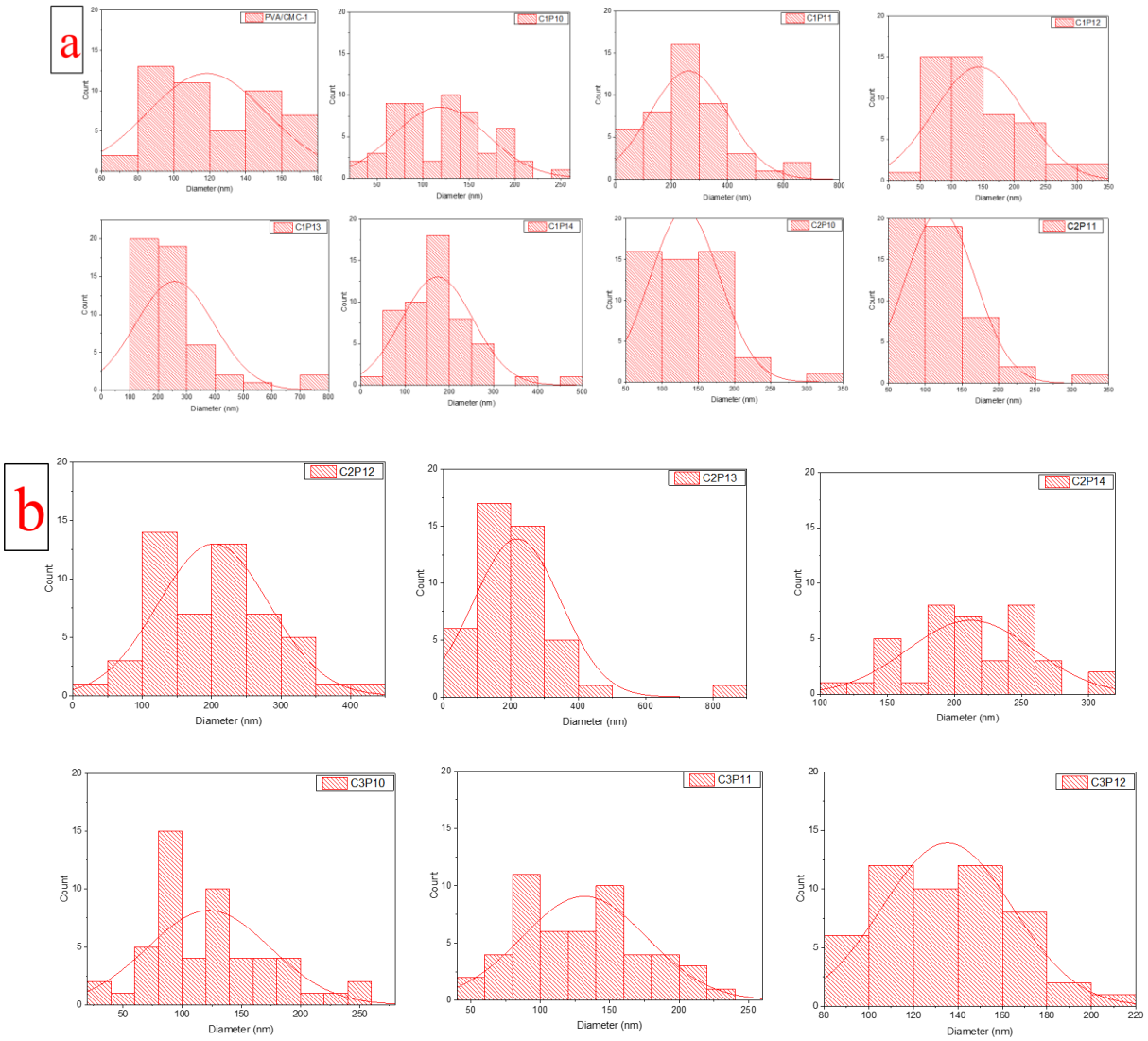

Figure 5.3 (a & b) Diameter distribution plots (histogram) of PVA/CMC, PVA/PVP, and tri-component composite nanofibers of PVA, PVP, and CMC

However, PVA/CMC-2 (having PVA:CMC = 6:2) did not show any sign of nanofiber formation. Addition of further CMC and PVP in PVA solution caused a bit diversity in diameter distribution of nanofibers.

However, it was observed that samples containing 12% PVP exhibited nanofibers of finer and uniform diameter range. It may be because of compatibility or formation of bonding among three polymers on this specific composition. However, this claim further needs confirmation after performing relevant test. As it can be observed in Figure *5.* and Figure *5.* that samples having 12% PVP and varying concentration of CMC exhibited uniform nanofibers without beads formation, as well as uniform diameter distribution.

5.3.4 Water contact angle (WCA)

Water holding capacity of any substance is generally dependent on hydrophilic or hydrophobic nature [18]. Hydrophilicity can be assessed by measuring water contact angle (WCA). WCA of PVA/CMC, PVA/PVP/CMC, and PVA/PVP was measured to evaluate hydrophilic capacity of electrospun nanofibers. Uncrosslinked PVA nanofibers generally have hydrophilic nature while crosslinked nanofibers exhibit hydrophobicity depending upon degree and type of crosslinking [19]. CMC and PVP are also highly hydrophilic polymers. Selection of hydrophilic polymers for a Tricomponent blend for enhanced adsorption and absorption properties was also one of the objectives of this research (however further testing will be carried out in future research regarding adsorption and absorption characteristics to evaluate usability of prepared blends for such applications commercially). Figure 5. represents WCA for composite nanofibrous mats. It can be seen that water contact angles for all of the nanofibrous mats are in the range of hydrophilic, however, samples a-d exhibited contact angle ranging from approx.15° to 20° while WCA values for samples e-o was found to be at 0° (except samples I and J, but average for these two samples were also well below 1°). It was observed that increasing PVP content did not bring any significant changes in water contact angles of composite nanofibers while increasing CMC content significantly decreased WCA values for composite nanofibers. Which indicates that CMC has more tendency towards water due to containing abundant hydroxyl groups in main chain as compared to that of PVA or PVP. Addition of optimum content of CMC will impart hydrophilicity to the composites. It is suggested that CMC should be added with hydrophobic polymers to increase their tendency towards hydrophilic nature. However compatibility of polymers should be properly examined before blending with CMC.

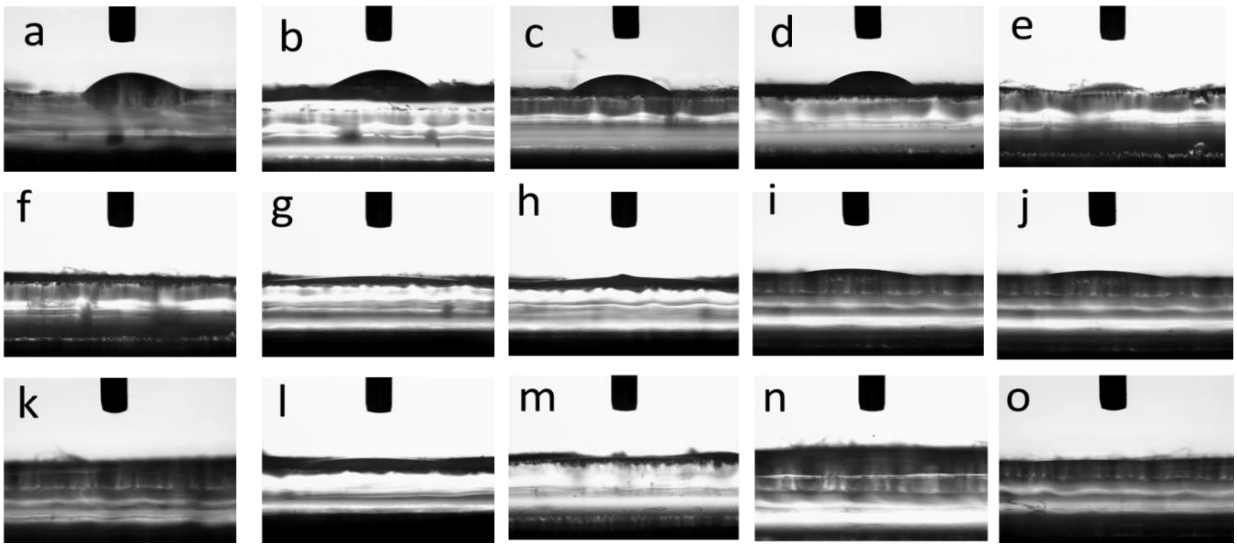

Figure 5.4 Water Contact Angles (WCA) for PVA/PVP, PVA/CMC, and PVA/PVP/CMC nanofibers: Effect of variation in weight ratios of PVP and CMC on water affinity of nanofibrous mats

5.3.5 Thermogravimetric analysis (TGA)

CMC is generally unstable above 280°C, while PVA and PVP are thermally stable well above 300°C. Figure *5.55* represents TGA curves of PVA/CMC, PVA/PVP, and PVA/PVP/CMC (with varying ratios of PVP and CMC). TGA plots in (a-c) have been divided in 3 groups due to overlapping of results. generally, a TGA curve is divided in 3 parts on the basis of temperature zones [39], first temperature zone is up to 100°C which indicates evaporation of high volatile components including impurities and vapors. Second zone starts from onset temperature and ends at offset temperature of substance. Second zone describes thermal stability of substance. While third and the last temperature zone starts from offset temperature of substance which shows burning or degradation of substance. For substances/polymers which are not thermally stable, the last zone is usually flatter as compared to that of thermally stable. It can be observed that onset temperatures for PVA/PVP nanofibrous mats was well above 300°C while onset temperature of nanofibers containing CMC was dropped to 220-250°C which indicated that addition of CMC in tri-component nanofibrous mats caused decrement in thermal stability of polymers. However, considering practical applications such as food packaging, water absorption/adsorption, the thermal stability of nanofibers is still enough to be used as it is. It was also observed that at lower weight ratios of CMC and PVP the 3rd onset was not so clearly visible

while increasing content of PVP and CMC, 3rd onset (curve) is clearly visible in TGA plot. Increasing CMC content also caused decrease in residue.

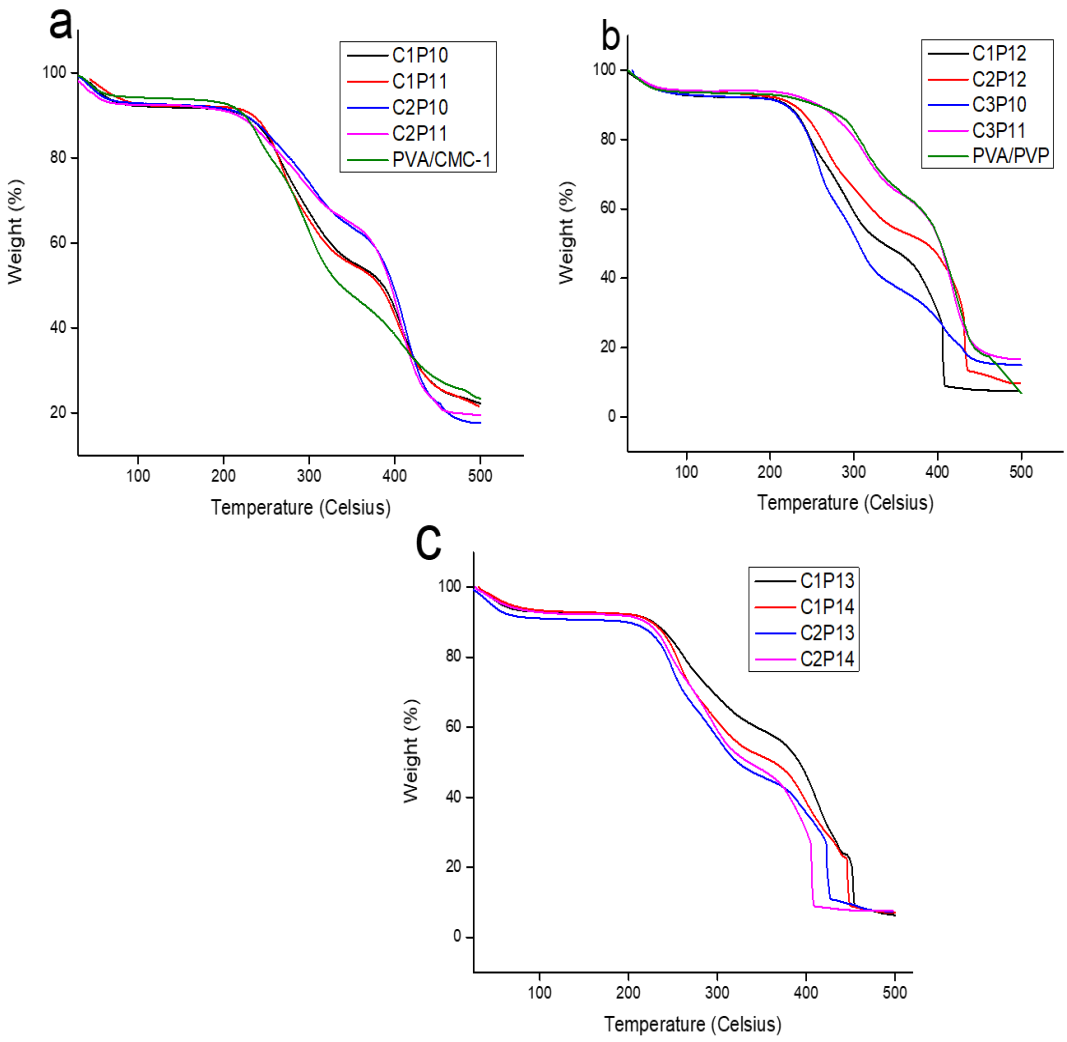

Figure 5.5 Thermogravimetric analysis (TGA) plot of PVA/PVP, PVA/CMC, and PVA/PVP/CMC nanofibers: Effect of variation in weight ratios of PVP and CMC on thermal properties of nanofibrous mats

5.4 Conclusions

Considering results and discussions of experimental section, it can be concluded that CMC is not suitable for electrospinning as a single component, however it can be processed by forming blends/composites with compatible polymers like PVA and PVP. It was observed that at specific concentrations of CMC and PVP formed highly uniformed nanofibers without any beads formation. Processability was also observed to be smoother specifically for samples containing 12 wt.% PVP. There was no significance on thermal

degradation due to addition of CMC. Water contact angle was further decreased to 0˚ with addition of CMC in tri-component nanofibers. Nanofibers having smoother morphology will have potential applications in the field of biomedical, agriculture, and environmental engineering.

References

[1] S. Ullah, A. Ullah, J. Lee, Y. Jeong, M. Hashmi, C. Zhu, K. Il Joo, H.J. Cha, I.S. Kim, Reusability Comparison of Melt-Blown vs Nanofiber Face Mask Filters for Use in the Coronavirus Pandemic, ACS Appl. Nano Mater. 3 (2020) 7231–7241. https://doi.org/10.1021/acsanm.0c01562.

[2] G. Mayakrishnan, S. Somasundaram, S. Ullah, I. Andivelu, K. Ick Soo, C. Ill Min, Facile Green Preparation of Rhodium Nanoclusters Supported Nano-Scaled Graphene Platelets for Sonogashira Coupling Reaction and Reduction of p-Nitrophenol, Catalysts. 9 (2019) 908. https://doi.org/10.3390/catal9110908.

[3] M. Gopiraman, S. Saravanamoorthy, S. Ullah, A. Ilangovan, I.S. Kim, I.M. Chung, Reducing-agent-free facile preparation of Rh-nanoparticles uniformly anchored on onion-like fullerene for catalytic applications, RSC Adv. 10 (2020) 2545–2559. https://doi.org/10.1039/c9ra09244g.

[4] S. Ullah, M. Hashmi, D. Kharaghani, M.Q. Khan, Y. Saito, T. Yamamoto, J. Lee, I.S. Kim, Antibacterial properties of in situ and surface functionalized impregnation of silver sulfadiazine in polyacrylonitrile nanofiber mats, Int. J. Nanomedicine. 14 (2019) 2693–2703. https://doi.org/10.2147/IJN.S197665.

[5] M. Hashmi, S. Ullah, I.S. Kim, Copper oxide (CuO) loaded polyacrylonitrile (PAN) nanofiber membranes for antimicrobial breath mask applications, Curr. Res. Biotechnol. 1 (2019) 1–10. https://doi.org/10.1016/j.crbiot.2019.07.001.

[6] S. Ullah, M. Hashmi, M.Q. Khan, D. Kharaghani, Y. Saito, T. Yamamoto, I.S. Kim, Silver sulfadiazine loaded zein nanofiber mats as a novel wound dressing, RSC Adv. 9 (2019) 268–277. https://doi.org/10.1039/C8RA09082C.

[7] N. Hussain, M. Yousif, A. Ali, M. Mehdi, S. Ullah, A. Ullah, F.K. Mahar, I.S. Kim, A facile approach to synthesize highly conductive electrospun aramid nanofibers via electroless deposition, Mater. Chem. Phys. (2020) 123614. https://doi.org/10.1016/j.matchemphys.2020.123614.

[8] X. Bie, M.Q. Khan, A. Ullah, S. Malik, D. Kharaghani, P.N. Duy, Y. Tamada, I.S. Kim, Fabrication and characterization of wound dressings containing gentamicin/silver for wounds in diabetes mellitus

patients, Mater. Res. Express. (2020). http://iopscience.iop.org/10.1088/2053-1591/ab8337.

[9] M.Q. Khan, D. Kharaghani, N. Nishat, Sanaullah, A. Shahzad, T. Hussain, K.O. Kim, I.S. Kim, The fabrications and characterizations of antibacterial PVA/Cu nanofibers composite membranes by synthesis of Cu nanoparticles from solution reduction, nanofibers reduction and immersion methods, Mater. Res. Express. 6 (2019). https://doi.org/10.1088/2053-1591/ab1688.

[10] D. Kharaghani, Y. Suzuki, P. Gitigard, S. Ullah, I.S. Kim, Development and characterization of composite carbon nanofibers surface-coated with ZnO/Ag nanoparticle arrays for ammonia sensor application, Mater. Today Commun. 24 (2020) 101213. https://doi.org/10.1016/j.mtcomm.2020.101213.

[11] D. Kharaghani, P. Gitigard, H. Ohtani, K.O. Kim, S. Ullah, Y. Saito, M.Q. Khan, I.S. Kim, Design and characterization of dual drug delivery based on in-situ assembled PVA/PAN core-shell nanofibers for wound dressing application, Sci. Rep. 9 (2019) 1–11. https://doi.org/10.1038/s41598-019-49132-x.

[12] M. Hashmi, S. Ullah, I.S. Kim, Electrospun Momordica Charantia Incorporated Polyvinyl Alcohol (PVA) Nanofibers for Antibacterial Applications, Mater. Today Commun. (2020) 101161. https://doi.org/https://doi.org/10.1016/j.mtcomm.2020.101161.

[13] M.Q. Khan, D. Kharaghani, Sanaullah, A. Shahzad, Y. Saito, T. Yamamoto, H. Ogasawara, I.S. Kim, Fabrication of antibacterial electrospun cellulose acetate/ silver-sulfadiazine nanofibers composites for wound dressings applications, Polym. Test. 74 (2019) 39–44. https://doi.org/10.1016/j.polymertesting.2018.12.015.

[14] M.Q. Khan, D. Kharaghani, Sanaullah, A. Shahzad, N.P. Duy, Y. Hasegawa, Azeemullah, J. Lee, I.S. Kim, Fabrication of Antibacterial Nanofibers Composites by Functionalizing the Surface of Cellulose Acetate Nanofibers, ChemistrySelect. 5 (2020) 1315–1321. https://doi.org/10.1002/slct.201901106.

[15] D. Kharaghani, M.Q. Khan, Y. Tamada, H. Ogasawara, Y. Inoue, Y. Saito, M. Hashmi, I.S. Kim, Fabrication of electrospun antibacterial PVA/Cs nanofibers loaded with CuNPs and AgNPs by an in-situ method, Polym. Test. 72 (2018) 315–321. https://doi.org/10.1016/j.polymertesting.2018.10.029.

[16] A. Ullah, S. Ullah, M.Q. Khan, M. Hashmi, P.D. Nam, Y. Kato, Y. Tamada, I.S. Kim, Manuka honey incorporated cellulose acetate nanofibrous mats: Fabrication and in vitro evaluation as a potential wound dressing, Int. J. Biol. Macromol. 155 (2020) 479–489. https://doi.org/10.1016/j.ijbiomac.2020.03.237.

[17] M. Khan, D. Kharaghani, S. Ullah, M. Waqas, A. Abbasi, Y. Saito, C. Zhu, I. Kim, Self-Cleaning Properties of Electrospun PVA/TiO2 and PVA/ZnO Nanofibers Composites, Nanomaterials. 8 (2018) 644. https://doi.org/10.3390/nano8090644.

[18] M. Hashmi, S. Ullah, A. Ullah, M.Q. Khan, N. Hussain, M. Khatri, X. Bie, J. Lee, I.S. Kim, An optimistic approach "from hydrophobic to super hydrophilic nanofibers" for enhanced absorption properties, Polym. Test. 90 (2020) 106683. https://doi.org/10.1016/j.polymertesting.2020.106683.

[19] S. Ullah, M. Hashmi, N. Hussain, A. Ullah, M.N. Sarwar, Y. Saito, S.H. Kim, I.S. Kim, Stabilized nanofibers of polyvinyl alcohol (PVA) crosslinked by unique method for efficient removal of heavy metal ions, J. Water Process Eng. 33 (2020) 101111. https://doi.org/10.1016/j.jwpe.2019.101111.

[20] X. Yang, S.K. Biswas, J. Han, S. Tanpichai, M.C. Li, C. Chen, S. Zhu, A.K. Das, H. Yano, Surface and Interface Engineering for Nanocellulosic Advanced Materials, Adv. Mater. 2002264 (2020). https://doi.org/10.1002/adma.202002264.

[21] J. Han, S. Wang, S. Zhu, C. Huang, Y. Yue, C. Mei, X. Xu, C. Xia, Electrospun Core-Shell Nanofibrous Membranes with Nanocellulose-Stabilized Carbon Nanotubes for Use as High-Performance Flexible Supercapacitor Electrodes with Enhanced Water Resistance, Thermal Stability, and Mechanical Toughness, ACS Appl. Mater. Interfaces. 11 (2019) 44624–44635. https://doi.org/10.1021/acsami.9b16458.

[22] Q. Ding, X. Xu, Y. Yue, C. Mei, C. Huang, S. Jiang, Q. Wu, J. Han, Nanocellulose-Mediated Electroconductive Self-Healing Hydrogels with High Strength, Plasticity, Viscoelasticity, Stretchability, and Biocompatibility toward Multifunctional Applications, ACS Appl. Mater. Interfaces. 10 (2018) 27987–28002. https://doi.org/10.1021/acsami.8b09656.

[23] C. Zheng, K. Lu, Y. Lu, S. Zhu, Y. Yue, X. Xu, C. Mei, H. Xiao, Q. Wu, J. Han, A stretchable, self-healing conductive hydrogels based on nanocellulose supported graphene towards wearable

monitoring of human motion, Carbohydr. Polym. 250 (2020). https://doi.org/10.1016/j.carbpol.2020.116905.

[24] J. Han, H. Wang, Y. Yue, C. Mei, J. Chen, C. Huang, Q. Wu, X. Xu, A self-healable and highly flexible supercapacitor integrated by dynamically cross-linked electro-conductive hydrogels based on nanocellulose-templated carbon nanotubes embedded in a viscoelastic polymer network, Carbon N. Y. 149 (2019) 1–18. https://doi.org/10.1016/j.carbon.2019.04.029.

[25] J. Ci, C. Cao, S. Kuga, J. Shen, M. Wu, Y. Huang, Improved Performance of Microbial Fuel Cell Using Esterified Corncob Cellulose Nanofibers to Fabricate Air-Cathode Gas Diffusion Layer, ACS Sustain. Chem. Eng. 5 (2017) 9614–9618. https://doi.org/10.1021/acssuschemeng.7b01970.

[26] J. Song, C. Chen, Z. Yang, Y. Kuang, T. Li, Y. Li, H. Huang, I. Kierzewski, B. Liu, S. He, T. Gao, S.U. Yuruker, A. Gong, B. Yang, L. Hu, Highly Compressible, Anisotropic Aerogel with Aligned Cellulose Nanofibers, ACS Nano. 12 (2018) 140–147. https://doi.org/10.1021/acsnano.7b04246.

[27] N. Dizge, E. Shaulsky, V. Karanikola, Electrospun cellulose nanofibers for superhydrophobic and oleophobic membranes, J. Memb. Sci. 590 (2019) 117271. https://doi.org/10.1016/j.memsci.2019.117271.

[28] M. Zhu, Y. Wang, S. Zhu, L. Xu, C. Jia, J. Dai, J. Song, Y. Yao, Y. Wang, Y. Li, D. Henderson, W. Luo, H. Li, M.L. Minus, T. Li, L. Hu, Anisotropic, Transparent Films with Aligned Cellulose Nanofibers, Adv. Mater. 29 (2017). https://doi.org/10.1002/adma.201606284.

[29] K. Boruvková, J. Wiener, M. Jakubičková, Preparation and properties of microporous structures based on cmc, NANOCON 2012 - Conf. Proceedings, 4th Int. Conf. (2012) 606–611.

[30] B. Tajeddin, N. Ramedani, Preparation and characterization (Mechanical and water absorption properties) of CMC/PVA/clay nanocomposite films, Iran. J. Chem. Chem. Eng. 35 (2016) 9–15.

[31] M. Golizadeh, A. Karimi, S. Gandomi-Ravandi, M. Vossoughi, M. Khafaji, M.T. Joghataei, F. Faghihi, Evaluation of cellular attachment and proliferation on different surface charged functional cellulose electrospun nanofibers, Carbohydr. Polym. 207 (2019) 796–805. https://doi.org/10.1016/j.carbpol.2018.12.028.

[32] S. Pouranvari, F. Ebrahimi, G. Javadi, B. Maddah, Chemical cross-linking of chitosan/polyvinyl

alcohol electrospun nanofibers, Mater. Tehnol. 50 (2016) 663–666. https://doi.org/10.17222/mit.2015.083.

[33] Y. Park, M. You, J. Shin, S. Ha, D. Kim, M.H. Heo, J. Nah, Y.A. Kim, J.H. Seol, Thermal conductivity enhancement in electrospun poly(vinyl alcohol) and poly(vinyl alcohol)/cellulose nanocrystal composite nanofibers, Sci. Rep. 9 (2019) 1–10. https://doi.org/10.1038/s41598-019-39825-8.

[34] M.Q. Khan, D. Kharaghani, N. Nishat, T. Ishikawa, S. Ullah, H. Lee, Z. Khatri, I.S. Kim, The development of nanofiber tubes based on nanocomposites of polyvinylpyrrolidone incorporated gold nanoparticles as scaffolds for neuroscience application in axons, Text. Res. J. (2018) 004051751880118. https://doi.org/10.1177/0040517518801185.

[35] M. Ignatova, N. Manolova, I. Rashkov, Novel antibacterial fibers of quaternized chitosan and poly(vinyl pyrrolidone) prepared by electrospinning, Eur. Polym. J. 43 (2007) 1112–1122. https://doi.org/10.1016/j.eurpolymj.2007.01.012.

[36] E.M. Abdelrazek, A.M. Abdelghany, A.E. Tarabiah, H.M. Zidan, AC conductivity and dielectric characteristics of PVA/PVP nanocomposite filled with MWCNTs, J. Mater. Sci. Mater. Electron. 30 (2019) 15521–15533. https://doi.org/10.1007/s10854-019-01929-2.

[37] R. Kaur, S.K. Tripathi, Study of conductivity switching mechanism of CdSe/PVP nanocomposite for memory device application, Microelectron. Eng. 133 (2015) 59–65. https://doi.org/10.1016/j.mee.2014.11.010.

[38] I.A. Safo, M. Werheid, C. Dosche, M. Oezaslan, The role of polyvinylpyrrolidone (PVP) as a capping and structure-directing agent in the formation of Pt nanocubes, Nanoscale Adv. 1 (2019) 3095–3106. https://doi.org/10.1039/c9na00186g.

[39] M.S. Irfan, Y.Q. Gill, S. Ullah, M.T. Naeem, F. Saeed, M. Hashmi, Polyaniline-NBR blends by in situ polymerization: Application as stretchable strain sensors, Smart Mater. Struct. 28 (2019). https://doi.org/10.1088/1361-665X/ab1df3.

Chapter 6

Conclusion

PAN/CuO nanofibers were successfully electrospun with varying concentrations of CuO in PAN nanofibers. Addition of copper oxide nanoparticles imparted strength to PAN nanofibers. Tensile strength of PAN/CuO nanofibers having 1.00% CuO nanoparticles was significantly increased (8.43 MPa). Morphological properties also exhibited uniformity and smooth production of nanofibers (beads free nanofibers). Prepared nanofiber mats presented excellent antimicrobial activity and release properties. Breathability test was performed which also resulted in significant breathability (performance of nanofibers was in medium range). MTT analysis also represented that more than 50% of total cells were survived after 120 hours of incubation. Air permeability of nanofiber mats was improved by addition of copper oxide nanoparticles. Analyzing above mentioned properties which include antimicrobial, drug release behavior, mechanical properties, thermal properties, breathability, air permeability, surface and structural properties, it can be concluded that copper oxide nanoparticles have significant potential for antimicrobial and structural applications. We recommend PAN/CuO nanoparticles for antimicrobial breath mask applications on the basis of above described results.

Momordica charantia (MC) extract (water soluble) was loaded on electrospinning in combination with PVA which is well known biocompatible polymer. PVA nanofibers are generally beads-free and more uniform in morphology. Addition of MC extract in PVA solution caused beads formation, and beads occurrence was increased with increasing MC concentration in PVA. Maximum of 50% (w/w) MC loading was run on electrospinning which resulted electro-sprayed PVA/MC nanofibers (less nanofibers, more beads). Samples having 40% MC was considered better as these samples presented better morphological, antibacterial, surface, and thermal properties, hence recommended for further production of nanofibers. Satisfactory results were obtained from toxicity test. But mechanical properties (tensile strength) were suppressed with increasing MC extract concentration in PVA/MC solution. However, our target application is more focused on antibacterial and biocompatibility of prepared nanofiber mats which both are satisfactory. It can be concluded that MC extract is suitable and sustainable replacement of antibacterial drug due to its excellent antibacterial activity against both gram positive and gram negative bacteria. WST-1 assay also showed that MC extract is suitable in applications such as wound dressings.

Keeping in mind all the results and discussions of prepared specimen, it is concluded that PAN has retained its structure and basic characteristics with addition of AgSD. Antibacterial activity test showed excellent antibacterial results for both PAN/AgSD (E.S) and PAN/AgSD (Immersion) nanofiber mats. From SEM results it is already discussed above that nanofiber structure was not much disturbed by AgSD. Surface of nanofiber became slightly rough which is considered to be helpful for antibacterial activity. FTIR spectra showed characteristic peaks of AgSD and PAN in nanofibers. There was no shift of peak observed so it can be referred to physical bonding between PAN and AgSD. XPS spectra clearly showed presence of Ag and S in nanofiber mats. It was observed that for all above mentioned characterizations, PAN/AgSD (Immersion) nanofibers showed prominent results. XRD analysis showed that crystalline structure of PAN was changes as peak at $2\theta = 17^{\circ}$, which was associated with hexagonal lattice of PAN, was decreased with addition of AgSD which was further observed in TGA study that thermal degradation of PAN/AgSD (E.S) and PAN/AgSD (Immersion) was lower than PAN nanofibers. Tensile strength and elongation at break was increased by addition of AgSD by immersion technique, while tensile strength was decreased with in situ addition of AgSD in PAN nanofibers during electrospinning. From all results it is concluded that PAN/AgSD (Immersion) nanofiber mats have better structural and antibacterial properties than that of PAN/AgSD (In situ) nanofiber mats. So, from our point of view, self-synthesized AgSD is recommended for further production of nanofiber mats for antibacterial applications.

Considering results and discussions of experimental section, it can be concluded that CMC is not suitable for electrospinning as a single component, however it can be processed by forming blends/composites with compatible polymers like PVA and PVP. It was observed that at specific concentrations of CMC and PVP formed highly uniformed nanofibers without any beads formation. Processability was also observed to be smoother specifically for samples containing 12 wt.% PVP. There was no significance on thermal degradation due to addition of CMC. Water contact angle was further decreased to 0° with addition of CMC in tri-component nanofibers. Nanofibers having smoother morphology will have potential applications in the field of biomedical, agriculture, and environmental engineering.

Chapter 7

Accomplishments

1. **Hashmi, M**.; Ullah, S.; Kim, I. S. Copper Oxide (CuO) Loaded Polyacrylonitrile (PAN) Nanofiber Membranes for Antimicrobial Breath Mask Applications. Curr. Res. Biotechnol. 2019, 1, 1–10. https://doi.org/10.1016/j.crbiot.2019.07.001.

2. **Hashmi, M**.; Ullah, S.; Kim, I. S. Electrospun Momordica Charantia Incorporated Polyvinyl Alcohol (PVA) Nanofibers for Antibacterial Applications. Mater. Today Commun. 2020, 101161. https://doi.org/https://doi.org/10.1016/j.mtcomm.2020.101161.

3. **Hashmi, M**.; Ullah, S.; Ullah, A.; Khan, M. Q.; Hussain, N.; Khatri, M.; Bie, X.; Lee, J.; Kim, I. S. An Optimistic Approach "from Hydrophobic to Super Hydrophilic Nanofibers" for Enhanced Absorption Properties. Polym. Test. 2020, 90 (June), 106683. https://doi.org/10.1016/j.polymertesting.2020.106683.

4. **Hashmi, M**.; Ullah, S.; Kim, I. S. Optimized loading of carboxymethyl cellulose (CMC) in tri-component electrospun nanofibers having uniform morphology, Polymers, 2020

5. Ullah, S.; Ullah, A.; Lee, J.; Jeong, Y.; **Hashmi, M**.; Zhu, C.; Joo, K. Il; Cha, H. J.; Kim, I. S. Reusability Comparison of Melt-Blown vs Nanofiber Face Mask Filters for Use in the Coronavirus Pandemic. ACS Appl. Nano Mater. 2020, 3 (7), 7231–7241. https://doi.org/10.1021/acsanm.0c01562.

6. Ullah, S.; **Hashmi, M^{+}**.; Khan, M. Q.; Kharaghani, D.; Saito, Y.; Yamamoto, T.; Kim, I. S. Silver Sulfadiazine Loaded Zein Nanofiber Mats as a Novel Wound Dressing. RSC Adv. 2019, 9 (1), 268–277. https://doi.org/10.1039/C8RA09082C.

7. Ullah, S.; **Hashmi, M^{+}**.; Kharaghani, D.; Khan, M. Q.; Saito, Y.; Yamamoto, T.; Lee, J.; Kim, I. S. Antibacterial Properties of in Situ and Surface Functionalized Impregnation of Silver Sulfadiazine in Polyacrylonitrile Nanofiber Mats. Int. J. Nanomedicine 2019, 14, 2693–2703. https://doi.org/10.2147/IJN.S197665.

8. Umar, M.; Ullah, A.; Nawaz, H.; Areeb, T.; **Hashmi, M**.; Kharaghani, D.; Kim, I. S. Wet-spun bi-component alginate based hydrogelfibers: Developmentandin-vitroevaluation as a potential moist wound care dressing. Int. J. Biol. Macromol. 168 (2021) 601-610.https://doi.org/10.1016/j.ijbiomac.2020.12.088

9. Ullah, A.; Ullah, S.; Khan, M. Q.; **Hashmi, M.**; Nam, P. D.; Kato, Y.; Tamada, Y.; Kim, I. S. Manuka Honey Incorporated Cellulose Acetate Nanofibrous Mats: Fabrication and In Vitro Evaluation as a Potential Wound Dressing. Int. J. Biol. Macromol. 2020. https://doi.org/https://doi.org/10.1016/j.ijbiomac.2020.03.237.

10. Kharaghani, D.; Khan, M. Q.; Tamada, Y.; Ogasawara, H.; Inoue, Y.; Saito, Y.; **Hashmi, M.;** Kim, I. S. Fabrication of Electrospun Antibacterial PVA/Cs Nanofibers Loaded with CuNPs and AgNPs by an in-Situ Method. Polym. Test. 2018, 72 (October), 315–321. https://doi.org/10.1016/j.polymertesting.2018.10.029.

11. Ullah, S.; **Hashmi, M^{+}.;** Hussain, N.; Ullah, A.; Sarwar, M. N.; Saito, Y.; Kim, S. H.; Kim, I. S. Stabilized Nanofibers of Polyvinyl Alcohol (PVA) Crosslinked by Unique Method for Efficient Removal of Heavy Metal Ions. J. Water Process Eng. 2020, 33 (December 2019), 101111. https://doi.org/10.1016/j.jwpe.2019.101111.

12. Hussain, N.; Ullah,S; Sarwar, M. N.; **Hashmi, M**.; Khatri, M.; Yamaguchi, T.; Khatri, Z.; Kim, I. S. Fabrication and characterization of novel antibacterial ultrafine Nylon-6 nanofibers impregnated by garlic sour. Fibers & Polymers (Accepted)

13. Irfan, M. S.; Gill, Y. Q.; Ullah, S.; Naeem, M. T.; Saeed, F.; **Hashmi, M.** Polyaniline-NBR Blends by in Situ Polymerization: Application as Stretchable Strain Sensors. Smart Mater. Struct. 2019, 28 (9). https://doi.org/10.1088/1361-665X/ab1df3.

14. Irfan, M. S.; Gill, Y. Q.; **Hashmi, M**.; Ullah, S.; Saeed, F.; Qaiser, A. A. Long-Term Stress Relaxation Behavior of Polyaniline-EPDM Blends Using the Time-Temperature-Strain Superposition Method. Mater. Res. Express 2018, 6 (2), 025318. https://doi.org/10.1088/2053-1591/aaf06a.

Chapter 8

Acknowledgment

I would love to express my gratitude to the Allah Almighty for his countless blessings. I would like to thank my advisor Prof. Kim Ick Soo for the support in my Ph.D studies and research, for his patience, motivation and knowledge. He helped me all time in research and writing this thesis.

I also want to thank all my lab mates Specially Mr. Azeem ullah, Mr. Nadir Hussain, Mr. Numan Sarwar and Mr. Muzammil for their support and motivation. My special thanks goes to administrative staff Ms. Yukari Katayam, Ms. Sumika Sano, Ms. Saito, Mrs. Akiko Kabuta and Japanese students Mr. Saito Yuske, Mr. Wada, Mr. Yamamoto, Ms. Mikoto for their immense support, without their support it was almost impossible to survive in japan.

I specially want to show my respect and love towards my family. My parents supported me with their advices and prayers. They made me what I am today.

I could never thank enough to my husband Mr. Sanaullah for his support in this journey. I could not have imagined having a best friend, soulmate and mentor like him in my life.

Last but not the least, all my love goes to my daughter Waniya Zarnish. She is my strength. Her cute smile made me the strongest woman in the world. She gave me the courage to vanquish the world for her.